An Introduction to Plasma Physics and its Space Applications

Dr. L. Conde

Department of Applied Physics
ETS Ingenieros Aeronáuticos
Universidad Politécnica de Madrid

March 5, 2014

These notes are not intended to replace any of the excellent textbooks (as Refs. [1, 2, 3, 4, 7]) cited in the bibliography, but to free to those attending this course of the thankless task of taking notes. The reader will find that are a very preliminary version that is far from being concluded. Some citations in the text to the references are still incomplete and the english requires of a major revision. I am responsible for all errors and/or omissions.

I took the liberty of borrowing some original figures and graphs from cited references to illustrate certain points. Also to allow to these students the calculations of relevant quantities using actual experimental data. Additionally, I also make use of two photographs of a solar eclipse from NASA that I found in the Wikipedia article on the solar chromosphere. My thanks to the authors for sharing these materials as well as for their unintentional collaboration.

L. Conde

Contents

1 Introduction

1.1 Ionized gases and plasmas

In essence, a *plasma* is a gas where a fraction of its atoms or molecules are ionized. This mixture of free electrons, ions and neutral gas atoms ($\alpha = i, e, a$) is denominated a *fully ionized plasma* when all neutral gas atoms are ionized and *partially ionized* otherwise.

In the thermodynamic equilibrium of a gas its atoms have a Maxwell Boltzmann velocity distribution determined by the temperature T of the system. This latter is usually expressed in units of energy $k_B T$ in Plasma Physics. In these conditions, the average velocity of these neutral particles is,

$$V_{a,Th} = \left(\frac{8\, k_B T}{\pi\, m_a} \right)^{1/2}$$

Then, for growing temperatures the kinetic energy of an increasing fraction of the atoms lies over the ionization threshold E_I of the the neutral gas. The collisions of these energetic particles may produce the ionization of a neutral gas atom. Consequently, the degree of ionization and the thermal temperature of the neutral gas are closely related magnitudes. This is why the plasma state is frequently associated with high temperature gases, because they reach an equilibrium state where its atoms become fully or partially ionized.

Nevertheless, the detailed derivation of the explicit relation between the equilibrium temperature T and the ionization degree of a gas will not be carried out here. The classical result is the *Saha equation*,

$$\frac{n_e n_i}{n_a} \simeq 2.4 \times 10^{21}\, T^{3/2}\, \exp(-E_I / k_b T)$$

where n_e, n_i and n_a respectively are the number of electrons, ions and neutral atoms per volume unit.

However, the above expression predicts very low ionization degrees even for high temperatures. Therefore, the thermodinamic equilibrium of partially ionized gases only take place for extremely high temperatures. This restrictive condition is seldom found in nature and most plasmas in nature and in the laboratory are physical systems *far from thermodynamic equilibrium*. The energy is lost by different physical mechanisms as the emission of visible light, electric current transport, ...etc. These energy losses are sustained by external energy contributions as external radiation, electromagnetic fields, ... etc.

1.2 Properties of plasmas

More precisely, the *plasma state of matter*[1] can be defined as the mixture of positively charged ions, electrons and neutral atoms which constitutes a *macroscopic electrically neutral medium that responds to the electric and magnetic fields in a collective mode.* These physical systems have the following general properties:

- The charged particles interact through long distance electromagnetic forces and the number of positive and negative charges is equal, so that the medium is *electrically neutral.*
- In the following, the electromagnetic interaction will be regarded as instantaneous, we will not cope with relativistic effects. The electromagnetic forces experienced by charged particles can be approximated by the Lorentz force.

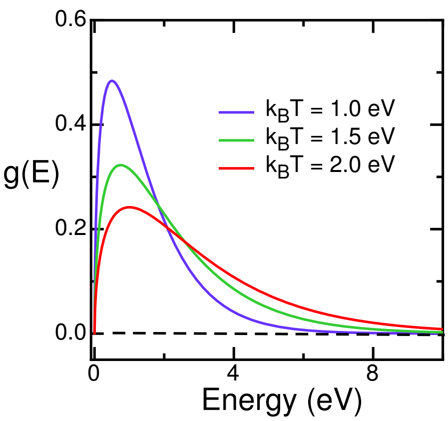

Figure 1.1: The Maxwell Boltzmann energy distribution function $g(E)$ for different temperatures $k_B T$.

A particular feature of plasmas is the *collective* response to external perturbations. In ordinary gases, the fluctuations of the pressure, energy, ...etc. are propagated by collisions between the neutral atoms. This requires the close approach of the colliding particles. In addition to this short scale interaction, the long range electromagnetic forces in plasmas also propagate the perturbations affecting the motion of large number of ions and electrons. Therefore, the response to the perturbations of electromagnetic fields is *collective*, involving huge numbers of charged particles.

Obviously, the *multicomponent plasmas* are constituted by a mixture of different kinds of atoms. Additionally, the *dusty plasmas* also include charged solid microparticles. The large mass and electric charge acquired by these dust grains introduce new properties in these physical systems.

For simplicity, we will limit in the following to one component classical plasmas composed by electrons and single charged ions.

1.3 The ideal Maxwellian plasma

Let us briefly recall some properties of the equilibrium Maxwell Boltzmann energy distribution for a neutral gas composed by a single kind of atoms with mass m. It may be shown that this

[1] Note that such statement is frequently, used but is somehow misleading because the different states of condensed matter may be found in thermodynamic equilibrium.

distribution *describes a gas in the thermodynamic equilibrium state* at the temperature $k_B T$. This distribution may be expressed as,

$$f(\boldsymbol{v}) = (\frac{m}{2\pi k_B T})^{3/2}\, exp\,(-\frac{m\,\boldsymbol{v}^2}{2k_B T}) \tag{1.1}$$

where $\boldsymbol{v}$ is the particle velocity. This velocity distribution only depends on $v = |\boldsymbol{v}|$ and the integral over all possible velocities gives,

$$\int_{-\infty}^{+\infty} f(\boldsymbol{v})\, d\boldsymbol{v} = \int_{-\infty}^{+\infty} f(\boldsymbol{v})\,(4\pi\, v^2)\, dv = 1$$

In the equilibrium the number n_o number of particles by unit volume is uniform and,

$$\int_{-\infty}^{+\infty} n_o\, f(\boldsymbol{v})\, d\boldsymbol{v} = n_o$$

Therefore $dn = n_o\, f(\boldsymbol{v})\, d\boldsymbol{v}$ represents the density of particles with velocities between $\boldsymbol{v}$ and $\boldsymbol{v} + d\,\boldsymbol{v}$. Equivalently, $dP = f(\boldsymbol{v})\, d\boldsymbol{v}$ is the probability of finding a particle with this velocity range by volume unit. Using the particle kinetic energy $E = mv^2/2$ in the Eq. (1.1) and integrating,

$$\int_0^{\infty} g(E)\, dE = 1 \quad \text{where,} \quad g(E) = \frac{2}{\sqrt{\pi}}\,\frac{\sqrt{E}}{(k_B T)^{3/2}}\, e^{-E/k_B T} \tag{1.2}$$

This energy distribution function $g(E)$ is equivalent to $f(\boldsymbol{v})$ in Eq. (1.1) and is represented in Fig. (1.1) for different temperatures $k_B T$.

As is evidenced in Fig. (1.1), the distribution becomes broader as the temperature increases and $dn = n_o\, g(E)\, dE$ represents the number of particles with kinetic energy between E and $E+dE$. The broadening of Fig. (1.1) shows the increment in the number of energetic particles for increasing $k_B T$.

The physical magnitudes are obtained from the equilibrium distributions (1.1) and (1.2) as averages. The kinetic energy by particle is e_i is,

$$e_i =< \frac{1}{2} m\boldsymbol{v}^2 >= \frac{1}{n_o}\int_{-\infty}^{+\infty} f(v)\,(\frac{1}{2}mv^2)\, d\boldsymbol{v} = \frac{1}{n_o}\int_0^{\infty} f(v)\,(\frac{1}{2}mv^2)\,(4\pi\, v^2)\, dv = \frac{3}{2}\, k_B T$$

and the internal energy of this monoatomic gas is therefore $E_i = n_o\, e_i$. Note in Fig. (1.1) hat while its maximum value is $e_{max} = k_B T/2$ the average kinetic energy by particle $e_c = 3\, k_B T/2$ is slightly higher.

Other different average speeds are currently defined for the Maxwell Boltzmann distribution function. As the *thermal velocity*, $v_{Th} = \sqrt{2k_B T/m}$ which may be used to rewrite Eq. (1.1) as,

$$f(v) = (\frac{1}{\pi^{3/2}\, v_{Th}^3})\, exp\,\left(-v^2/v_{Th}^2\right)$$

The *average speed* is defined as $\bar{v} =< |\boldsymbol{v}| >$ and,

$$\bar{v} =< \sqrt{\boldsymbol{v}\cdot\boldsymbol{v}} >= \int_0^{+\infty} f(\boldsymbol{v})\, v\, (4\pi\, v^2\,)\, dv = \left(\frac{8k_BT}{\pi\, m}\right)^{1/2} \tag{1.3}$$

Since the Maxwell Boltzmann distribution only depends on $|\boldsymbol{v}|$ the average along a fixed direction,

$$< v_x >=< v_y >=< v_z >= 0$$

This reflects the fact that in the equilibrium of an ideal gas there is no privileged direction for the particle speed. On the contrary, the average,

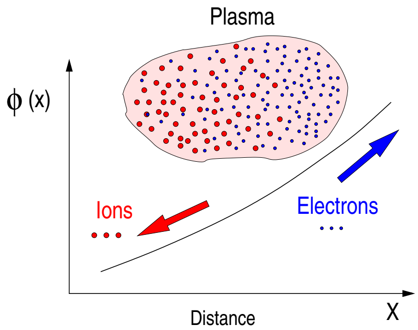

Figure 1.2: Polarization of a plasma cloud under an external electric field $\boldsymbol{E} = -\nabla\phi(x)$.

$$< |v_x| >= \left(\frac{2k_BT}{\pi\, m}\right)^{1/2} = \frac{1}{2}\,\bar{v}$$

represents the average speed of particles crossing an imaginary plane drawn perpendicular to the x direction within the gas bulk. The *random flux of particles* Γ crossing such surface is,

$$\Gamma = \frac{1}{2} n < |v_x| >= \frac{1}{4}\, n_o\, \bar{v}$$

where the factor $1/2$ accounts for the two possible directions of incident particles.

As for neutral gases, the Maxwell Boltzmann distributions (1.2) and (1.2) may be used to describe the *thermodynamic equilibrium state* of an *ideal plasma* [2]. This physical situation is roughly characterized by:

1. The energy distribution function of each specie (ions electrons and neutral atoms) is a Maxwellian with a common kinetic temperature k_BT for all species. This latter is also the temperature of the thermodynamic equilibrium state of the plasma.

2. In order to preserve the bulk electric charge neutrality, the ion and electron volume densities $n_{io} \simeq n_{eo} = n_o$ are equals. This property is denominated the *plasma quasineutrality* and results in a negligible electric field $\boldsymbol{E} \simeq 0$ in the plasma bulk.

3. The plasma potential $\phi(\boldsymbol{r}) \simeq \phi_o$ is therefore uniform in space, so that no currents nor transport of particles takes place in a Maxwellian plasma.

4. The kinetic temperatures k_BT are also uniform in space and are usually expressed in energy units. They are currently measured in electron volts (eV) in Plasma Physics because of the large energies involved ($1\ eV = 11{,}605\ K$).

A rising temperature increments the average kinetic energy and the energy distribution function becomes wider as shown in Fig. (1.1). The limit $k_BT = 0$ for a *cold plasma* corre-

[2] The use of the term *ideal* should be remarked. The requisites for the thermodynamic equilibrium of a plasma are extremely restrictive and plasmas essentially in *stationary states* far from the thermodynamic equilibrium.

sponds to a monoenergetic particle population and its energy distribution could be approximated by a Dirac delta function. In this case, all particles have exactly the same velocity and there is no energy spread around a mean value, contrary to the case $k_B T \neq 0$ corresponding to a *finite temperature* plasma.

Therefore, in the *ideal* plasma in *thermodynamic equilibrium* the kinetic temperature $k_B T$ is the same for all species, while the electron and ion thermal speeds differ,

$$v_{e,Th} = \sqrt{2\, k_B T/m_e} \quad \text{and,} \quad v_{i,Th} = \sqrt{2\, k_B T/m_i} = v_{e,Th}\, \sqrt{m_e/m_i}$$

The ion velocity $v_{i,Th}$ is lower than the electron thermal speed, because of their different masses. As we will see later, when the plasma *is far from thermodinamic equilibrium* the temperatures of the species $k_B T_e$ are also different and is frequently found that $k_B T_i \ll k_B T_e$.

1.4 The Maxwellian plasma under an external electric field

In order to introduce some basic properties we will consider an ideal, fully ionized plasma of ion and electrons. The initial charged particle densities n_{io}, n_{eo} and temperature $k_B T$ are constant in time and uniform in space.

This initial equilibrium is perturbed by an *external*[3], one dimensional electric field $\boldsymbol{E} = -\nabla \phi(\boldsymbol{r})$. After reaching an stationary state, both charged species separate as shown in Fig. (1.2). The electrons (blue dots) are attracted towards the high potential side whereas the ions (red dots) move on the opposite direction.

The disturbance introduced by the electric potential profile $\phi(x)$ brings the plasma out of equilibrium and produces a one dimensional spatial profile of the electron $n_e(x)$ and ion $n_i(x)$ densities. However, the strength of this external electric field is not too strong, so that the charge separation along the plasma potential profile $\phi(x)$ is not complete. The *electrostatic energy* ($\sim e\,\phi(x)$) is of the same order than the *thermal energy* ($\sim k_B T$) of ions and electrons and therefore both charge species coexist along the spatial profile $\phi(x)$.

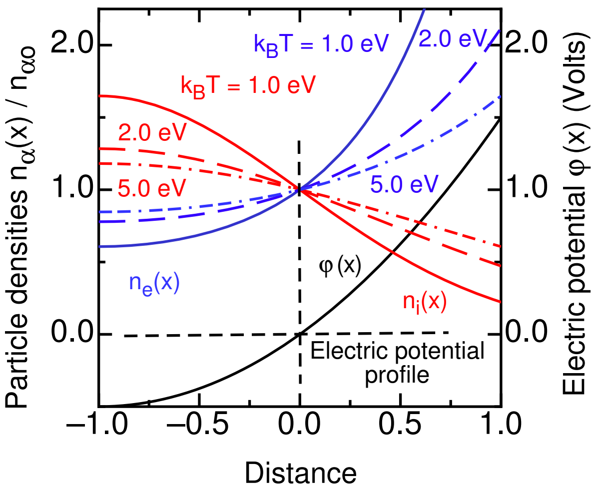

Figure 1.3: The applied electric potential $\phi(x)$, electron $n_e(x)$ and ion $n_i(x)$ densities as a function of the distance X.

In these conditions the energy of each charged particle ($\alpha = i, e$) is $E_\alpha = m_\alpha v^2/2 + q_\alpha\, \phi(\boldsymbol{r})$ where $q_\alpha = \pm e$ and the Maxwellian energy distribution (Eq. 1.1) for each specie is,

$$f_\alpha(\boldsymbol{v}) = (\frac{m_\alpha}{2\pi k_B T})^{1/2} \exp\left(-\frac{m_\alpha\, v_\alpha^2 + 2\, q_\alpha\, \phi(\boldsymbol{r})}{2 k_B T}\right) \tag{1.4}$$

Integrating over v_α we obtain for ions,

[3] This point is emphasized because this potential profile $\phi(x)$ is essentially produced by an external electric field, the contribution of charged particles is neglected.

$$n_i(x) = n_{io}\, \exp\,(-\frac{e\,\phi(x)}{k_B T}) \tag{1.5}$$

and for electrons,

$$n_e(x) = n_{eo}\, \exp\,(\frac{e\,\phi(x)}{k_B T}) \tag{1.6}$$

In Fig. (1.3) are represented the plasma potential profile $\phi(x)$ (black solid line, right axis between -0.5 V and 1.5 V) and the corresponding densities of charged particles given by Eqs. (1.5) and (1.6), which reproduces the situation depicted in the scheme of Fig. (1.2).

Since the values for $\phi(x)$ in Fig. (1.3) are moderate and similar to the plasma temperatures $k_B T \simeq$ 1-5 eV both charged species coexist in the range $-1 \leq x \leq 1$. The electron densities $n_e(x)$(blue curves) increase for $\phi(x) < 0$ ($x < 0$) when $k_B T$ grows and the same effect takes place for ions for $\phi(x) > 0$ ($x > 0$).

The electron densities $n_e(x)$ (blue curves) dominate for positive potentials ($x > 0$ and $\phi(x) > 0$) where ions are rejected whereas the opposite situation occurs for $x < 0$ where $\phi(x) < 0$. At the point $x = 0$ the electric potential is null and the Eqs. (1.5) and (1.6) recover the equilibrium particle densities $n_{eo} = n_{io}$. In the figure (1.3) the spatial profiles for electrons and ions are not equivalent with respect to the vertical dashed line at $x = 0$ because the electric potential $\phi(x)$ is asymmetric.

This increment of $n_e(x)$ for $x < 0$ (equivalently, $n_i(x)$ for $x > 0$) with the plasma temperature takes place because the Maxwellian electron (ion) energy distribution $g_e(E)$ (for ions $g_i(E)$) becomes broader when $k_B T$ grows as shows the Fig. (1.1). For points close to $x \simeq -0.5$ an increasing fraction of electrons have enough thermal energy to overcome the electrostatic potential energy $e\,\phi(x)$. The situation is similar for the ions at the point $x \simeq 0.5$.

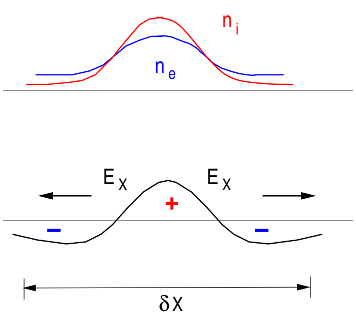

Figure 1.4: The space fluctuation of the electron $n_e(x)$ and ion $n_i(x)$ densities produce a local electric field E_x in the plasma.

In the case of a *cold plasma* $k_B T \simeq 0$ the charged particles have no thermal energy. They only move under the external electric field and both species separate in space. On the contrary, in a *finite temperature plasma* ($k_B T$ >0) and despite the charged particle α is rejected when $q_\alpha\, \phi(x) < 0$, a fraction of them have *thermal energy* enough to jump the electric potential barrier. For *finite temperatures* the *thermal energy* competes with the magnitude of the *electrostatic energy* of the plasma electric potential profile.

The thermal energy of charged particles considered in Eqs. (1.5) and (1.6) brings a relevant property of plasmas: Their ability to *shield out the electromagnetic perturbations*. When moderate electric fields are externally applied or low amplitude electric fluctuations occur in the plasma bulk, the thermal motion of charged particles shields the perturbations as in Fig.

(1.3) by electrons and ions with energy enough to overcome the potential barrier.

1.5 The plasma parameters

The physical description of a plasma requires of a characteristic time and length scales and additionally, a minimum number of charged particles by unit volume. These parameters are related with the attenuation of the small amplitude fluctuations of the equilibrium state of the plasma.

As indicated in Fig. (1.4), when an small charge fluctuation $\delta q = e\,\delta(n_i - \delta n_e)$ occurs in a plasma in equilibrium, the local positive and negative charged particle densities $n_i(x)$ and $n_i(x)$ become slightly different along the perturbation length δX. This departure from quasineutrality produces an intense electric field in the plasma bulk that moves the charged particles. In the absence of other forces, the motion of charges in the plasma tends to cancel the perturbation and to restore the local electric neutrality as the Fig. (1.4) suggests.

The space fluctuations are damped out along a characteristic distance λ_D denominated *Debye length*. This characteristic distance might be also understood as the length scale along the spatial average of electric charge in the plasma is cancelled. Only longitudes $L > \lambda_D$ over the Debye length are usually considered in Plasma Physics because for distances below $L < \lambda_D$ the electric fields are local, very variable and they are regarded as microscopic.

By other hand, the damping of the charge fluctuations takes place during a time scale τ_{pe} which defines the *electron plasma frequency* $f_{pe} = 1/\tau_{pe}$. The minimum time of response against local time dependent fluctuations corresponds to the faster particles (electrons) and turns to be the shortest time scale possible in the plasma.

Finally, the electric charge shielding processes in the plasma bulk require of a number of free charges to cancel the fluctuations of the local electric field. So we need to have a minimum density of charged particles and this determines the so called *plasma parameter* [4]. In the Table (1.1) are compared the typical values and magnitudes for different plasmas in nature and in the laboratory.

1.5.1 The Debye length

We consider again a quasineutral ($n_e = n_i = n_o$) plasma where a small plasma potential fluctuation $\phi(\boldsymbol{r})$ is produced by the electric charge $\delta\rho_{ext} = q\,\delta(\boldsymbol{r})$, where $\delta(\boldsymbol{r})$ is the Dirac delta function. Thus, q only introduces small changes in the electric potential $\phi(\boldsymbol{r}) \ll 1$ close to the origin $\boldsymbol{r} = 0$.

The electric charge fluctuations becomes,

$$\delta\rho_{sp} = e\,[n_i(\boldsymbol{r}) - n_e(\boldsymbol{r})]$$

and therefore, the locally perturbed charge density is,

$$\delta\rho = \delta\rho_{ext} + \delta\rho_{sp} = q\,\delta(\boldsymbol{r}) \; + e\,[n_i(\boldsymbol{r}) - n_e(\boldsymbol{r})]$$

[4] Useful expressions for the characteristic length, time and plasma parameter are summarized in Table (1.2).

We left open in this case the possibility of having different temperatures for electrons $k_B T_e$ and for ions $k_B T_i$ [5]. However, we assume that the electric potential fluctuation introduced by the charge disturbance q is small when compared with the thermal energies of charged particles $|e\,\phi(\boldsymbol{r})/k_B\,T_\alpha| \ll 1$ (with $\alpha = e, i$). Then, we may approximate the Eqs. (1.5) and (1.6) by,

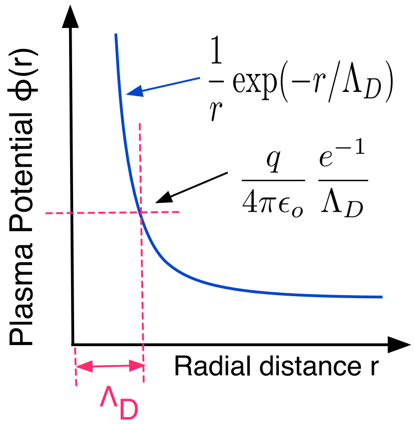

Figure 1.5: Exponential damping for the space fluctuations of $\phi(x)$ along distances in the order of Λ_D.

$$n_\alpha(\boldsymbol{r}) \simeq n_o\left(1 \pm \frac{e\,\phi(\boldsymbol{r})}{k_B T_\alpha}\right) \tag{1.7}$$

Substituting in the Poisson equation,

$$\nabla^2\phi = -\frac{\delta\rho}{\epsilon_o} = -\frac{1}{\epsilon_o}\left[\delta\rho_{ext} + \frac{e^2\,n_o}{k_B T_i}\,\phi(\boldsymbol{r}) + \frac{e^2\,n_o}{k_B T_e}\,\phi(\boldsymbol{r})\right]$$

For the plasma potential fluctuations $\phi(\boldsymbol{r})$ we obtain,

$$\left(\nabla^2 - \frac{1}{\Lambda_D^2}\right)\phi(\boldsymbol{r}) = -\frac{q}{\epsilon_o}\,\delta(\boldsymbol{r}) \quad \text{where,} \quad \frac{1}{\Lambda_D^2} = \frac{1}{\lambda_{Di}^2} + \frac{1}{\lambda_{De}^2}$$

The characteristic lengths λ_{Di} and λ_{De} respectively are the *ion* and *electron Debye lengths*,

$$\lambda_{Di} = \sqrt{\frac{\epsilon_o\,k_B T_i}{e^2\,n_o}} \quad , \quad \lambda_{De} = \sqrt{\frac{\epsilon_o\,k_B T_e}{e^2\,n_o}}$$

and both have units of distance. Assuming spherical symmetry the plasma potential $\phi(\boldsymbol{r})$ is the solution of the differential equation,

$$\frac{\partial^2\phi}{\partial r^2} + \frac{2}{r}\frac{\partial\phi}{\partial r} - \frac{\phi}{\Lambda_D^2} = -\frac{q}{\epsilon_o}\,\delta(\boldsymbol{r})$$

Then, introducing, $\phi(r) = a\,f(r)/r$ where a is constant,

$$\frac{a}{r}\left(\frac{d^2 f}{dr^2} - \frac{1}{\Lambda_D^2}\,f\right) = -\frac{q}{\epsilon_o}\,\delta(\boldsymbol{r})$$

Therefore, for $r > 0$ $a > 0$ this equation reduces to,

$$\frac{d^2 f}{dr^2} - \frac{1}{\Lambda_D^2}\,f = 0 \quad \text{with solutions} \quad f(r) = \exp(\pm\,r/\Lambda_D)$$

The solution proportional to $\exp(r/\Lambda_D)$ is unphysical because the spatial perturbations would be amplified in this case. In order to recover the potential for a point charge when $r/\Lambda_D \ll 1$. we have $a = q/(4\pi\epsilon_o)$. Finally, the electric potential for $r > 0$ is,

$$\phi(r) = \frac{q}{4\pi\epsilon_o}\,\frac{e^{-r/\Lambda_D}}{r}$$

[5] As we shall see, this is a frequent situation in nonequilibrium laboratory plasmas

As shown in Fig. (1.5) the perturbation introduced in the plasma potential exponentially decays along the distance at a rate $1/\Lambda_D$. Equivalently, the local charge perturbation q becomes shielded out by a cloud of opposite charge with a radius proportional to Λ_D.

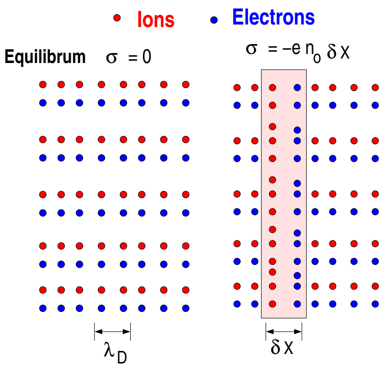

Figure 1.6: The electric field produced by a fluctuation of the local charge density along the distance δX.

The electron and ion Debye lengths measure the contribution of each charged specie to this shielding and are only equals when $k_B T_e = k_B T_i$. Because of electron temperature is usually higher $k_B T_e \gg k_B T_i$ the electron Debye length is then larger and is often considered as the *plasma Debye length*.

The Debye length considers the *thermal effect*, and relies on the charged particle temperatures $k_B T_\alpha$ and density n_o of the plasma. The Debye shielding is more efficient for rising plasma densities n_o whereas a growing thermal energy $k_B T_\alpha$ enlarges the region perturbed by the charge fluctuation q.

The Debye shielding is realistic when the magnitude of the perturbation introduced by the electric charge q is moderate. When $|\, q\,\phi/k_B T\,| > 1$ additional terms needs to be considered in the power expansion of Eq. (1.7) for $n_\alpha(\boldsymbol{r})$ and hence, the Poisson equation becomes nonlinear and the above approximation is no longer valid. Under these conditions, intense electric fields might develop in the plasma volume extended over many Debye lengths, as well as complex plasma structures as are the denominated *plasma double layers*.

These structures are shown in Fig. (2.5) and are composed of different concentric plasma shells separated by abrupt changes in luminosity. These boundaries corresponds to plasma potential jumps (double layers) separating the different plasmas of the structure

1.5.2 The plasma frequency

The shorter time scale of the plasma response to time dependent external perturbations is related the fast oscillations of electrons around the heavy ions. This process is illustrated in Figs. (1.4), (1.6) and (1.7) in one dimension where are shown the local departures from the equilibrium electric neutrality (quasineutrality) of an ideal plasma along the small distance $s = \Delta X$.

These deviations takes place in Fig. (1.7) along an infinite plane perpendicular to the X direction. This produces the electric field E_x that is calculated as shown in Fig. (1.7), where the negative charge of electrons $Q = -e\, n_o\, A\, \Delta x$ is within the pillbox of area A and Δx of height. The electric field in the plasma bulk at the bottom of the pillbox is null ($n_{eo} = n_{io}$ and hence $\boldsymbol{E} = 0$) as well as the components of $\boldsymbol{E}$ parallel to the plane. We have $-A\, E_x = -e\, n_o\, A\, \Delta x/\epsilon_o$ by using the Gauss theorem and therefore,

$$E_x = \frac{e}{\epsilon_o}\, n_o\, \Delta X$$

The equation of motion for the electrons inside the upper pillbox results,

$$m_e\, \frac{d^2}{dt^2} \Delta X = -\frac{e}{\epsilon_o}\, n_o\, \Delta X \quad \text{hence,} \quad \frac{d^2 \Delta X}{dt^2} + \frac{e\, n_o}{m_e\, \epsilon_o}\, \Delta X = 0$$

and therefore the electrons perform harmonic oscillations with frequency,

$$\omega_{pe} = \sqrt{\frac{n_o\, e^2}{m_e\, \epsilon_o}}$$

The electrons oscillate around the ions with a frequency ω_{pe} which is called *electron plasma frequency* $f_{pe} = \omega_{pe}/(2\pi)$ [6]. Similar arguments apply for ions and the *ion plasma frequency* f_{pi} is also defined for the positive charges. The ratio between the electron and ion frequencies is,

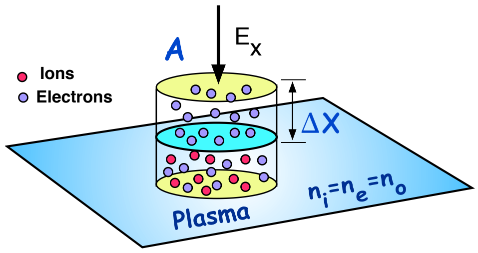

Figure 1.7: The electric field E_z produced by a small local charge fluctuation along the small distance ΔX.

$$f_{pi} = f_{pe}\sqrt{\frac{m_e}{m_i}} \ll f_{pe}$$

and f_{pe} is usually called *plasma frequency*. It should be underlined that both ion and electron plasma frequencies only rely on the equilibrium charged particle density n_o and are independent on the temperature $k_B T_\alpha$ of the charged particle species.

The electron plasma frequency provides the shortest time scale $\tau_{pe} = 1/f_{pe}$ for the propagation of perturbations in the plasma. So that, the motion of ions could be regarded as frozen when compared with the faster electron motion over the time scale $\tau_{pe} > \tau > \tau_{pi} = 1/f_{pi}$. The frequency f_{pe} determines the fast time scale of the plasma, where the lighter particles (electrons) respond to the time dependent fluctuations of the local electric field.

We may also interpret the time scale associated to the plasma frequency τ_{pe} as proportional to the time that a thermal electron (with velocity $V_{Te} = \sqrt{2k_B T_e/m_e}$) travels along a Debye length,

$$\tau_{pe} = \frac{1}{f_{pe}} \simeq \frac{\lambda_D}{V_{Te}} \simeq \left(\frac{\epsilon_o m_e}{2\, n_e\, e^2}\right)^{1/2} = \frac{1}{\sqrt{2}\, f_{pe}}$$

1.5.3 The plasma and coupling parameters

Finally, in order to shield out the perturbations of the electric field an ideal plasma requires of a number of electric charges inside an sphere with radius of a Debye length. This defines the *electron plasma parameter* as,

$$N_{De} = n_e\, \frac{4}{3}\, \pi\, \lambda_{De}^3$$

as well as the equivalent definition of N_{Di} for ions. The collective behavior of plasmas requires a large number of charged particles and then $N_{De} \gg 1$, otherwise the Debye shielding would no be an statistically valid concept. Usually $N_{De} \gg N_{Di}$ because the ion and electron temperatures frequently are $k_B T_e \gg k_B T_i$ and therefore $\lambda_{De} \gg \lambda_{Di}$.

The plasma parameter is also related with the *coupling parameter* $\Gamma = E_{el}/E_{th}$ which compares the electrostatic potential energy of nearest neighbors E_{el} with the thermal energy $E_{th} \sim k_B T$. The potential energy of two repelling charged particles ($\alpha = e, i$) is,

[6] Sometimes ω_{pe} is also called Langmuir frequency as in Ref. [2].

$$E(r, v_\alpha) = \frac{1}{2} m_\alpha v_\alpha^2 - \frac{e^2}{4\pi\epsilon_o r}$$

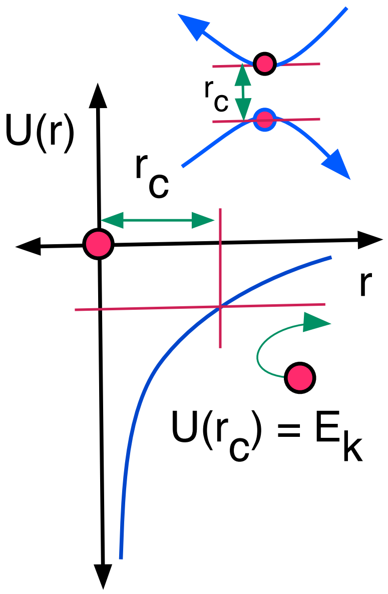

Figure 1.8: The minimum distance of approach r_c between two repelling charged particles.

Their minimum distance of approach r_c (see Fig. 1.8) takes place when $E(r_c, v_\alpha) = 0$ and using the thermal speed $v_{T\alpha} = \sqrt{2k_BT/m_\alpha}$ of the equilibrium plasma we have on average,

$$r_c = \frac{e^2}{4\pi\epsilon_o k_b T}$$

The *coupling parameter* Γ is the ratio between r_c and the average separation r_d between particles provided by the plasma density $r_d \sim n_o^{-1/3}$,

$$\Gamma = \frac{r_c}{r_d} = \frac{e^2 n_o^{1/3}}{4\pi\epsilon_o k_B T} \sim \frac{< E_{el} >}{< E_{th} >}$$

Respectively we have,

$$< E_{el} > \sim \frac{e^2}{4\pi\epsilon_o r_d} \quad \text{and,} \quad < E_{th} > \sim k_B T$$

for the average electrostatic and thermal energies. When $\Gamma = r_c/r_d$ is large, the electric interaction dominates and the kinetic energies are small compared with the electrostatic energy of particles. The relation with the plasma parameter is found by,

$$\Gamma = \frac{e^2 n_o^{1/3}}{4\pi\epsilon_o k_B T} = \frac{1}{4\pi} \times \frac{n_o e^2}{4\pi\epsilon_o k_B T} \times n_o^{1/3} = \frac{1}{4\pi} \times \frac{n_o e^2}{4\pi\epsilon_o k_B T} \times n_o^{-2/3} = \frac{1}{4\pi} \times \frac{1}{[n_o \lambda_D^3]^{2/3}}$$

We might introduce the number $N_D \sim n_o \lambda_D^3$ proportional to the number of charged particles contained into an sphere of radius λ_D and results,

$$\Gamma \sim \frac{1}{4\pi} \frac{1}{(n_o \lambda_D^3)^{2/3}} \sim \frac{1}{4\pi} \frac{1}{N_D^{2/3}}$$

The coupling parameter Γ is large in a *strongly coupled plasma* where $N_D \ll 1$ and the Debye sphere is scarcely populated. In the opposite case of a *weakly coupled* $\Gamma \ll 1$ we have $N_D \gg 1$ and a large number of particles are contained within the Debye sphere.

An alternative way to understand the meaning of the plasma parameter the ratio $|e\phi/k_BT|$ already employed in Eqs. (1.5) and (1.6). Since the average distance between two repelling plasma particles is $r_d \sim n_o^{-1/3}$ and the electric potential $\phi(r_d) = e/(4\pi\epsilon_o r_d)$ we have,

Plasma	n_o	$k_B T$	f_{pe}	λ_{De}	Γ	N_D
Fusion reactor	10^{15}	10^4	3.0×10^{11}	2.4×10^{-3}	1.45×10^{-4}	5.4×10^7
Laser plasmas	10^{20}	10^2	9.0×10^{13}	7.4×10^{-7}	0.67	1.7×10^2
Glow discharge	10^8	2	9.0×10^7	0.1	3.0×10^{-3}	5×10^5
Arc discharge	10^{14}	1	9.0×10^{10}	8.0×10^{-5}	0.67	1.7×10^2
Earth ionosphere	10^6	5×10^{-2}	9.0×10^6	0.2	2.9×10^{-2}	2.0×10^4
Solar corona	10^6	10^2	9.0×10^6	7.4	1.45×10^{-5}	1.7×10^9
Solar atmosphere	10^{14}	1	9.0×10^{10}	7.4×10^{-5}	0.67	1.7×10^2
Interestelar plasma	1	1	9.0×10^3	740	1.45×10^{-5}	1.7×10^9

Table 1.1: Typical values of plasma densities n_o in cm^{-3}, the temperatures $k_B T_e$ are in eV, the plasma frequencies f_{pe} in s^{-1} while the electron Debye lengths λ_{De} are in cm. The plasma parameter Γ is dimensionless and N_D is the number of charges contained into a Debye sphere.

$$\Gamma \sim \frac{e\,\phi}{k_B T} = \frac{e^2}{4\,\pi\,\epsilon_o\,r_d} \times \frac{1}{k_B T} = \frac{1}{4\,\pi} \times \frac{e^2}{\epsilon_o\,k_B T} \times n_o^{1/3} = \frac{1}{4\,\pi} \times \frac{1}{[n_o\,\lambda_D^3]^{2/3}} \sim \frac{1}{4\,\pi} \times \frac{1}{N_D^{2/3}}$$

The amount of charges contained within a sphere of radius λ_D, or equivalently, the value of N_D, has to be high if the approximation previously used to derive the Debye length was correct.

As we see, strongly coupled plasmas are dense and cold while weakly coupled plasmas are more diffuse and warm. The ideal Maxwellian plasmas are weakly coupled and a large number of charged particles are affected by fluctuations with typical lengths over the Debye length.

1.6 Magnetized plasmas

In *magnetized plasmas* the local magnetic field is high enough to alter the trajectories of the charged particles. In the nonrelativistic approximation the charges q_α $(\alpha = e, i)$ in the plasma are accelerated by the Lorentz force,

$$\boldsymbol{F}_\alpha = q_\alpha\,n_\alpha\,(\boldsymbol{E} + \boldsymbol{v}_q \wedge \boldsymbol{B})$$

in the frame of reference where the magnetic field lines of $\boldsymbol{B}$ remains at rest. Note that in a magnetized plasma moving with speed $\boldsymbol{v}_q$ the electric field $\boldsymbol{E} = -\boldsymbol{v}_q \wedge \boldsymbol{B}$ *is not affected* by the Debye screening and is null the frame that moves with the plasma bulk.

The force experienced by the charges in a magnetized plasma is zero in the direction parallel to $\boldsymbol{B}$ while along the perpendicular direction the charges make circular orbits with a *ciclotron frequency* or *girofrequency*,

$$\Omega_\alpha = \frac{q_{\alpha\, B}}{m_\alpha}$$

The *Larmor radius* or *giroradius* of a charged particle α is the ratio between the component of the velocity $\boldsymbol{v}_\perp$ perpendicular to the magnetic file lines and the girofrequency Ω_α,

$$R_{l\alpha} = \frac{v_\perp}{\Omega_\alpha}$$

This magnitude is estimated using l_α where $v_\perp$ the particle thermal speed $V_{T,\alpha} = \sqrt{2k_B T_\alpha / m_\alpha}$ is employed in place of $v_\perp$ and then,

$$l_\alpha = \frac{V_{T\alpha}}{\Omega_\alpha} \quad \text{and therefore,} \quad l_e = \sqrt{\frac{m_e}{m_i}}\, l_{li}$$

Therefore, the plasma is said *magnetized* when $l\alpha$ is comparable with the relevant length scale L and *unmagnetized* otherwise. In accordance to the magnitude of $\boldsymbol{B}$ we found situations where $l_e/L \sim 1$ while $l_i/L \ll 1$ so that *electrons are magnetized* while ions are not. However, when we refer to a *magnetized plasma* we usually mean that both species, ions and electrons are magnetized.

	Definition	**Expression**
Velocities		
Electron thermal	$V_{Te} = \sqrt{8\,k_B T_e/\pi\,m_e}$	$V_{Te} = 6.71 \times 10^7 \sqrt{k_B T_e}$ cm/s
Ion thermal	$V_{Ti} = \sqrt{8\,k_B T_i/\pi\,m_i}$	$V_{Ti} = 1.56 \times 10^6 \sqrt{k_B T_i/A}$ cm/s
Electron with energy E	$V_e = \sqrt{2\,E/m_e}$	$V_e = 5.9 \times 10^7 \sqrt{E}$ cm/s
Ion sound speed	$C_{is} = \sqrt{2\,k_B T_e/m_i}$	$C_{is} = 1.54 \times 10^5 \sqrt{k_B T_e}$ cm/s
Plasma parameters		
Debye length	$\lambda_D = \sqrt{\epsilon_o\,k_B T_e/e^2\,n_e}$	$\lambda_D = 740 \times \sqrt{k_B T_e/n_e}$ cm
Electron plasma frequency	$\omega_{pe} = \sqrt{n_e\,e^2/\epsilon_o\,m_e}$	$f_{pe} = 9.0 \times 10^3 \sqrt{n_e}$ Hz
Ion plasma frequency	$\omega_{pi} = \sqrt{n_i\,e^2/\epsilon_o\,m_i}$	$f_{pi} = 4.9 \times\ A \sqrt{n_i}$ Hz
Larmor radius for electrons	$l_e = V_{Te}/\Omega_e$	$l_e = 2.38 \sqrt{k_B T_e}\,/\,B$ cm
Larmor radius for ions	$l_i = V_{Ti}/\Omega_i$	$l_i = 4.38 \times 10^3\ (\sqrt{k_B T_i/A})\,/\,B$ cm
Plasma parameter	$\Gamma = 1/(4\,\pi\,\lambda_D^2\,n^{2/3})$	$\Gamma = 1.45 \times 10^{-5}\,(n^{1/3}/k_B T_e)$ cm
N$_D$	$N_D = \frac{4\,\pi}{3}\,n\,\lambda_D^3$	$N_D = 1.7 \times 10^9\,(k_B T)^{3/2}/\sqrt{n}$
Collisions		
Mean free path.	$\lambda_{pb} = 1/(\sigma_{pb}\,n_b)$	See section 4.1 in page 26.
Collision frequency	$\nu_{pb} = \sigma_{pb}\,n_b\,V_{pb}$	See section 4.1 in page 26.

Table 1.2: The results are in CGS units except the energies and temperatures ($k_B T_e$, $k_B T_i$) that are in electron volts, A is the atomic number. The collision cross section is σ_{pb} and V_{pb} the relative speed of colliding species.

2

The plasmas in space and in the laboratory.

2.1 The plasma state of condensed matter

The physical parameters introduced before allow us to refine the early definition of the plasma state of matter of page 2. The Debye length λ_D introduced before provides the physical length scale for a plasma, and an upper bound for the plasma time scale $\tau = f_{pe}^{-1}$ is introduced by the electron plasma frequency. The collective plasma response requires of a critical number density of charged particles introduced by the plasma parameter N_D. Additionally, the coupling parameter Γ compares the thermal and electrostatic energies. In Table (1.2) are summarized these previous definitions of the different plasma parameters as well as their shorthand expressions. In first place let us summarize the main characteristics of classical plasmas.

- The plasma is an electrically neutral medium. The average charge density is null over macroscopic volumes with typical sizes larger than λ_D^3. This requires an average equal number of positive and negative densities of charged particles inside a Debye sphere.
- The typical longitudes L considered will be always are larger than the Debye length $L \gg \lambda_D$. Therefore, the characteristic distances L_{sh} for the Debye electric shielding are $L_{sh} \simeq \lambda_D \ll L$ are also smaller $L \gg L_{sh}$.
- The number of electrons (and ions) N_D contained within a sphere of radius λ_D must be large enough to allow the Debye shielding the internal and external low amplitude fluctuations of electromagnetic fields.
- In accordance to the magnitude of the magnetic field, the plasmas are classified as *magnetized* or *unmagnetized*. In magnetized plasmas the Larmor radius R_l of electrons (or ions) is smaller than the characteristic distance $L < R_l$.

The plasmas are frequently produced by the partial ionization of a neutral gas. In accordance to the ionization degree the plasmas are termed as *fully ionized* when the neutral atom densities n_a are negligible compared with the charged particle densities $n_a, n_e \gg n_a$ and *partially ionized* otherwise. In *weakly ionized* plasmas the neutral atom densities $n_a, n_e \ll n_a$ are larger than those of charged particles.

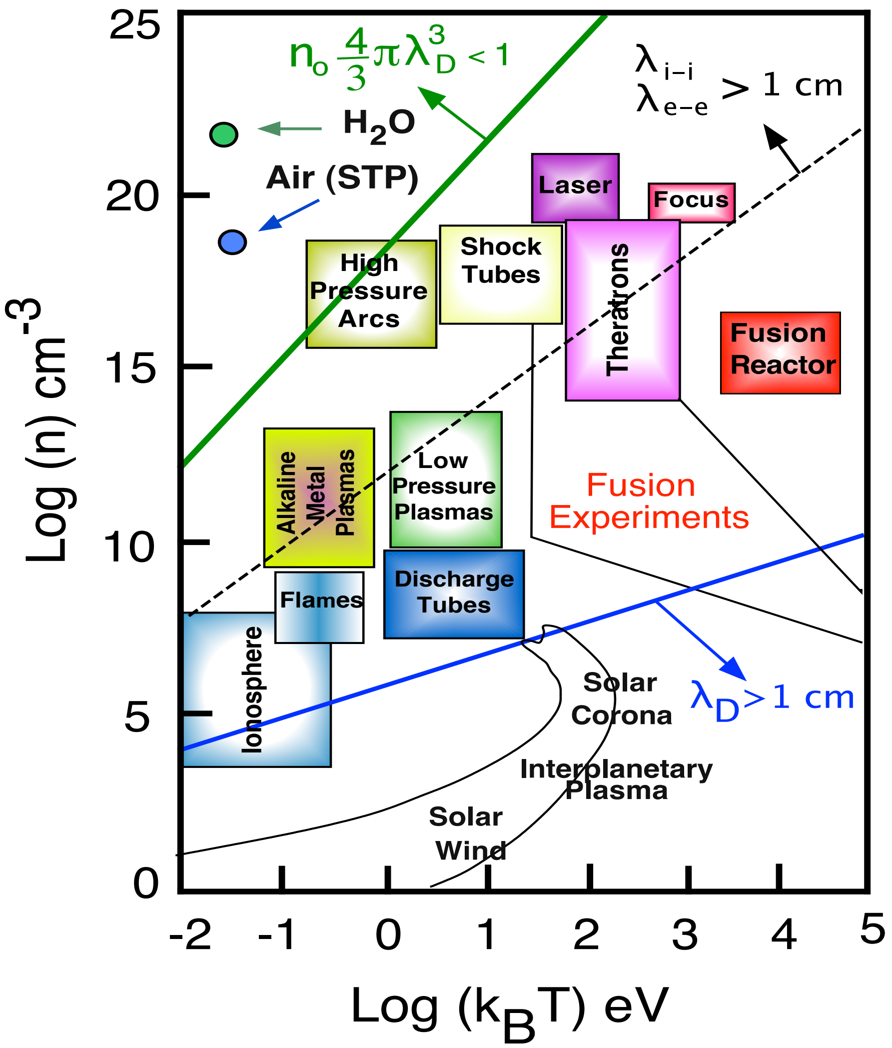

Figure 2.1: The characteristic densities and temperatures of different plasmas in nature and produced in the laboratory.

Since only Coulomb collisions between charged particles are relevant in fully ionized plasmas, the collisional processes with neutral atoms introduce additional features.

- Partially ionized plasmas are said *collisional* when the mean free path $\lambda \ll L$ for the relevant collisional processes are much smaller than the dimensions L of the medium.
- The elastic and inelastic collisions between neutrals and charged particles in collisional plasmas give rise to a large number of physical processes as ionization, light emission, ...etc.

The plasmas can be roughly characterized by its kinetic temperature $k_B T$ and charged particle density density n. In Fig. (2.1) are classified a number of those found in nature and also produced in the laboratory. As we can see, the possible values for the particle densities in this figure covers twenty orders of magnitude (from 1 up to 10^{25} charges by cubic centimeter). The corresponding temperature range is extended along seven orders of magnitude (from 10^{-2} up to 10^5 eV).

In order to grasp the huge extent of these scales it would be enough to introduce in the diagram of Fig. (2.1) the point corresponding to the water at room temperature $n \simeq 2.1 \times 10^{22}$ cm^{-3}, and for the ordinary air; the Loschmidt number $n \simeq 2.7 \times 10^{19}$ cm^{-3} at STP conditions. The particle densities of air and liquid water only differ by a factor 10^3. Between the ordinary water and the density of a white dwarf star this factor raises up to 10^{15}, much shorter than the plasma density range of Fig. (2.1).

2.2 Plasmas in astrophysics

The cold $k_B T \cong 10^{-2} - 10{-}1$ eV *interestellar* plasma has a very low density of 10^{-5} cm^{-3} and does not appear in Fig. (2.1). This concentration as low as 0.1 charged particle by cubic meter leads Debye lengths in the order of 8 meters, that are used to scale the plasma equations. Thus, because of the huge distances involved the equations of magnetohidrodynamics could still be used to describe the plasma transport over galactic distances.

Figure 2.2: The Sun chromosphere observed during an eclipse

The plasma inside the Sun core where thermonuclear reactions take place has an estimated temperature about $k_B T \cong 10^5$ eV and the densities are $n \sim 10^{25}$. At the solar corona the temperature decreases down to $k_B T \cong 10 - 10^2$ eV and the density $n \sim 10^5$ decreases about 15 orders of magnitude over the surface of the Sun.

The *stellar atmospheres* are constituted by a gases hot enough to be fully ionized and the plasma at the Sun chromosphere could be observed during solar eclipses as in Fig. (2.2). This plasma is later accelerated by different physical mechanisms to form the *solar flares* and the *solar wind* that reach the Earth ionosphere following the interplanetary magnetic field lines [3].

The *solar wind* is constituted by an stream of charged and energetic particles coming from the the sun. The typical solar wind parameter are $n = 3 - 20$ cm^{-3}, $k_B T_i < 50$ eV and $k_B T_e \leq 100$ eV. The drift velocities of these charged particles close to the Earth are about 300-800 Km s^{-1}. This flow of charged particles reaches the Earth orbit and interacts with the geomagnetic field forming a complex structure denominated *magnetosphere* that protects the Earth surface from these high energy particle jets. The average properties of the *interplanetary plasma* in our solar system *solar corona* and *solar wind* are also in Fig. (2.1) [3].

2.3 Geophysical plasmas

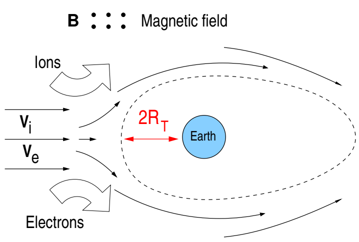

Figure 2.3: The deviation of charged particles by the geomagnetic field.

The interplanetary plasma and the solar wind interact with the geomagnetic field to for a complex structure. The geomagnetic field is a centered magnetic dipole $\sim 1/r^3$ up to distances about two Earth radii ($R_T = 6.371$ Km) inclined 11^o with respect to the planet axis. For distances over $2\,R_T$ interacts with the solar wind and gives raise to a complex structure denominated *magnetosphere* [3, 5]

The basic physical mechanism is outlined in Fig. (2.3). The Earth magnetic field decreases with the distance in the direction towards the dayside where a stream of particles comes from the sun. The Lorentz force resulting from the perpendicular geomagnetic field deviates the flux charged particles around the Earth. The weak local magnetic field is in turn affected by this current of charged particles resulting a complex structure of magnetic field and electric currents around the Earth. Within the magnetosphere are located the Van Allen belts around the Earth that are constituted by energetic particles trapped by the geomagnetic field [3, 5]

At the North and south poles, the Earth magnetic field is connected with the Sun magnetic field lines. The particles moving with parallel velocity to the field lines do not experience a deflecting force and precipitate towards the Earth surface. The stream of charged particles is aligned with the local geomagnetic field and this is the origin of polar auroras which are strongly influenced by the solar activity. The existence of magnetospheres around the planets is a common feature in the solar system that prevents the energetic particles from reach most of the surface of planets [3, 6].

All the planets in the solar system have a ionosphere connecting the high altitude atmosphere with the outer space. They have different characteristic in accordance to the particular

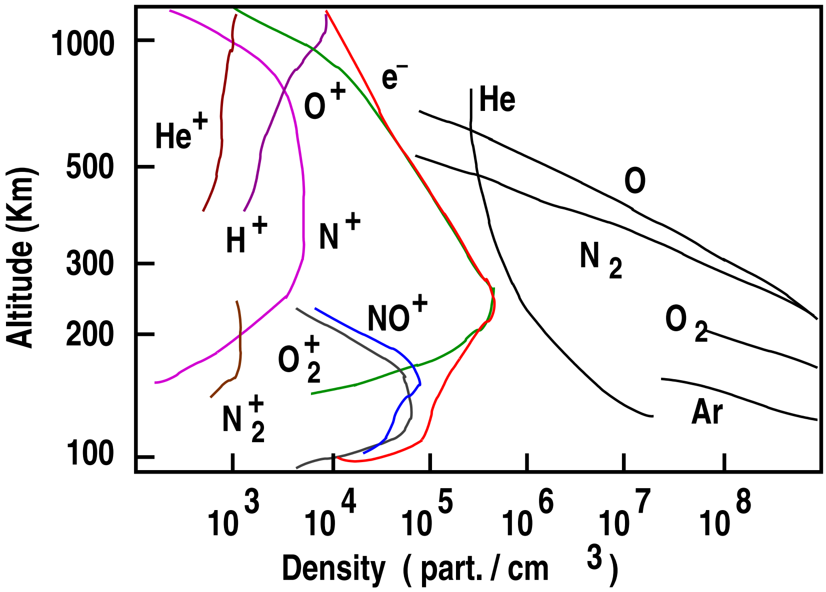

Figure 2.4: The altitude dependent chemical composition of the Earth ionosphere from Ref. [16].

properties of the planetary magnetic field and the chemical composition of its atmosphere. The *Earth's ionosphere* is a weakly ionized plasma present between 50 and 1000 Km of altitude below the magnetosphere ver the neutral atmosphere. The altitude dependent particle density relies on the sun activity and also on the night/day cycle. The orbiting spacecrafts move immersed into this cold ($k_B T \leq 0.1$ eV and tenuous plasma with densities of $n = 10^3 - 10^7$ cm^{-3} and a altitude dependent chemical composition as shown in Fig. (2.4) [6, 7, 16].

In Table (2.1) are the main properties of ionospheric plasma for different altitudes. Here $n_{e,i}$ are respectively the electron and ion densities, λ_D the Debye length, and the average mass of the ion is $\bar{m}_i$. The temperatures are respectively $T_{e,i}$ and the collisional mean free paths $\lambda_{e,i}$. The typical orbital speed is V_o, the local gas pressure P_a and T_a the gas temperature [16]

2.4 Laboratory plasmas

The plasmas produced in the laboratory or for technological applications are also appear in the scheme of Fig. (2.1) covering from cold discharge plasmas up to the experiments in controlled fusion.

The *electric discharges in gases* are the most traditional field of plasma physics investigated by I. Langmuir, Tonks and their co-workers since 1920. In fact, the nobel laureate Irvin Langmuir coined the term *plasma* in relation to the peculiar state of a partially ionized gas. Their original objective was to develop for General Electric Co. electric valves that could withstand large electric currents. However, when these valves were electrically connected low pressure *glow discharges* triggered inside. The low pressure inert gases become partially ionized, weakly ionized plasmas.

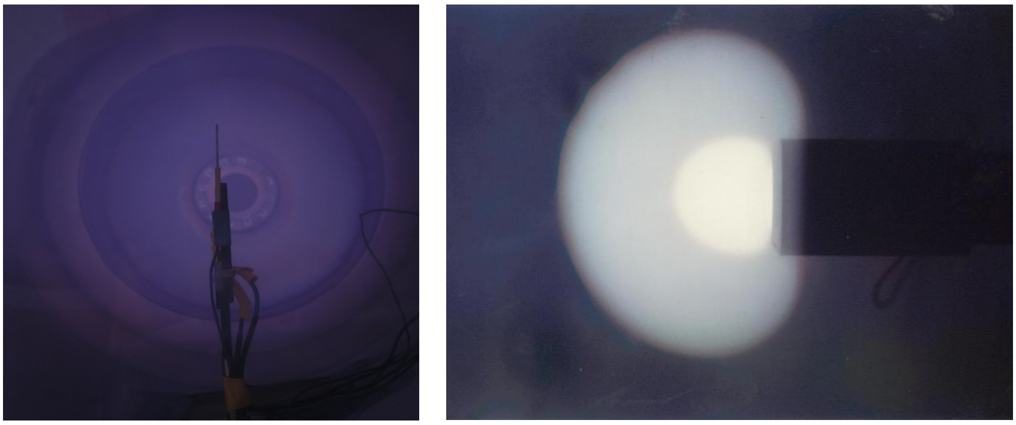

Figure 2.5: A laboratory experiment with an argon electric glow discharge (left) and an stable structure of different plasmas separated by double layers (right).

Two examples of a low pressure argon discharge plasmas are in Fig. (2.5). The typical low pressure discharges are weakly ionized plasmas with densities between 10^6 - 10^{14} cm^{-3} and temperatures of $k_B T \cong 0.1 - 10$ eV in the scheme of Fig. (2.1). In our everyday life these electric discharges are widely used in a large number of practical applications, as in metal arc welding, fluorescent lamps, ...etc.

The relatively cold plasmas ($k_B T_e$ = 0.05-0.5 eV) of high pressure arc discharges are employed in metal welding and are dense quite dense; up to 10^{20}. On the opposite limits are *flames* which in most cases cannot be strictly considered as a plasma because of their low ionization degree.

The physics of the discharge plasmas and its applications constitutes a branch of Plasma Physics and Refs. [10] and [13] are two comprehensive books on this subject.

The *plasma thrusters* are employed for space propulsion and they impart momentum to an spacecraft by means an accelerated plasma stream where the ions are accelerated along a fixed direction. Contrary to classical chemical thrusters, may be continuously working and the specific impulse of these devices is quite better than chemical thrusters. More than 700 models have been flown in particular for deep space exploration and orbit station keeping. The plasmas of these devices are produced by low pressure electric discharges with densities up to 10^{14} and temperatures in the range 1-2 eV. The basic Plasma Physics involved in space propulsion and new developments are discussed in Refs. [14, 15].

The *themonuclear controlled fusion* is the more promising application of plasma physics since 1952. The controlled thermonuclear reaction of deuterium and/or tritium atoms and is intended in order to produce waste amounts of energy. The reaction cross sections are appreciable for energies of reacting particles over 5 KeV. This would require to produce an stable plasma with temperatures in the range of 10 KeV. The plasma heating and confinement of such hot plasma still remains a unsolved problem and active field of research. We can see in Fig. (2.1) the plasma densities reached today in these experiments are around $10^{10} - 10^{13}$ cm $^{-3}$ with the temperatures $k_B T_e \cong 10^2 - 10^3$ eV.

The design and operation of the future plasma fusion reactor is a scientific and technological

Altitude	(Km)	**150**	**200**	**400**	**800**	**1200**
V_o	m/s	7.83×10^3	7.80×10^3	7.68×10^3	7.47×10^3	7.26×10^3
$N_{i,e}$	cm^{-3}	3.0×10^5	4.0×10^5	1.0×10^6	1.0×10^5	1.0×10^4
k_BT_i	K	700	1100	1600	2200	2600
k_BT_e	K	1000	2000	2800	3000	3000
$\bar{m}_i$	uma	28	24	20	14	10
λ_D	cm	0.40	0.49	0.37	1.20	3.78
$\lambda_{e,i}$	cm	5.0×10^5	1.0×10^5	1.0×10^5	1.0×10^6	1.0×10^7
P_a	Torr	3.75×10^3	7.5×10^{-10}	1.5×10^{-11}	-	-
T_a	K	635	859	993	-	-

Table 2.1: The characteristics of ionospheric plasmas for different altitudes from Ref. [16]. The ion k_BT_i and electron k_BT_e temperatures are in Kelvin degrees, the average ion mass $\bar{m}_i$ is in atomic mass units and the local pressure in Torrs.

challenge that requires intense international collaboration. Such a reactor must work with plasmas where $n = 10^{13} - 10^{16}$ cm $^{-3}$ and $k_BT \cong$ 0.5-1.0 $\times 10^4$ eV.

3

Bibliography, texbooks and references

There are excellent textbooks on the Physics of Plasmas and these notes are not intended to replace them. They serve as a support for the lectures and therefore, it seems advisable to provide a complementary bibliography for the reader.

3.1 Textbooks

The following books are general texts of Plasma Physics. The first one is very popular at elementary level while the others contain chapters with more advanced topics.

- Introduction to plasma physics and controlled fusion. Vol 1: Plasma physics. 2nd ed. F.F. Chen. Plenum Press New York, USA (1984).
- Introduction to plasma physics. R.J. Goldston and P.H. Rutherford. Institute of Physics Bristol, UK (1995).
- Physique de Plasmas. Jean-Marcel Rax. Dundod, Paris, France (2007).

The following references are introductory books to Plasma Physics with an special emphasis on astrophysical and space problems. The first is a comprehensive collection of articles covering many fields of interest and the second is a textbook on the Physics of Space Plasmas. Finally, the last one is of elementary level and includes sections with applications of fluid dynamics in astrophysics and its connections with plasma physics.

- Introduction to Space Physics, edited by M.G. Kivelson and C.T. Russel. Cambridge University Press, New York, (1995).
- Physics of Space Plasmas, an Introduction, GK Parks. Addison Wesley, Redwood City CA. USA, (1991).
- Physics of Fluids and Plasmas. An Introduction for Astrophysicists. A. Rai Choudhuri. Cambridge University Press, Cambridge U.K. (1998).

3.2 Bibliography on space plasmas

These references cover two particular topics of interest in this course. The first is a through reference regarding the structure and properties of the Earth ionosphere. The orbiting spacecrafts and satellites move into and also interact with this particular medium, these issues are discussed in the two additional references.

- The Earth's Ionosphere: Plasma Physics and Electrodynamics. M.C. Kelley. International Geophysical Series, Academic Press, San Diego CA, USA (1989).
- A review of plasma Interactions with spacecraft in low Earth orbit. D. Hastings, *J Geophys. Res.* **79**, (A13), 1871-1884, (1986).
- Spacecraft environment interactions. S.D. Hastings. Cambridge University Press, Cambridge, UK (2004).

3.3 References on gas discharge physics

The following references on the physics of electric discharges are indispensable to calculate numeric estimates of transport coefficients, ionization rates, ... etc.

- Basic data of plasma physics: The fundamental data on electrical discharge in gases. S.C. Brown. American Vacuum Society Classics American Institute of Physics, New York, USA (1994).
- Gas discharge physics. Y.P. Raizer. Springer-Verlag, Berlin, Germany (1991).

3.4 Additional material

One can be found easily in servers across the internet lots of information regarding topics covered in this course. Some of them also include free useful computer codes codes. This is not an exhaustive list but provides some reference web pages.

- **On the Physics of Plasmas:**

  http://plasma-gate.weizmann.ac.il/directories/plasma-on-the-internet/

  This web page contains links to practically all large groups of Plasma Physics around the world. It covers software, references, conferences, ...etc and remains continuously updated.

- **Space Physics Groups at NASA:**

  http://xd12srv1.nsstc.nasa.gov/ssl/PAD/sppb/

  NASA has a wide range of activities in physics from space and a full division dedicated to Plasma Physics issues.

- **Naval Research Laboratory:**

  http://wwwppd.nrl.navy.mil

  The naval research laboratory in the U.S. has a division of plasma physics which publishes a free and well-known *NRL plasma physics formulary* of commonly used formulas.

- **Plasma Simulation Group. Berkeley University:**

  http://ptsg.eecs.berkeley.edu

  This group dedicated to the development of PIC codes to simulate plasmas and gaseous discharges. The codes These codes have a good graphical interface are open and can be downloaded from this server for free.

4 The elementary processes and the plasma equilibrium

In ordinary fluids the energy and momentum is transported by the short range molecular collisions of the neutral particles. Their properties determine the transport coefficients of the neutral gas, as its viscosity or thermal conductivity. These atomic and molecular encounters also are the relaxation mechanism that brings the system from a perturbed state back into a new equilibrium.

Most plasmas (see Fig. 2.1) of interest in space are weakly coupled, the average kinetic energy of particles dominates and is much larger than their electrostatic energies. These plasmas are constituted by electrons, atoms, molecules and eventually charged dust grains, in a dynamic equilibrium where a large number of collisional processes between the plasma particles take place. As for ordinary fluids, the collisions at atomic and molecular level also determine both, the transport properties and the relaxation of perturbations towards the equilibrium state.

The atomic and molecular encounters determine the response of fluids and plasmas to external perturbations. They also couple the motions of the different particle species that contribute to the transport properties. Additionally, the long range Coulomb forces in plasmas are involved in collisions between charged and neutral species.

The physical and chemical properties of plasmas in nature are determined by the characteristics of the elementary processes at atomic and molecular level, and the number of possible collisional processes is huge. In Tables (4.3) and (4.1) are shown the more relevant involving the ions, electrons and neutral atoms or molecules. The chemical nature of the parent neutral gas (or gas mixture) influences the plasma properties. While most ions are produced by electron impact in noble gases as Argon the formation of negative ions is important in electronegative gases as is the molecular oxygen O_2.

The degree of ionization in the plasma also determines the relevant molecular processes. In weakly ionized plasmas, the concentration of charged particles n_e and n_i are much lower than the neutral atom background density $n_a \gg n_e, n_i$; the ratio n_e/n_a could be as low as $1/10^5$. Therefore, the collisions between charged particles and neutrals dominate. On the contrary, in fully ionized plasmas the long range Coulomb collisions between charged particles are the relevant collisional processes.

Not all possible of atomic collisions are equal likely and the relevance of a particular molecular process introduces additional length and times scales characterized by its *mean free path* and *collision frequency*. In this section are introduced some simple concepts from kinetic theory in order to relate the properties of atomic and molecular collisions with the transport properties of low density plasmas. In the following we will restrict ourselves to *binary* collisions that involve two particles. These are dominant in weakly coupled plasmas while those with more than two particles are important in denser strongly coupled plasmas. This connection between the transport properties and the properties of molecular and and atomic collisions is throughly discussed in the classical Refs. [17] and [18] and a modern approach is found in Ref. [19].

4.1 The collision cross section

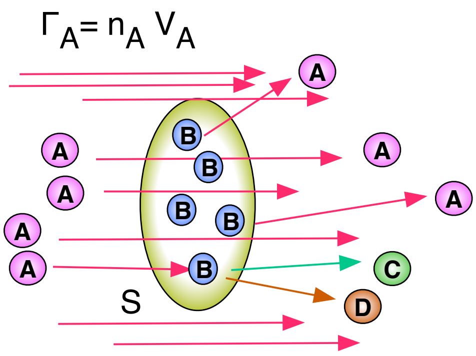

Figure 4.1: The one dimensional stream of particles A across the surface S with particles B.

The classical concept of *collision cross section* could be traced back to the early atomic models of Thomson and Rutherford and considers the typical velocity of particles v large enough so that their quantum wavelengths $\lambda = h/m\,v$ are negligible. In this classical picture the particles are represented by spherically symmetric centers of force and the quantum effects as well as its internal structure are neglected.

The basic concept may be introduced using the scheme of Fig. (4.1). The flux $\Gamma_A = n_A\,V_A$ of monoenergetic incident particles pass through the surface S and collide with the B target particles. The particles A and B only react or are scattered when reaching a minimum distance R_o or -equivalently- when lie within the equivalent surface $\sigma_o = \pi R_o^2$. The number of such collision events Q_{AB} produced by a single molecule B by time unit is,

$$\frac{dQ_{AB}}{dt} = \dot{Q}_{AB} = \sigma_o \times \Gamma_A = \sigma_o \times (n_a\,V_A) \tag{4.1}$$

representing the number of A particles that cross σ_o by time unit. Thus, the *total cross section* σ_o may be defined as the ratio,

$$\sigma_o = \frac{\dot{Q}_{AB}}{\Gamma_A} = \frac{\dot{Q}_{AB}}{n_a V_A} \tag{4.2}$$

Next, the number q_{AB} of collisions by volume and time units is obtained from by multiplying Eq. (4.1) by the number density n_B of particles,

$$\frac{d\,q_{AB}}{dt} = n_B\,\dot{Q}_{AB} = \sigma_o\,n_b\,n_a\,V_A$$

When the particles A are lost by the reaction $A + B \rightarrow C + D$ the rate $\dot{n}_A = -\dot{q}_{AB}$ and,

$$\frac{dn_A}{dt} = -\sigma_o\,n_A\,n_B\,V_A < 0 \quad \text{while for the } C \text{ and } D \text{ particles,} \quad \dot{n}_C = \dot{n_D} = -\dot{n}_A > 0$$

Therefore, we obtain a differential equation for n_A that can be integrated in time,

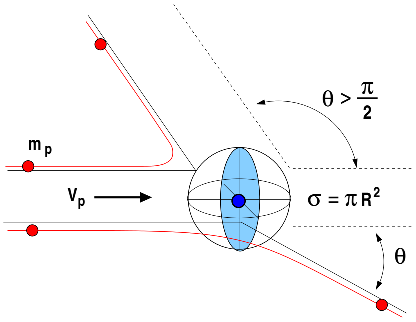

Figure 4.2: Dispersed particles under large $\theta > \pi/2$ and small $\theta < \pi/2$ scattering angles.

$$\frac{dn_A}{n_A} = -(\sigma_o \, n_B \, V_A) \, dt \quad \text{which gives,} \quad n_A(t) = n_{Ao} \, e^{-\nu \, t} > 0$$

where,

$$\nu = \sigma_o \, n_B \, V_A$$

is the *collision frequency*. This magnitude represents the number of collisions of a given process by unit time. We may also introduce the length $\nu = V_A/\lambda$ which gives *collision mean free path*,

$$\lambda = 1/(\sigma_o \, n_B)$$

representing the average length that the A particle travels between two successive collisions among the background of particles n_B. Alternatively, using $dx_A = V_A \, dt$ we also obtain,

$$n_A(x) = n_{Ao} \, e^{-x/\lambda}$$

The equations for $n_A(x)$ and $n_A(t)$ respectively represents the attenuation in the number of particles with the beam depth x, and the decay in number with time. The collision cross section is involved in λ and ν and measures the characteristic time and length.

The cross section $\sigma_o \sim \pi \, R_o^2$ essentially measures the extent of the region with average radius R_o where A and B interact. Note that in addition to the reactions the collisions also scatter the particles along large $\theta > \pi/2$ or small $\theta < \pi/2$ deflection angles as in Fig.(4.2). For two hard spheres with radius d_A and d_B the cross section is,

$$\sigma_o = \pi R_o^2 \qquad \text{with,} \qquad R_o = \frac{1}{2} \, (d_A + d_B)$$

When a particles experience different kinds of collisions with cross sections $\sigma_{tot} = \sigma_1 + \sigma_2 + \ldots$ the total collision frequency in above equation becomes $\nu_{tot} = \nu_1 + \nu_2 + \ldots$.

4.2 The total and differential cross sections.

In the general, the cross section essentially depends on the relative velocity $|\boldsymbol{v}_A - \boldsymbol{v}_B| = |\boldsymbol{g}| = g$ of the colliding species and therefore the could no be considered as a constant value. Equivalently, on the kinetic energy E of the incoming particle in the frame where the target remains at rest (laboratory frame). The incident particles also could be scattered along large or small scattering angles θ as in Fig. (4.2) or –because of the internal properties of colliding particles– along a privileged direction. This situation is depicted in the schemes of (4.3) and (4.4).

As a first step we generalize the Eq. (4.1) by considering the number $\Delta \dot{Q}_{AB}$ of collision events by time unit between the A particles within the interval of velocity $\Delta \boldsymbol{v}_A$ as,

$$\frac{\Delta \dot{Q}_{AB}}{\Delta \boldsymbol{v}_A} \sim \frac{d\dot{Q}_{AB}}{d\boldsymbol{v}_A}$$

Therefore, for a particular collisional process, the energy dependent *total cross section* is defined as,

$$d\dot{Q}_{AB} = n_A\, \sigma_T(|\boldsymbol{v}_A - \boldsymbol{v}_B|)\, |\boldsymbol{v}_A - \boldsymbol{v}_B|\, d\boldsymbol{v}_A \tag{4.3}$$

As in the Eq. (4.1) $d\dot{Q}_{AB}$ represents the number of collision events produced by a target molecule B for velocities of the incoming A particles between $\boldsymbol{v}_A$ and $\boldsymbol{v}_A + d\boldsymbol{v}_A$. The total cross section may be also introduced by generalizing the Eq. (4.2) as the ratio,

$$\sigma_T(|\boldsymbol{v}_A - \boldsymbol{v}_B|) = \frac{(d\dot{Q}_{AB}/d\boldsymbol{v}_A)}{\Gamma_A} = \frac{(d\dot{Q}_{AB}/d\boldsymbol{v}_A)}{n_A\, |\boldsymbol{v}_A - \boldsymbol{v}_B|}$$

The total cross section $\sigma_T(|\boldsymbol{v}_A - \boldsymbol{v}_B|)$ characterizes the energy dependent scattering of A particles irrespective of their dispersion angles.

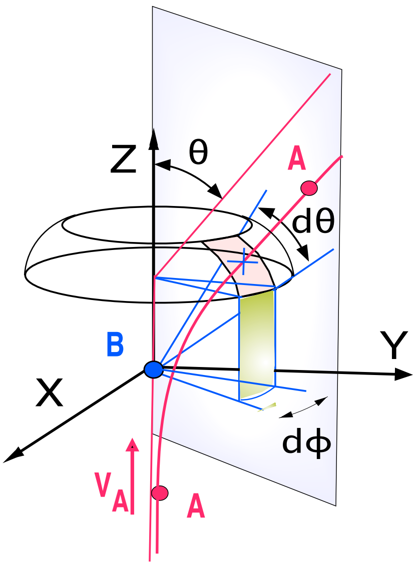

Figure 4.3: The scheme of an atomic collision.

However, in accordance to their internal states, the incident particle A could be scattered over a preferred direction along the angle θ. The *differential cross section* $\sigma_{AB}(g, \theta)$ accounts for this *anisotropic* scattering as indicated in Fig. (4.3).

The incident particle moves along the Z axis and is scattered by the particle at rest located at the origin. The dispersion is independent of the angle ϕ [1] and the trajectory of the incoming particle and the Z axis are contained in the plane indicated in Fig. (4.3). Again, as in Eq. (4.1) the number collision events Q_{AB} by time unit of A particles emerging within the solid angle $d\Omega = \sin\,\theta\, d\theta\, d\phi$,

$$d\dot{Q}_{AB}(\theta, g) = n_A\, \sigma_{AB}(g, \theta)\, |\boldsymbol{v}_A - \boldsymbol{v}_B|\, \sin\,\theta\, d\theta\, d\phi \tag{4.4}$$

Again, the differential cross section could be also introduced using the Eq. (4.2) as the ratio,

$$\sigma_{AB}(|\boldsymbol{v}_A - \boldsymbol{v}_B|) = \frac{(d\dot{Q}_{AB}/d\boldsymbol{v}_A d\Omega)}{\Gamma_A} = \frac{(d\dot{Q}_{AB}/d\boldsymbol{v}_A d\Omega)}{n_A\, |\boldsymbol{v}_A - \boldsymbol{v}_B|}$$

This represents the ration between the number of particles by time unit that appear over the solid angle $d\Omega$ after collide over the flux of incoming A particles.

The integration over the angles $d\phi$ and $d\phi$ of Fig. (4.3) recovers the total cross section,

$$d\sigma_T(|\boldsymbol{v}_A - \boldsymbol{v}_B|) = \sigma_{AB}(\theta, |\boldsymbol{v}_A - \boldsymbol{v}_B|)\, d\Omega$$

therefore,

$$\sigma_T(|\boldsymbol{v}_A - \boldsymbol{v}_B|) = \int_0^{2\pi} \int_\pi^0 \sigma_{AB}(\theta, |\boldsymbol{v}_A - \boldsymbol{v}_B|)\, \sin\,\theta\, d\theta\, d\phi$$

and we obtain the Eq. (4.3),

[1] The collisions may also depend on ϕ of Fig. (4.3) and the cross section would be as $\sigma(E, \theta, \phi)$, but this situation is caused by the existence of internal states in the colliding molecules, however is unusual in atomic

$$\sigma_T(|\boldsymbol{v}_A - \boldsymbol{v}_B|) = 2\pi \int_0^{\pi} \sigma_{AB}(|\boldsymbol{v}_A - \boldsymbol{v}_B|, \theta) \, \sin\theta \, d\theta$$

The values for the cross section are essentially determined in experiments where are analyzed the dispersion of an incident particle beam by a target material [2]. Additionally, the values for $\sigma_{AB}(\theta, |\boldsymbol{v}_A - \boldsymbol{v}_B|)$ could be theoretically calculated by means of physical models that predicts the dispersion angles of particles observed in the experiments.

In Figs. (4.6), (4.5) and (4.10) are some useful experimental values for the total cross section for the collisions of interest in laboratory plasmas. These are discussed in [10] and [13] in the context of the physics of electric discharges. The differential cross sections for elastic collisions between low energy electrons and neutral Argon atoms are in Fig. (4.7). Finally, the differential cross sections in relation with transport properties in plasmas are also discussed in Refs. [20, 21].

4.3 Cross section and impact parameter

The concepts of *impact parameter* and *cross section* are closely related and useful in atom and molecular collision experiments. For simplicity in the following we will consider the elastic dispersion of A particles by the B targets, but similar arguments apply to reactive collisions.

In the classical experiments of particle scattering, the measurements essentially relate the so called *impact parameter* $b(\theta, E)$ and the energy E of the incident particle and its dispersion angle θ. This situation is depicted scheme of Fig. (4.4) in the frame where the target particle B remains at rest. We consider the symmetry around the angle ϕ and the incoming particle A moves again with relative speed $\boldsymbol{g} = \boldsymbol{v}_A - \boldsymbol{v}_B$. After the collision event, the particle A is scattered along the angle θ with respect of its initial direction.

The number of incoming particles by time unit entering into the dashed annular surface $\delta S = b\, db\, d\phi$ of Fig. (4.4) is,

$$\left(\frac{dn_A}{dt}\right)_{in} = n_A\, |\boldsymbol{g}|\, \delta S = n_A\, |\boldsymbol{g}|\, (b\, db\, d\phi)$$

where b is denominated the *impact parameter*. These particles are found after the encounter at the distance r from the dispersion center B within the spherical sector $2\pi\, r\, sin\,\theta\, d\theta$.

According to Eq. (4.4) the number of A particles emerging from the collision within the solid angle $d\Omega = \sin\theta\, d\theta\, d\phi$ may be expressed as,

$$\left(\frac{dn_A}{dt}\right)_{out} = n_A\, |\boldsymbol{g}|\, \sigma_{AB}(\theta, g) \sin\theta\, d\theta\, d\phi$$

Here, the differential cross section is $\sigma_{AB}(g, \theta)$ and is adjusted to give,

$$\left(\frac{dn_A}{dt}\right)_{in} = \left(\frac{dn_p}{dt}\right)_{out} \tag{4.5}$$

then,

and molecular encounters in gases.

[2] In the next section is discussed the useful Eq. (4.7) relating the cross section with the impact parameter.

$$(n_{AB}\,|\boldsymbol{g}|)\,b\,db\,d\phi = (n_{AB}\,|\boldsymbol{g}|)\,\sigma_{AB}(g,\theta)\,\sin\theta\,d\theta\,d\phi \tag{4.6}$$

and we finally obtain the relation between the differential cross section and the impact parameter,

$$\sigma_{AB}(\theta,g) = \frac{b}{\sin\theta}\left|\frac{db}{d\theta}\right| \tag{4.7}$$

Therefore the cross section $\sigma_{AB}(\theta,g)$ measures the variation of in the flux $\Gamma = n_A\,|\boldsymbol{g}|$ of A particles in the collision along the scattering direction defined by the angle θ. The absolute value is introduced because $b(E,\theta)$ is usually a decreasing function of θ, the particles with large impact parameter b are scattered along smaller angles θ.

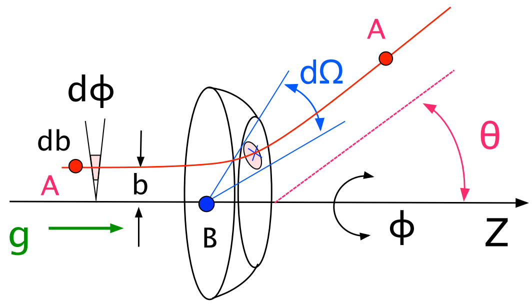

Figure 4.4: The A particle with impact parameter b collides with relative velocity $\boldsymbol{g} = \boldsymbol{v}_A - \boldsymbol{v}_B$ and is scattered along the direction θ.

The theoretical models for molecular collisions provide expressions for $b(E,\theta)$ that can be compared with the results of the experiments using Eq. (4.7). These concepts may be extended to reactive encounter. In this case, the particle found along the line defined by θ is the result of the reaction $A + B$ and the Eqs. (4.5) and (4.6) the number of molecular reactions.

4.4 The atomic collisions in plasmas

In plasmas electrons and charged particles are not bounded moving freely within the plasma bulk. The number of different collisional processes in the plasma is huge and scale with the number of particles involved. The more relevant processes for electrons are in Table (4.1) and for ions and neutral atoms in Table (4.3). All collisional processes could be roughly categorized [14] as;

- *Elastic*: The total kinetic energy of colliding particles is conserved and also retain their charges and initial internal states.
- *Inelastic*: A fraction of kinetic energy is transferred to alter the initial internal state of one (or both) colliding particles. Also to produce an additional particle, as in ionizing collisions.
- *Superelastic*: A collision where potential energy is transformed into kinetic energy so that the total kinetic energy of colliding object is greater after the collision than before[3].
- *Radiative*: When a fraction of the kinetic energy is radiated in any range of the electromagnetic spectrum.
- *Charge exchange*: The electric charge state of colliding particles is interchanged. An electric charge is transferred from one to other.

[3] This occurs for example in the electron ion recombination.

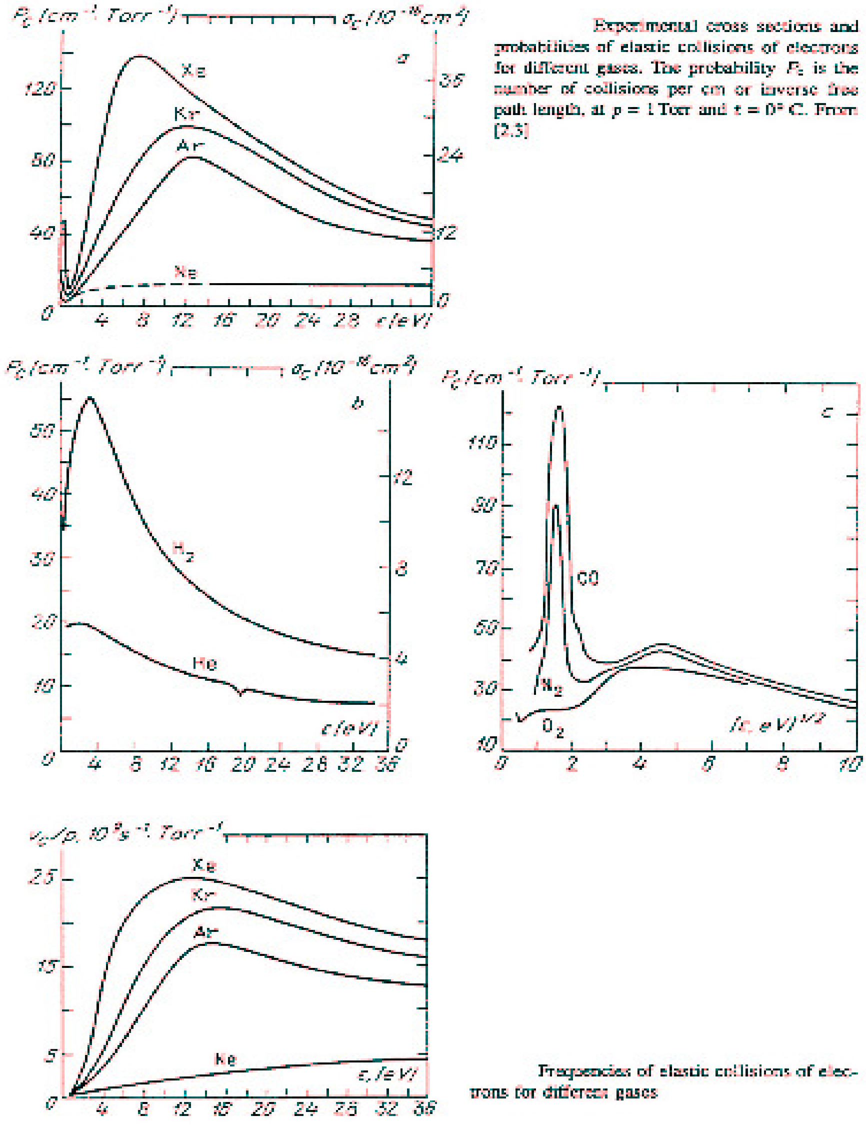

Figure 4.5: Experimental data of the elastic cross sections and collision probabilities between electrons and neutrals for different gases from Ref. [10].

The detailed description of each atomic collision depends of the energy of incident particles and their internal states. Our objective is not to review the elementary processes in detail but we will briefly examine their more relevant features for the low energy range of our interest. For more details on the theoretical models for cross sections end their experimental data the reader is referred to the literature on this subject. The Refs. [10], [11] and [12] discuss in detail the kinetic of charged particles and plasma chemistry.

4.4.1 The electron collisions with neutrals

Electrons are the more mobile particles in a plasma and when the gas is *partially* or *weakly ionized*, the collisions between electrons and neutral atoms are dominant. Collisions with neutrals require the close approach of colliding pand therefore are of short range. In weakly ionized plasmas these cross sections are the major contribution to the plasma transport coefficients.

4.4.1.1 The elastic collisions

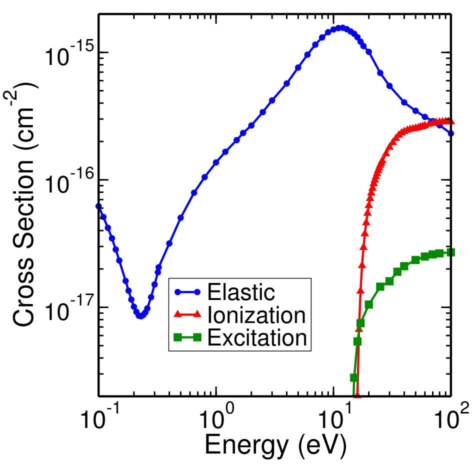

Figure 4.6: The total cross sections of Argon for elastic and inelastic collisions between electron and neutral atoms.

In these collisions there is a negligible exchange (in the order of $\delta = (2m_e/m_a)$ of kinetic energy between the electron and the neutral atom. Then, the energy of colliding particles is practically conserved without changes in the internal states of the neutral atom,

$$e^- + A \rightarrow e^- + A$$

The total elastic cross sections for low electron energies in are Fig. (4.5) and exhibit strong variations and an important angular dependence for the electron scattering as shows the Fig. (4.7).

The electron energy energy profiles (see Fig. 4.5) differ within an order of magnitude according to the chemical nature of molecular (N_2, CO, O_2) and atomic (Ar, Kr, Xe) gases. The values are about $\sigma(E) \sim 5.0 - 35.0 \times 10^{-16}$ cm^{-2} for noble gases.

The elastic collisions take place for any energy of the incoming electron and the cross section decreases for large energies. The peak in the cross section for very low energies correspond to a quantum mechanical effect denominated *Ramssauer effect*, which could be appreciated for Argon at low electron energies in Fig. (4.6).

This growth of the cross section takes place when the characteristic size of the atom ($\sim 10^{-8}$ cm) is in the order of the electron wavelength $\lambda_e = h/mv_e$. In this case the electron wave function interacts with those of electrons at the external shells of the atom. On practical grounds the Ramssauer effect is negligible in most plasmas because the typical average electron energy leads a negligible number of low energy electrons.

4.4.1.2 Inelastic collisions

In the *inelastic collisions* a fraction of the initial electron kinetic energy is transferred and produces changes in the internal state of the target particle. In this category are included

Electron collisions with atoms and molecules			
Scheme		**Process**	**Macroscopic effect**
1	$e^- + A^+ \rightarrow e^- + A^+$	Elastic Coulomb collision between electron and ions	Transport and energy transfer in highly ionized plasmas
2	$e^- + A \rightarrow e^- + A$	Elastic collision between electron and neutral atoms	Electron transport and diffusion. Electron mobility
3	$e^- + A \rightarrow e^- + A^*$	Excitation of neutrals by electron impact	Multiplication of metastable neutral atoms
4	$e^- + AB \rightarrow e^- + AB^*_\nu$	Vibrational excitation	Energy tranfer to vibrational levels of molecules
5	$e^- + A \rightarrow 2e^- + A^+$	Electron impact ionization	Multiplication of ion and electrons from the ground state.
6	$e^- + A^* \rightarrow 2e^- + A^+$	Multistep ionization	Ionization of neutral atoms from an excited state
7	$e^- + AB \rightarrow A + B^-$	Dissociative attachement	Production of negative ions in molecular gases
8	$e^- + A + B \rightarrow AB^-$	Three body attachment	Production of negative ions in electronegative gases
9	$e^- + AB \rightarrow 2e^- + A + B^+$	Dissociative ionization	Production atomic ions in electronegative gases
10	$e^- + AB \rightarrow e + A + B$	Molecule dissociation by electron impact	Production of neutral atoms in molecular gases
11	$e^- + A^* \rightarrow e^- + A$	De-excitation of neutrals (quenching)	Destruction of metastable neutral atoms
12	$2e^- + A^+ \rightarrow e^- + A^*$	Three body recombination	Relevant in dense highly ionized plasmas
13	$e^- + A^+ \rightarrow h\nu + A$	Radiative recombination	Relevant in dense highly ionized plasmas
14	$e^- + AB^+ \rightarrow A + B^*$	Dissociative recombination	Important in weakly ionized molecular plasmas
15	$e^- + A^- \rightarrow 2e + A$	Detachment by electron impact	Loss of negative ions in electronegative gases

Table 4.1: The most relevant electron collisional processes in plasmas for energy exchange (1-4) production of particles (5-10) and losses (11-15). The neutral atom is A, its metastable state A^* and A^+ represents the corresponding single charged ion. The molecules or diatomic gases are indicated as AB.

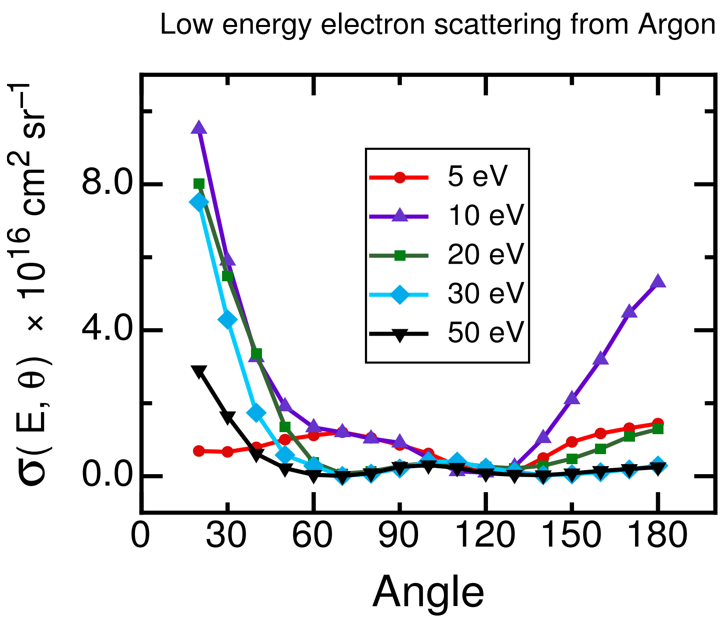

Figure 4.7: Experimental data of the differential cross section for low energy electrons with Argon atoms from Ref. [8].

the collisions that transfer a fraction of the electron energy to the neutral atom in which a bounded electron jumps into excited state as,

$$e^- + A^* \rightarrow e^- + A^+$$

The corresponding cross section depends of the excited state of the neutral atom. This latter is ionized in the *electron impact ionization*,

$$e^- + A \rightarrow 2\,e^- + A^+$$

when the energy of the incident electron lies over the ionization energy E_I of the neutral atom. The ionization of a neutral produces an electron-ion pair and the newly released electron is called *secondary electron*.

A plasma stable in time requires of an dynamic equilibrium between the charge production (ionization) and losses (recombination). The number of produced electron-ion pairs needs to be equal to the number of those lost in order to obtain a plasma density constant in time.

These inelastic collisions provide excited neutral atoms and ions, and the electron impact ionization is usually the main charge production mechanism in the plasma. Both require of a threshold energy for the impacting electron.

The elastic, excitation (only the more relevant transition is depicted) and ionization cross section or argon are compared[4] in Fig. (4.6). The qualitative dependence with the electron energy is similar in most gases.

[4] Note that the energies are represented in logarithmic scale.

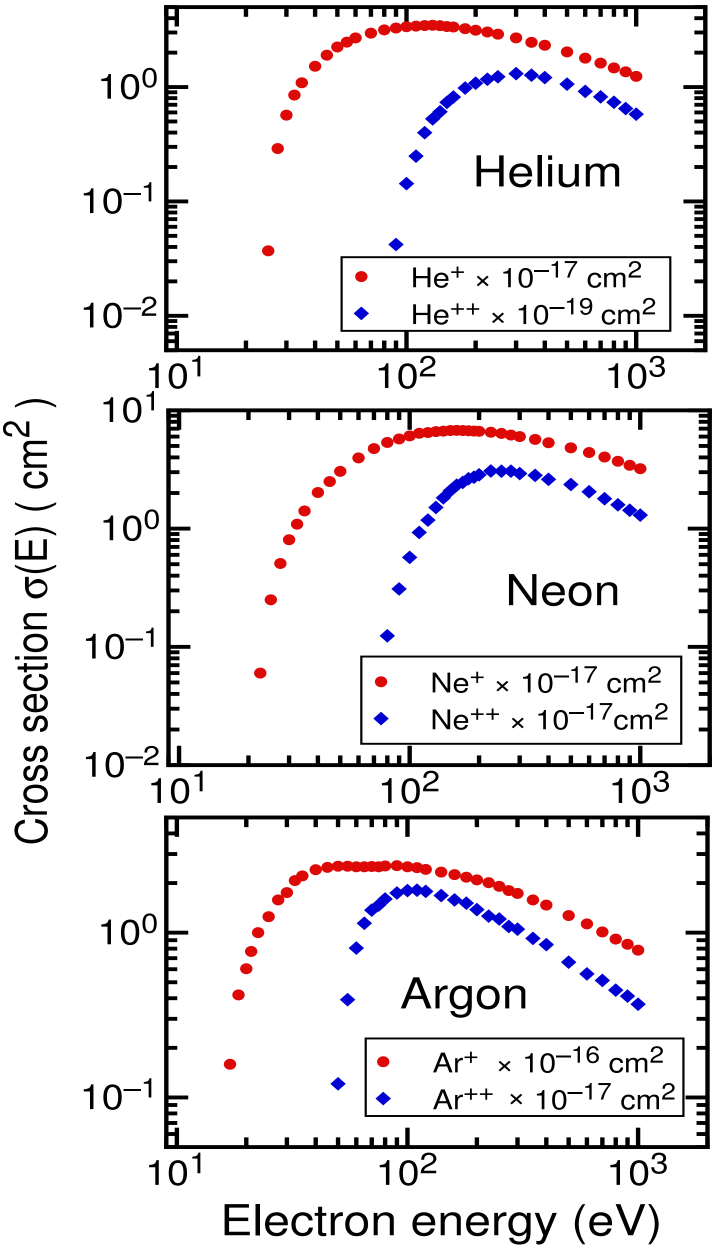

Figure 4.8: Experimental data from Ref. [9] for the electron impact ionization cross sections of different rare gases.

The excitation and ionization require of a threshold value for the energy of the colliding electron and after a sharp growth decreases smoothly for high energies. When the transition of the bounded electron to the target neutral atom is allowed according to the spectroscopy selection rules, the tail of $\sigma(E)$ trend to decrease as $\sigma(E) \sim \ln(E)/E$ while it falls as $\sigma(E) \sim 1/E$ or faster when is forbidden. In both inelastic collisions, the dispersed electrons are concentrated more around the forward direction than for the elastic collisions (see Fig. 4.7) and this tendency increases with the electron energy.

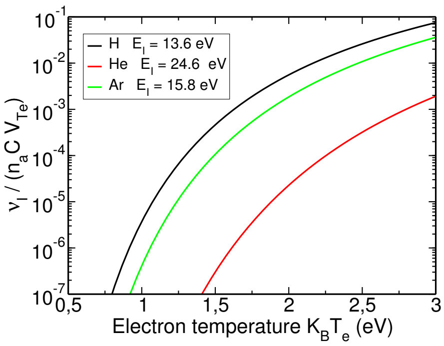

Figure 4.9: The growing of the ionization frequency with $k_B T_e$ for atomic H, He and Ar using the Eq. (4.10).

The inelastic collisions with a threshold energy produce changes in the electron energy distribution function. Since most excitation potential of gases are in the order of few eV, each collision event reduces the energy of the impacting electron by an amount E_I. Therefore, the average energy of fast electrons in the tail of the energy distribution decreases, and these electrons return to the low energy group.

The ionization rate could be calculated using the Eq. (4.3). The number $\dot{Q}_I$ of ionization events by target neutral atom in the frame where they remain at rest is,

$$d\dot{Q}_I = n_e\, \sigma_I(v_e)\, |\boldsymbol{v}_e|\, d\boldsymbol{v}_e$$

The number of incoming electrons with velocities between $\boldsymbol{v}_e$ and $\boldsymbol{v}_e + d\boldsymbol{v}_e$ is therefore,

$$n_e\, d\boldsymbol{v}_e = n_{eo}\, f_e(\boldsymbol{v}_e)\, d\boldsymbol{v}_e$$

and in the case of a *isotropic* electron distribution $f_e(\boldsymbol{v}_e) = f_e(|\boldsymbol{v}_e|)$ also,

$$n_e\, d\boldsymbol{v}_e = n_{eo}\, g_e(E)\, dE$$

and $g_e(E)$ is the electron energy distribution function. Then,

$$d\dot{Q}_I = n_{eo}\, \sigma_I(v_e)\, v_e\, f_e(v_e)\, d\boldsymbol{v}_e = n_{eo}\, \sigma_I(v_e)\, v_e\, g_e(E)\, dE$$

where $\sigma_I(E)$ is the cross section for electron impact ionization. The energy of the colliding electron needs to be over the ionization threshold $E_I = m_e v_I^2/2$ of the neutral atom, so that $\sigma_I(E) = 0$ for $E < E_I$. Therefore,

$$\dot{Q}_I = n_{eo} \int_{v_I}^{\infty} \sigma_I(v_e)\, v_e\, f_e(\boldsymbol{v_e})\, d\boldsymbol{v}_e \tag{4.8}$$

or equivalently,

$$\dot{Q}_I = n_{eo} \int_{E_I}^{\infty} \sigma_I(E)\, v_e\, g_e(E)\, dE \tag{4.9}$$

Gas	He	H_2	Ne	N_2	O_2
C	0.13	0.59	0.16	0.85	0.68

Table 4.2: Coefficient C in the electron impact cross section for ionization (Eq. 4.10) for different gases from Ref. [10].

Higher ionization levels of ions as double ionized ions (as A^{++}, ...etc) have lower cross sections and require of higher energies for ionizing electrons. This fact is evidenced in the experimental data of Fig. (4.8) where the energy threshold for the double ionization of rare gases corresponds to higher energies of the impacting electron.

As observed in Fig. (4.6) the ionization cross section grows fast $\sigma_I(E)$ grows fast for electron energies over $E \geq E_I$. Therefore, in Eq. (4.8) is usually approximated by a piecewise linear function,

$$\sigma_I(E) = \begin{cases} 0 & \text{if} \quad E < E_I \\ C\,(E - E_I) & \text{if} \quad E \geq E_I \end{cases} \tag{4.10}$$

where C is an empirical value and in Table (4.2) are their values for different gases. For a Maxwellian electron energy distribution function (Eqs. 1.1 and 1.2) with temperature $k_B T_e$ in Eqs. (4.8) and (4.9) we obtain,

$$\nu_I = A\,(1 + 2 k_B T_e)\,\exp(-E_I / k_B T_e) \tag{4.11}$$

where $A = n_a\, C\, \bar{v}_e$ and $\bar{v}_e$ is given by Eq.(1.3).

In Fig. (4.9) is represented the ratio ν_I / A which only rely on the electron temperature. As it could be observed, the ionization frequency grows several orders of magnitude with the electron temperature. The increasing value of $k_B T_e$ produce a wider Maxwellian distribution for electrons and the number of electrons in the tail for energies $E > E_I$ also increments. A higher number of electrons with energy enough to produce a ionization event increases the ionization rate in the plasma.

The ionization from the ground state of the neutral atom is not the only possibility. The ion could also be produced by two successive collisions, from an excited level of the of the neutral,

$$A \,+\, e^- \,\rightarrow\, A^* \,+\, e^-$$

and then,

$$A^* \,+\, e^- \,\rightarrow\, A^+ \,+\, e^-.$$

Finally, the electrons could be also los in certain gases by *attachment*. A negative ion in formed by capturing an electron as,

$$N_2 \,+\, e^- \,\rightarrow\, N_2^-$$

This occurs for certain molecular gases in accordance to their electron affinity.

4.4.2 Ion collisions with neutrals

In plasma whit low ionization degrees the elastic collisions between ions and neutral atoms are frequent. An important process is the collision between a neutral and an ion where an electron is interchanged, denominated *charge exchange* collision,

$$A^+ + B \rightarrow B^+ + A$$

and these collisions are dominant in partially and weakly ionized plasmas.

The charge exchange is *resonant* when both colliding atoms have similar ionization energies and *non resonant* otherwise. As it can be deduced from the experimental data of Figs. (4.10) and (4.5) this reaction has a cross sections[5] comparable with those for elastic collisions between electrons and neutral atoms and contributes to distribute the positive charges within the plasma. In weakly ionized plasma where the number of ions is low and the neutral atom concentration high, these collisions represent and important mechanism for energy transfer between both species.

The electrons are not the only particle producing the ionization of a neutral. There exits ion neutral collisions where charges are produced as in the *dissociative ionization* where two neutrals collide, one of them excited,

$$A^* + B \rightarrow A^+ + B + e^-.$$

Again, a large number of possible molecular and atomic collisions are possible and the details are beyond the scope of these notes.

4.4.3 Photoprocesses

In *radiative* collisions or *photoprocesses* the photon is the second particle involved and the kinetic energy of a particle may be transformed in electromagnetic radiation. For example, in the *photoionization* process the ionizing particle is a quantum of light (photon) with energy $E_\nu = h\,\nu$. When the energy $E_\nu > E_I$ is over the ionization potential of the neutral atom,

$$A + h\nu \rightarrow A^+ + e^-.$$

The number of ionization events by time and volume is proportional to the concentration of neutral atoms $\nu_I = I(\nu)\,n_a$, multiplied by a function $I(\nu)$ which rely in the light intensity (that is, to the number of available photons) and the frequency ν of light.

Additionally, the *photoexcitation* could increment the energy of an electron in the external shell of the neutral atom which is eventually ionized later by an electron impact,

$$A + h\nu \rightarrow A^*$$
$$A^* + e^- \rightarrow A^+ + e^-$$

[5] Some authors ambiguously use *total* cross section also for the sum of different total cross sections as in Fig. (4.10).

Ion and neutral atom collisions			
Scheme		**Process**	**Macroscopic effect**
1	$A + A \to A + A$	Elastic collision between neutral atoms	Transport of neutrals and energy thermalization
2	$A^+ + A \to A^+ + A$	Elastic collision between ions and neutral atoms	Transport of ions, diffusion and thermalization of energy
3	$A + B^+ \to A^+ + B$	Resonant or nonresonant charge exchange	Ion transport, diffusion and thermalization of energy
4	$A + A^* \to A^* + A$	Collision between metastable and neutral atoms	Diffusion of metastable atoms
5	$A^* + B \to e^- + A + B^+$	Penning ionization	Production ions in gas mixtures
6	$A + B^* \to e^- + AB^+$	Associative ionization	Production of molecular ions in diatomic or gas mixtures
7	$A + B^+ + C \to A + BC^+$	Ion association	Production of molecular ions in gas mixtures
8	$A^* + A^* \to e^- + A^+ + A$	Cross Penning reaction	Production of ions from metastable atoms
9	$AB^- + AB^+ \to AB + AB$	Ion-ion recombination	Loss of negative ions in electronegative or diatomic gases

Table 4.3: Relevant collisional processes between ions and neutral atoms in plasmas involving energy exchange (1-4) ion production (5-8) and losses. The neutral atom is A, its metastable state A^* and A^+ represents the corresponding single charged ion. The molecules or diatomic gases are indicated as AB

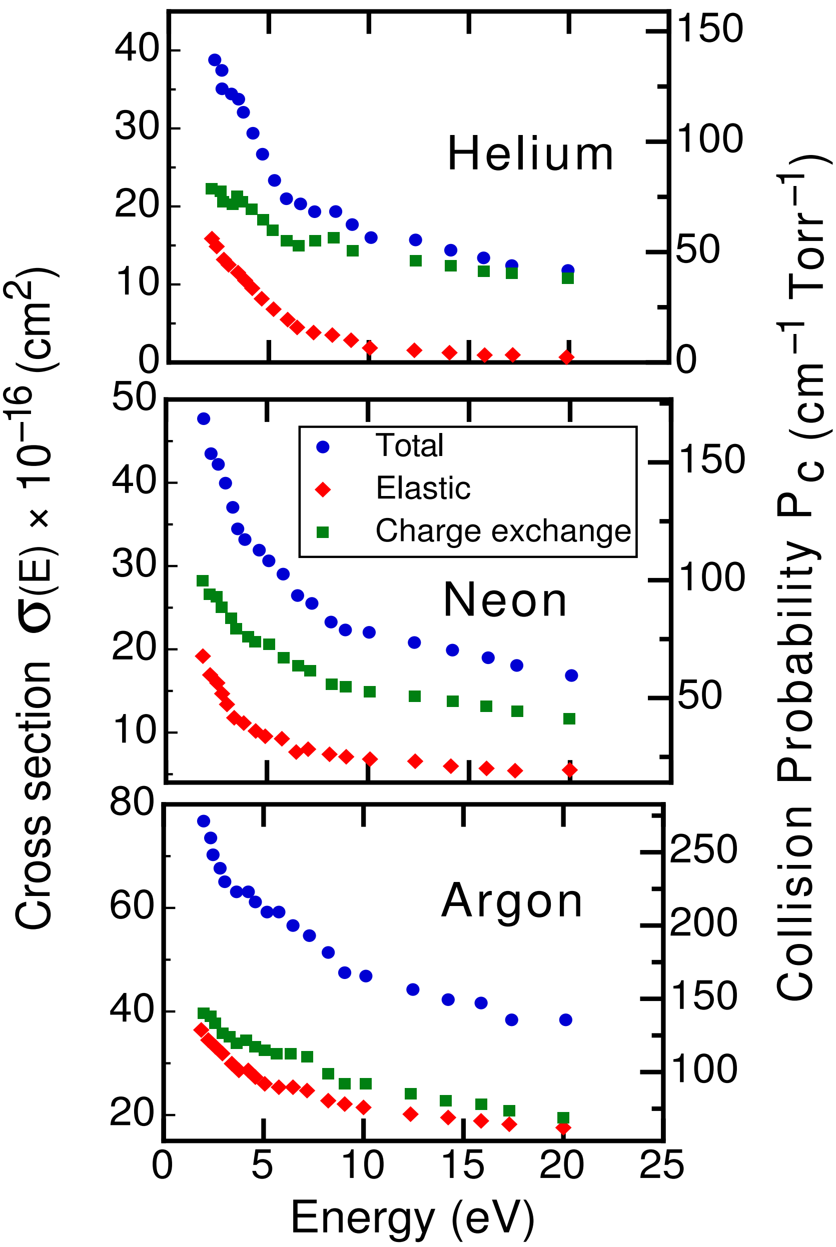

Figure 4.10: Experimental data from Ref. [10] for cross section and probabilities of elastic collisions between ions and neutral atoms for different inert gases as a function of the ion energy. The data correspond to elastic collisions (diamonds), charge exchange (squares) and the sum of both (solid bullets).

The frequencies of light involved in photoexcitation are in the order of 1-5 eV, within the range of visible light (E = 2.26 eV or λ = 550 nm). The visible light emitted by plasmas comes mostly from these processes atomic excitation and processes caused by the large number of free electrons with energies in the range 1-5 eV. However, the energies required to ionize the neutral atoms from their ground state corresponds to the ultraviolet part of the electromagnetic spectrum.

4.4.4 The collisions of charged particles

The number of encounters between charged particles depend on the ionization degree,

$$\alpha = n_i/(n_i + n_a)$$

of the neutral gas. The plasmas may be roughly considered as fully ionized and the coulomb collisions dominant when the ionization degree is over few parts over one thousand, while can be neglected in weakly ionized plasmas. The long range electric force between two charged particles is more intense and is exerted at much longer distances that the average atomic dimensions. The corresponding cross sections are therefore much larger than in collisions with neutral particles. Again, there are different possible collisions between charged particles and we only discuss the more relevant.

4.4.4.1 The electron and ion recombination

The reverse process of ionization is the *recombination* of an electron e^- and the ion A^+ to produce a neutral atom. There exists different possible atomic and molecular processes that end with the production of a neutral atom. However, the average number of ions lost by volume and time units is proportional to the concentration of ions and electrons,

$$(\frac{dn_i}{dt})_{rec} = k_R \, n_e \, n_i. \tag{4.12}$$

Here k_R is the *recombination rate*, and a plasma stable in time and electrically neutral requires $n_i = n_e = n$. This leads to the following differential equation,

$$\frac{dn}{dt} = -k_R \, n^2$$

and integrating we obtain,

$$\frac{1}{n} = \frac{1}{n_o} + k_R \, t$$

where n_o is the ion (or electron) concentration at $t = 0$. The recombination coefficient k_R could be experimentally determined by its linear relation of $1/n$ with time. The typical values found are $k_R \simeq 10^{-7}$ cm^3 seg^{-1}.

In addition to the electron impact ionization, the neutrals could be ionized and the ions recombined by different collisional processes. It must be emphasized that the corresponding reaction rate constants and the involved energies may differ by orders of magnitude. The relevance of each particular recombination process in the above average needs to be examined.

The number of charged particles in a plasma in equilibrium is therefore related with the ionization frequency ν_I (or equivalently with the reaction rate k_I) and the reaction rate k_R. The equilibrium between charge production and recombination is determined by the quotient,

$$\frac{n_i}{n_a} = \frac{k_I}{k_R}$$

In laboratory plasmas, the ions are lost mainly by recombination at the walls of the device, not in the plasma bulk. Because of the low ionization degrees, the typical recombination mean free path is larger than the physical dimensions of the plasma container. On the contrary, most of ions reach the plasma chamber walls without a recombining collision that would transform the ion into a neutral atom.

4.4.4.2 The Coulomb collisions

The long range Coulomb collisions of the form,

$$A^+ + e^- \rightarrow A^+ + e^-.$$

transfer energy and momentum between the charged species. These collisions are dominant in fully ionized plasmas and in dense plasma may involved more than two particles.

This is not the place for a detailed description of these collisions, however, it may be shown the using $\tau = \lambda_{ei}/V_{th}$ the average collision time between electrons and ions in MKSC units respectively are,

$$\tau_e = \frac{6\sqrt{2}\,\pi^{3/2}\epsilon_o\sqrt{m_e}\,T_e^{3/2}}{\Lambda\, e^4\, n} \tag{4.13}$$

and

$$\tau_i = \frac{12\,\pi^{3/2}\epsilon_o\sqrt{m_i}\,T_i^{3/2}}{\Lambda\, e^4\, n} \tag{4.14}$$

Here, $\Lambda = \ln(d_{max}/d_{min})$ is the *Coulomb logarithm* proportional to the logarithm of the ratio the maximum and minimum impact parameters. The shortest approaching distance is d_{min} and $d_{min} \simeq r_c = e^2/4\pi\epsilon_o T$ determined by,

$$\frac{m_{e,i}u_{e,i}^2}{2} - \frac{e^2}{4\pi\epsilon_o\, r_c} = 0$$

Because the electric potential is shielded $d_{max} = \lambda_d$ (the Debye length). The Coulomb logarithm is an smooth function of the density and plasma temperature.

4.5 Numerical estimates

The mean free paths, collision frequencies are estimated from the experimental data for cross sections. In addition, most of these quantities are somehow related with the neutral gas pressure, that we associate with the neutral atom density n_a through,

$$n_a = \frac{1}{k_B}\frac{P}{T} = 7.24 \times 10^{22}\,\frac{P}{T}$$

with the pressures in Torr 1 Pa = 133 Torr and neutral atom densities in cm^{-3} we have,

$$n_a\,[\mathrm{cm}^{-3}] = 9.63 \times 10^{18}\,\frac{P\,[\mathrm{Torr}]}{T\,[\mathrm{K}]}$$

for the $T_a = 273$ K we have

$$n_a\,[\mathrm{cm}^{-3}] = 3.53 \times 10^{16}\,P\,[\mathrm{Torr}]$$

The actual parameter measured in the experiments is the *collision probability* P_c, which is defined as *the average number of collisions experienced by a particle when traveling 1 cm of length at the temperature of ^oC and at the pressure of 1 mm Hg.*

The relation between P_c and σ is simple. Being n_b the density of *target* particles and ν the collision frequency $P_c = \nu\,\Delta t$ (1 cm), and because $\Delta t(1\text{ cm}) = 1/v_T$ where v_T is the corresponding thermal velocity,

$$P_c = \nu\,\Delta t(1\text{ cm}) = (n_b\,\sigma\,v_T) \times \left(\frac{1\text{ cm}}{v_T}\right) = n_b\,\sigma$$

For example, in collisions between neutrals and electrons (see Fig. 4.5) we have, $P_c = n_a\,\sigma_{ea}$ we have,

$$\lambda_{ea} = \frac{1}{n_a\,\sigma_{ea}} = \frac{1}{p_o P_c}$$

and for the frequency,

$$\nu_{ea} = \frac{v}{\lambda_{ea}} = p_o\,P_c\,v_{Te}$$

where p$_o$=1 mm Hg, and for the total cross section we have,

$$\sigma_{ea}\,[\mathrm{cm}^{-2}] = 0.283 \times 10^{-16}\,\mathrm{P}_c$$

The cross sections are frequently expressed as,

$$\sigma = \pi a_o^2 = 8.797 \times 10^{-17}\,\mathrm{cm}^{-2} = 0.88\,\text{Å}^2$$

and results $\sigma = 0.322\,\mathrm{P}_c\,[\text{Å}^2]$.

The experimental cross section for the elastic and inelastic collisions between electrons and neutral atoms for different gases as a function of the energy of the incident particle are in Figs. (4.5) and (4.6). Additionally, the cross sections for elastic and charge exchange collisions of ions with neutrals are in Fig. (4.10).

4.6 The equilibrium states of a plasma

As we have seen, not all the above reactions between the plasma species have equal probability. Their cross sections are different, the collision rates also rely on the degree of ionization, the concentration of ions, electrons, ...etc.

Consequently, the plasma in *thermodynamic equilibrium* is a rather unusual situation in nature. Strictly speaking, it would require the balance of all collisional and radiative processes by the reverse reactions. So that the charge production and ionization rates must be equals, the emission and absortion of electromagnetic radiation by the plasma particles, ...etc. We conclude that,

> A plasma (or any other statistical population of particles) is in *thermodynamic equilibrium* when the rates of collisional and radiative processes are balanced by their reverse reactions.

In such situation, the plasma is fully characterized by its thermodynamic magnitudes; the equilibrium pressure, volume and temperature. The energy distribution of each specie in the plasma is a Maxwell Boltzmann distribution with a common temperature for all species in the system. In this thermodynamic equilibrium state,

- The physical properties properties of the plasma are uniform in space and constant in time.
- The plasma is said *optically thick*. The balance of forward and backward reaction requires that the light produced by inelastic particle collisions is later absorbed and cannot leave the plasma region. In consequence, a plasma in thermodynamic equilibrium has a black body radiation spectrum.

Obviously, these requisites are very restrictive and plasmas in thermodynamic equilibrium are seldom found in nature nor in laboratory. In practice we always deal with plasmas *far from thermodynamic equilibrium* where the lack of balance of some elementary processes leads to a *hierarchy of partial equilibrium states.*

> The plasma is in *local equilibrium* when all collisional processes for charge production are balanced with those of particle recombination, but not the radiative processes.

Under these conditions, the plasma in *local equilibrium* emits light, since it comes from radiative processes, as i.e. from electron impact excitation and deexcitation of bounded electrons of neutrals atoms. This radiation leaves the plasma and therefore can be detected. However, the balance of all collisional processes between charged and neutral species implies that they are in equilibrium, and consequently, are again characterized by the Maxwell Boltzmann energy distribution with the same kinetic temperature.

Finally, because of their the different cross sections in plasmas confined in small volumes only *some collisional processes are balanced.* This brings the next kind of plasma equilibrium.

The plasma is in *partial equilibrium* when only an small number of elementary processes are balanced.

This is the more frequent situation in laboratory plasmas because the charge production occurs within the plasma volume but the recombination of charged particles takes place at the walls of the plasma container or over the surface of the metallic electrodes.

The reason is the electron impact ionization cross section, which is often much larger than the recombination cross section. Consequently, the ionization mean free path is shorter than for recombination. The charges are originated inside the plasma bulk but leave the experimentation volume without experience the corresponding recombining collision.

4.6.1 Multithermal equilibrium

A particular feature of plasmas is the possibility of the coexistence of charged particle populations with different average energies. This means a *partial equilibrium* where the electron k_BT_e and ion k_BT_i temperatures differ.

The energy exchange between the different particle species is determined by the nature and frequency of collisions among them. Because of the disparity between the electron and ion masses the energy exchange is low in the elastic collisions between electrons and neutral atoms. The fraction of exchanged energy is proportional to $\delta = 2\, m_e/m_i$ which typically lies between 10^{-4} and 10^{-5}.

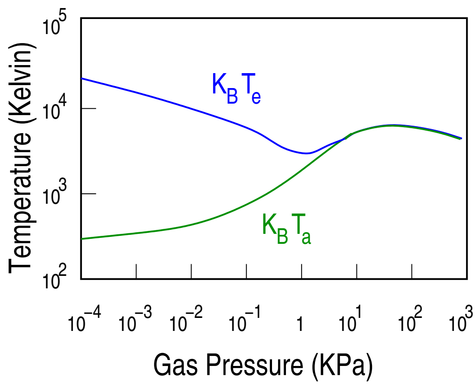

Figure 4.11: The neutral gas k_BT_a and electron k_BT_e temperatures as a function of the gas pressure.

The electron impact inelastic collisions produce transitions between energy levels of bounded electrons of atoms and vibrational and/or rotational energy levels of molecules. The typical energy transfer rate for these inelastic collisions is one or two orders of magnitude higher, between 10^{-3} and 10^{-2}. On the contrary, for elastic and charge exchange collisions between ions and neutral atoms the energy exchange rate is much larger because colliding particles have similar masses. In other words, ions and neutrals share energy fast while electrons retain their kinetic energies during longer times.

This effect of energy transfer between two plasma species is evidenced in Fig. (4.11) where are represented the electron k_BT_e and neutral gas k_BT_a temperatures as a function of the neutral gas pressure p_a. The electrons acquire energy from the low electric field in the plasma and transfer a fraction of this energy to the neutral gas, essentially by elastic collisions.

For low neutral pressures the collisions are scarce, the energy transfer between both species remains low and their respective temperatures are different. For higher gas pressures the collision frequency increases and both temperatures approach because the collisional energy transfer grows. In this partial equilibrium state of electrons ions and neutral atoms the average electron kinetic energy per particle is different from those of ions and neutrals.

Therefore the electron kinetic temperature $k_BT_e \gg k_BT_i$ differs from ion and neutral atom temperatures $k_BT_i \simeq k_BT_a$. In the *multithermal equilibrium* state or *two temperature plasma* each charged particle specie is characterized by a different energy distribution function and contrary to a plasma in local equilibrium. This partial equilibrium state of a plasma is often found in nature and in the laboratory but obviously requires of an external source of energy to exist.

4.6.2 The local equilibrium

As we have seen, the Maxwell Boltzmann distribution corresponds to a plasma in thermodynamic equilibrium with parameters as temperatures and density constant in time and uniform in space. This fact excludes the possibility of transport of charged or neutral particles, momentum, energy, ...etc. Such situation has no practical interest because we usually deal with plasmas far from equilibrium. The determination of the nonequilibrium velocity (or energy) distribution function $f_\alpha(\boldsymbol{v}, \boldsymbol{r}, t)$ for all plasma species ($\alpha = a, e, i$) is a difficult task and one of the main objectives of the kinetic theory of plasmas.

However, when certain conditions are met we may *locally approximate* this undetermined nonequilibrium energy distribution function by Eq. (1.1). That is, to consider the plasma species as *locally Maxwellians* by using,

$$f_\alpha(\boldsymbol{v},\, \boldsymbol{r}\ t) = n_\alpha(\boldsymbol{r},\, t)\, (\frac{m_\alpha}{2\pi k_B T_\alpha(\boldsymbol{r},\, t)})^{3/2}\, \exp\left(-\frac{m_\alpha \boldsymbol{v}^2}{2k_B T_\alpha(\boldsymbol{r},\, t)}\right) \tag{4.15}$$

where the density $n_\alpha(\,\boldsymbol{r},\, t)$ and temperature $k_B T_\alpha(\,\boldsymbol{r},\, t)$ are non-uniform and/or time dependent.

This approximation has the implicit assumption of the existence of fast energy relaxation processes in the plasma, or equivalently, of large collision frequencies. The collisions lead the energy fluctuations to relax fast to an local equilibrium state described by the Maxwell Boltzmann distribution. This *local Maxwellian* approximation is therefore valid when the spatial and time changes in the plasma properties are much lower that the characteristic time and length scales for collisions.

Then, the essential requisite is that the plasma properties slowly vary in time and have smooth changes in space. The local Maxwellian distribution of the Eq. (4.15) may be understood as resulting from an small perturbation $f^1_\alpha(\boldsymbol{v},\, \boldsymbol{r},\, t)$ of Eq. (1.1) as,

$$f_\alpha(\boldsymbol{v},\, \boldsymbol{r}\ t) = f^o_\alpha(\boldsymbol{v})\ + f^1_\alpha(\boldsymbol{v},\, \boldsymbol{r},\, t)$$

where $|f^1_\alpha| \ll |f^o_\alpha|$.

Then, the properties of this plasma obviously are neither constant in time nor homogeneous in space. The restrictive requisites for thermodynamic equilibrium condition are therefore weaken, and non equilibrium phenomena, as the particle transport are considered. Nevertheless, it should be stressed that the local Maxwellian plasma *constitutes a useful approximation* but *is not the actual velocity distribution function* of the plasma species.

5

The physical models for plasmas

In Chapter 1.1 we introduced the plasmas as a mixture of interacting electrons, ions and neutral atoms in thermodynamic equilibrium. In this situation, all particle species are described by a Maxwell Boltzmann energy distribution with a common temperature $k_B T_e = k_B T_i = k_B T_a$. The plasma parameters (plasma frequency, Debye length and plasma parameter) were introduced for this ideal Maxwellian plasma in Sec. (1.5). However, as discussed in Sec. (1.3), the transport of neither particles, momentum nor energy is possible in this restrictive equilibrium state. The ideal Maxwellian plasmas are scarcely found in both, neither in nature nor the laboratory as discussed in Sec. (4.6). Most plasmas usually are found in *partial equilibrium*, as the glow discharge plasma of Fig. (2.5) in Sec. (2.4) where visible light is emitted and the electric current flows through the plasma bulk.

In order to account for the non equilibrium properties properties of plasmas new concepts and more involved physical models are required. In the scheme of Fig. (5.1) are represented the essential stationary and time dependent macroscopic and microscopic approaches. The plasma state is placed at the top as an electrically neutral fluid like medium of interacting particles as discussed in Sec. (2.1).

The *macroscopic models* consider this medium as a continuum where a huge number of particles are contained within volumes with characteristic sizes $V \sim \lambda_D^3 \ll L^3$ much smaller that the macroscopic lengths L involved. The *microscopic* theories are based upon the fact that plasmas are constituted by interacting atoms and/or molecules. The calculations of the physical magnitudes require of new concepts and are obtained as statistical averages over a large number of particles.

The *thermodynamics* is the macroscopic theory concerned with equilibrium fluids at rest. They are described by time independent variables, uniform in space as the temperature T, density ρ, enthalpy h, ...etc. The thermodynamics also relies on additional material dependent relations, as the *equations of state* or the specific heats which may be supplied by either the experiments or other considerations.

In the macroscopic approach, the equation for the fluid motion are directly derived by the application of the conservations of mass, momentum and energy, ignoring most particular details of the constituent particles. The motions of fluids are described by using mechanical magnitudes as the velocity $\boldsymbol{u}(\boldsymbol{r}, t)$ and density $\rho(\boldsymbol{r}, t)$, ...etc. More relations, as the transport

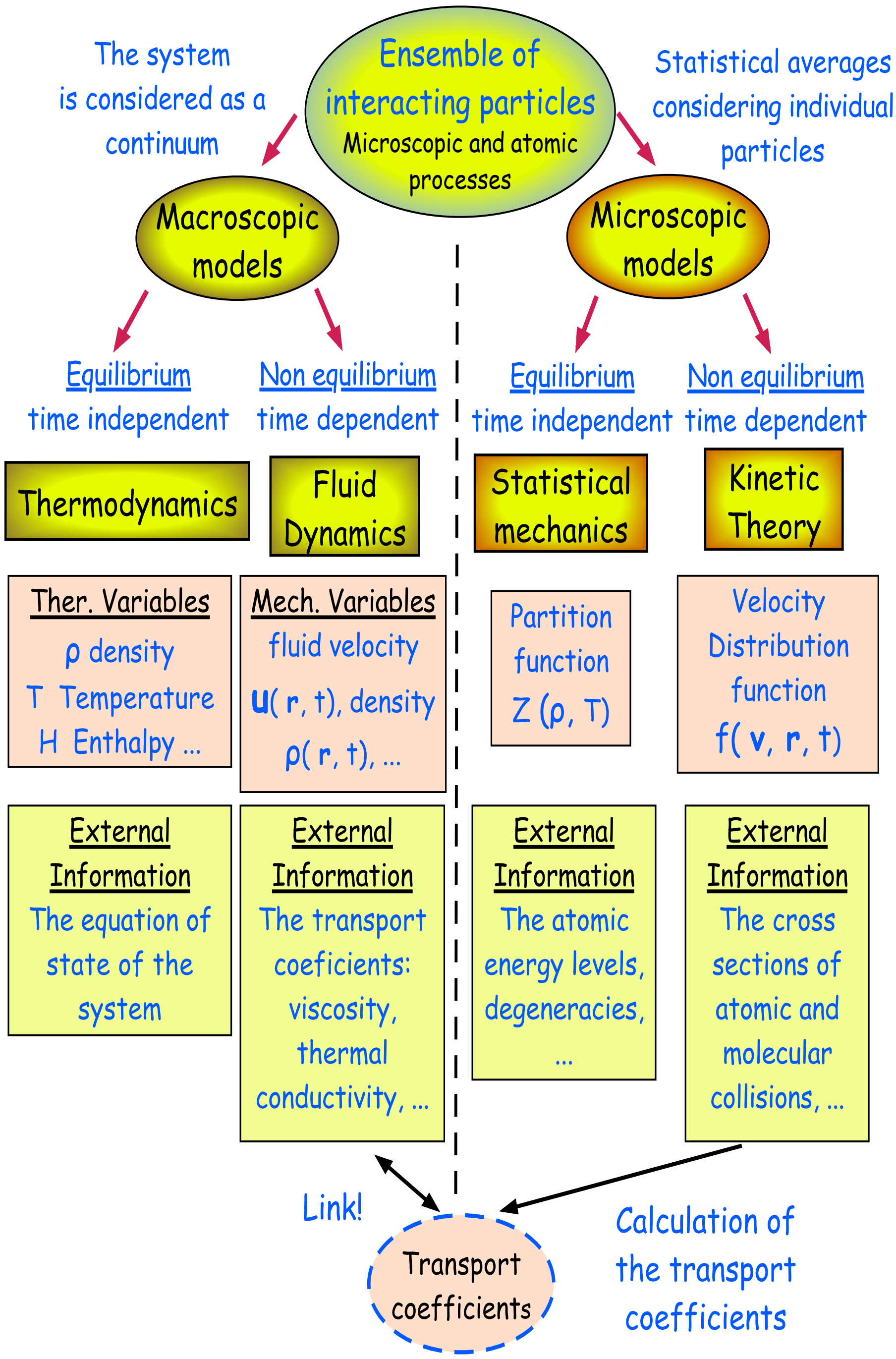

Figure 5.1: The more relevant physical models for an statistical ensemble of interacting particles.

coefficients, are needed to close the fluid equations. Then, the viscosity, thermal conductivity, ...etc also need to be supplied by external considerations or obtained from the experiments.

The microscopic approaches are less dependent on experimental information. The *statistical mechanics* is concerned from the microscopic point of view with the same kind of systems than equilibrium thermodynamics. The fundamental concept is the partition function from which may be derived material dependent relations not available in thermodynamics as the equation of state or the specific heats. The calculations require of microscopic information obtained from the experiment as the atomic or molecular energy levels its degeneracy, ...etc.

In this chapter we are mainly concerned with the *kinetic* description of plasmas. The *kinetic theories* make use of an statistical approach based on the velocity distribution function $f_\alpha(\boldsymbol{r}, \boldsymbol{v}, t)$ that may be different for each particle specie (α = e, i, a) in the plasma. These probabilistic functions depend on the particle speed $\boldsymbol{v}$ its position $\boldsymbol{r}$ and also may evolve in time. The macroscopic properties, as the local gas pressure or temperature result from averages of $f_\alpha(\boldsymbol{r}, \boldsymbol{v}, t)$ using appropriate operators for the physical magnitudes. The ideal Maxwell Boltzmann distribution $f_\alpha(\boldsymbol{r}, \boldsymbol{v}, t) \simeq f_\alpha(|\boldsymbol{v}|)$ is recovered in the limit of the thermodynamic equilibrium.

These kinetic models essentially apply when $f_\alpha(\boldsymbol{r}, \boldsymbol{v}, t)$ appreciably changes along the typical length L and/or the time scale T of the plasma. In particular, when the mean collisional free paths λ are comparable to the characteristic size of the plasma volume considered. However, these models are quite complex even for the simplest physical situations.

The fluid equations are more intuitive compared with the kinetic theories and this fact makes the fluid models attractive. However, they are essentially only valid when $f_\alpha(\boldsymbol{r}, \boldsymbol{v}, t)$ changes smoothly along typical distances $L \gg \lambda$ much larger than the relevant collisional mean free path λ. This slowly varying distribution function over distances much larger than λ justifies the *local Maxwellian* approximation previously discussed in Sec. (4.6.2).

In both, the fluid and kinetic descriptions the properties of the elementary processes, as the elastic and inelastic particle collisions discussed in Sec. (4.4) need to be introduced. For instance, the energy transfer between particle species by elastic collisions, the ionization and recombination rates, ...etc. In the kinetic description they are incorporated by means of *collision operators* that account for the changes introduced in $f_\alpha(\boldsymbol{r}, \boldsymbol{v}, t)$ by the collisional processes.

These operators provide the coupling between the velocity distributions $f_\alpha(\boldsymbol{r}, \boldsymbol{v}, t)$ for the different species of the plasma. The transport coefficients of required by the fluid equations are also calculated by averaging over the collisional operators. This is indicated by the link in the scheme of Fig. (5.1). For example, as we shall see, this is the origin of the particle source and sink terms in the fluid continuity equation.

5.1 The kinetic description of plasmas

The kinetic description considers the velocity distribution function $f_\alpha(\boldsymbol{v}, \boldsymbol{r}, t)$ for the three plasma species $\alpha = e, i, a$ of electrons, ions and neutral atoms. The governing equation for the spatial an temporal evolution of $f_\alpha(\boldsymbol{v}, \boldsymbol{r}, t)$ is the *Boltzmann equation* which accounts for the particle sink and source terms as well as the forces acting on each plasma species.

The solution of this partial differential equation are the time dependent velocity distribution functions $f_\alpha(\boldsymbol{r},\boldsymbol{v},t)$ for the nonequilibrium states.

As we shall see, the fluid equations for a plasma could be deduced from averages of the Boltzmann equation by using an unspecified nonequilibrium distribution $f_\alpha(\boldsymbol{r},\boldsymbol{v},t)$ for the plasma species. Nevertheless, a key point still remains open, the explicit expression for $f_\alpha(\boldsymbol{r},\boldsymbol{v},t)$ is needed for the calculation of the transport coefficients (thermal conductivity, viscosity, ...etc). Therefore, additional approximations and/or assumptions are required for the closure of the fluid transport equations.

The number of particles dN_α with velocities between $\boldsymbol{v}$ and $\boldsymbol{v}+d\boldsymbol{v}$ of each specie contained in the infinitesimal volume $d\boldsymbol{r} = d^3r$ located at the point $\boldsymbol{r}$ is given by,

$$dN_\alpha = f_\alpha(\,\boldsymbol{v},\,\boldsymbol{r},\,t)\,d\boldsymbol{v}\,d\boldsymbol{r}$$

The particle density $n_\alpha(\boldsymbol{r},t)$ at the point $\boldsymbol{r}$ is obtained by integration of all possible velocities of particles contained into d^3r and,

$$n_\alpha(\,\boldsymbol{r},\,t) = \int_{-\infty}^{+\infty} f_\alpha(\,\boldsymbol{v},\,\boldsymbol{r},\,t)\,d\boldsymbol{v} \quad \text{and then,} \quad N_\alpha = \int_{-\infty}^{+\infty} n_\alpha(\,\boldsymbol{r},\,t)\,d\boldsymbol{r} \tag{5.1}$$

Therefore, the velocity distribution function could be also considered as a probability distribution using $\hat{f}_\alpha = f_\alpha/n_\alpha(\boldsymbol{r},t)$. Then,

$$1 = \frac{1}{n_\alpha}\int_{-\infty}^{+\infty} f_\alpha(\,\boldsymbol{v},\,\boldsymbol{r},\,t)\,d\boldsymbol{v} \ \text{ or equivalently, } \ 1 = \int_{-\infty}^{+\infty} \hat{f}_\alpha(\,\boldsymbol{v},\,\boldsymbol{r},\,t)\,d\boldsymbol{v} \tag{5.2}$$

and we may interpret $\hat{f}_\alpha\,d\boldsymbol{v}$ as the probability of finding a particle α in the volume $dr^3 = d\boldsymbol{r}$ with velocity within the range $\boldsymbol{v}$ and $\boldsymbol{v}+d\boldsymbol{v}$. Then the average local velocity is,

$$\boldsymbol{u}_\alpha(\,\boldsymbol{r},\,t) = \frac{1}{n_\alpha(\,\boldsymbol{r},\,t)}\int_{-\infty}^{+\infty} \boldsymbol{v}\,f_\alpha(\,\boldsymbol{v},\,\boldsymbol{r},\,t)\,d\boldsymbol{v} = \int_{-\infty}^{+\infty} \boldsymbol{v}\,\hat{f}_\alpha(\,\boldsymbol{v},\,\boldsymbol{r},\,t)\,d\boldsymbol{v} \tag{5.3}$$

In addition,

- The velocity distribution function is said *inhomogeneous* when changes with $\boldsymbol{r}$ and *homogeneous* otherwise.
- When $f_\alpha(\boldsymbol{v},\boldsymbol{r},t)$ depends on the direction of the speed de $\boldsymbol{v}$ it is said *anisotropic* and *isotropic* when is a function of $v = |\boldsymbol{v}|$.
- The velocity distribution function $f_\alpha(\boldsymbol{v},\boldsymbol{r})$ is *stationary* when $(\partial f_\alpha/\partial t = 0)$.

The distribution function $f_\alpha(t,\boldsymbol{r},\boldsymbol{v})$ depends on seven independent variables and its time derivative is,

$$\frac{df_\alpha}{dt} = \frac{\partial f_\alpha}{\partial t} + \sum_i \left(\frac{\partial f_\alpha}{\partial x_i}\frac{dx_i}{dt}\right) + \sum_i \left(\frac{\partial f_\alpha}{\partial v_i}\frac{dv_i}{dt}\right)$$

that may be cast as,

$$\frac{df_\alpha}{dt} = \frac{\partial f_\alpha}{\partial t} + \boldsymbol{v} \cdot \nabla_{\mathbf{r}} \, f_\alpha + \boldsymbol{a} \cdot \nabla_{\mathbf{v}} \, f_\alpha$$

The operators,

$$\nabla_{\boldsymbol{r}} \equiv \left(\frac{\partial}{\partial x} \, \boldsymbol{i} + \frac{\partial}{\partial y} \, \boldsymbol{j} + \frac{\partial}{\partial z} \, \boldsymbol{k} \right) \qquad \text{and,} \qquad \nabla_{\boldsymbol{v}} \equiv \left(\frac{\partial}{\partial v_x} \, \boldsymbol{e}_{v_x} + \frac{\partial}{\partial v_y} \, \boldsymbol{e}_{v_y} + \frac{\partial}{\partial v_z} \, \boldsymbol{e}_{v_z} \right)$$

are the ordinary gradient and $\nabla_{\boldsymbol{v}}$ is the gradient operator with the unit vectors, $(\boldsymbol{e}_{v_x}, \boldsymbol{e}_{v_y}, \boldsymbol{e}_{v_z})$. In order to derive the Boltzmann equation we rewrite the previous expressions and we introduce the force by unit of mass $\boldsymbol{a} = \boldsymbol{F}/m_\alpha$, which is independent of the particle speed $\boldsymbol{v}$. The Eq. for df_α/dt may be simplified using the general expression,

$$\nabla_{\mathbf{v}}(\boldsymbol{A}\phi) = (\nabla_{\mathbf{v}} \cdot \boldsymbol{A}) \, \phi + \boldsymbol{A} \cdot \nabla_{\mathbf{v}} \phi$$

For the acceleration we have,

$$\nabla_{\mathbf{v}} \cdot \boldsymbol{a} = q_\alpha \, (\underbrace{\nabla_{\mathbf{v}} \cdot \boldsymbol{E}}_{\text{null } \boldsymbol{E} \neq \boldsymbol{E}(\boldsymbol{v})}) + q_\alpha \, \nabla_{\mathbf{v}} \cdot (\boldsymbol{v} \wedge \boldsymbol{B}) = q_\alpha \, \nabla_{\mathbf{v}} \cdot (\boldsymbol{v} \wedge \boldsymbol{B})$$

Because the electric $\boldsymbol{E}(\boldsymbol{r}, t)$ and magnetic $\boldsymbol{B}(\boldsymbol{r}, t)$ fields are independent of $\boldsymbol{v}$ therefore, $\nabla_{\mathbf{v}} \cdot \boldsymbol{E} = \nabla_{\mathbf{v}} \cdot \boldsymbol{B} = 0$ Furthermore, $\nabla_{\mathbf{v}} \cdot (\boldsymbol{v} \wedge \boldsymbol{B}) = \boldsymbol{B} \cdot (\nabla_{\mathbf{v}} \wedge \boldsymbol{v}) + \boldsymbol{v} \cdot (\nabla_{\mathbf{v}} \wedge \boldsymbol{B})$ and because $\nabla_{\mathbf{v}} \wedge \boldsymbol{v} = 0$ we may write,

$$\boldsymbol{a} \cdot \nabla_{\mathbf{v}} f_\alpha = q_\alpha \, (\boldsymbol{E} + \boldsymbol{v} \wedge \boldsymbol{B}) \cdot \nabla_{\mathbf{v}} \, f_\alpha = \nabla_{\mathbf{v}} \cdot (\boldsymbol{a} \, f_\alpha)$$

By other hand, using again the identity, $\nabla_{\mathbf{r}} \cdot (\boldsymbol{A} \, \phi) = \phi \, (\nabla_{\mathbf{r}} \cdot \boldsymbol{A}) + \boldsymbol{A} \cdot \nabla_{\mathbf{r}} \, \phi$ and because $\nabla_{\mathbf{r}} \cdot \boldsymbol{v} = 0$ we have,

$$(\boldsymbol{v} \cdot \nabla_{\boldsymbol{r}} \, f_\alpha) = \nabla_{\boldsymbol{r}} \cdot (\boldsymbol{v} \, f_\alpha)$$

and we obtain for the time derivative,

$$\left(\frac{df_\alpha}{dt} \right) = \frac{\partial f_\alpha}{\partial t} + \nabla_{\mathbf{r}} \cdot (\boldsymbol{v} \, f_\alpha) + \nabla_{\mathbf{v}} \cdot (\boldsymbol{a} \, f_\alpha) \tag{5.4}$$

The nonequilibrium velocity distribution functions could eventually remain unaltered during the time evolution of the system. This occurs when $\partial f_\alpha/\partial t \neq 0$ and $df_\alpha/dt = 0$ and in this case the Eq. (5.4) is denominated *Vlasov equation* and its solutions are functions of the constants of motions as also the distribution function itself.

The plasma particles interchange energy and momentum during the collisional processes which are in the origin of the changes in the particle distribution function of colliding species. Hence, $df_\alpha/dt \neq 0$ and we may write,

$$\left(\frac{df_\alpha}{dt} \right) = \left(\frac{\partial f_\alpha}{\partial t} \right)_{col.} = C_s(f_\alpha)$$

where $C_s(f_\alpha)$ is an operator that we will be develop in Sec. (5.1.1) accounting for the variations introduced in $f_\alpha(\boldsymbol{v},\boldsymbol{r},t)$ by all collisional processes. This term in Eq. (5.4) couples the time and space evolution of the distribution functions for the different species. For the α particles we obtain,

$$\frac{\partial f_\alpha}{\partial t} + \nabla_{\mathbf{r}} \cdot (\boldsymbol{v}\, f_\alpha) + \nabla_{\mathbf{v}} \cdot (\frac{\boldsymbol{F}}{m_\alpha}\, f_\alpha) = \, C_s(f_\alpha) \tag{5.5}$$

where $\boldsymbol{F} = \boldsymbol{F}_g + q_\alpha\,(\boldsymbol{E} + \boldsymbol{v} \wedge \boldsymbol{B})$ is the electromagnetic force, q_α the electric charge and $\boldsymbol{F}_g$ other additional forces, as the gravity, ...etc. The operators $\nabla_{\mathbf{r}}$ y $\nabla_{\mathbf{v}}$ respectively represents the gradients defined above.

The resulting equation (5.5) where the collisional operator $C_s(f_\alpha)$ is still undefined is denominated *Boltzmann equation*. This operator relates the changes in $f_\alpha(\boldsymbol{v},\boldsymbol{r},t)$ with the particular properties of each elementary process where the particle specie α is involved. The Boltzmann equation 5.5 is essentially a continuity equation for the velocity distribution function in the phase space $(\boldsymbol{r},\boldsymbol{v},t)$ where the source and sink term $C_s(f_\alpha) = (df_\alpha/dt)_{col.}$ accounts for the time and space evolution introduced by collisions.

The electromagnetic fields inside the plasma bulk are self consistent. They result from the coupling between the fields produced by charged particles in the plasma and the externally applied electromagnetic fields. The Boltzmann equation (5.5) for the evolution of $f_\alpha(\boldsymbol{v},\boldsymbol{r},t)$ needs to be complemented with the Maxwell equations for the electric $\boldsymbol{E}(\boldsymbol{r},t)$ and magnetic $\boldsymbol{B}(\boldsymbol{r},t)$ fields in the plasma.

The probability distribution function $f_\alpha(\boldsymbol{v},\boldsymbol{r},t)$ of Eq. (5.5) also defines the plasma density of charged particles ρ_c and the transported current density $\boldsymbol{J}_c$ are,

$$\rho_c = \sum_\alpha \rho_{e\alpha} = \sum_\alpha q_\alpha n_\alpha(\boldsymbol{r},t) \tag{5.6}$$

$$\boldsymbol{J}_c = \sum_\alpha \boldsymbol{J}_{e\alpha} = \sum_\alpha q_\alpha n_\alpha \boldsymbol{u}_\alpha = q_\alpha \int_{-\infty}^{+\infty} \boldsymbol{v}\, f_\alpha(\,\boldsymbol{v},\,\boldsymbol{r},\,t)\, d\boldsymbol{v} \tag{5.7}$$

and should be introduced in the Maxwell equations,

$$\begin{aligned} \nabla \cdot \boldsymbol{E} &= \rho_c/\epsilon_o & \qquad \nabla \wedge \boldsymbol{E} &= -\frac{\partial \boldsymbol{B}}{\partial t} \\ \nabla \cdot \boldsymbol{B} &= 0 & \qquad \nabla \wedge \boldsymbol{B} &= \frac{1}{c^2}\frac{\partial \boldsymbol{E}}{\partial t} + \frac{\boldsymbol{J}_c}{\epsilon_o c^2} \end{aligned}$$

in order to calculate the electromagnetic fields $\boldsymbol{E}(\boldsymbol{r},t)$ and $\boldsymbol{B}(\boldsymbol{r},t)$.

From a formal point of view, without a proper formulation of the collisional operator, the kinetic approach the plasma physics may be understood as the closure of the Maxwell equations for $\boldsymbol{E}(\boldsymbol{r},t)$ and $\boldsymbol{B}(\boldsymbol{r},t)$ using Boltzmann equation (5.5). Once the particle distribution functions are obtained the physical magnitudes as the local particle density $n_\alpha(\boldsymbol{r},t)$ in Eq. (5.1) or the local velocity $\boldsymbol{u}_\alpha(\boldsymbol{r},t)$ in Eq. (5.3) could be calculated.

5.1.1 The Boltzmann collision integral

In the Boltzmann equation (5.5) *the collision term* accounts for the changes in time introduced in $f_\alpha(\boldsymbol{r}, \boldsymbol{v}_\alpha, t)$ by collisions,

$$\left(\frac{\partial f_\alpha}{\partial t}\right)_{col} = C_s(f_\alpha) = \sum_\beta C(f_\alpha, f_\beta) \tag{5.8}$$

and also denominated *Boltzmann collision integral*. The operator $C(f_\alpha, f_\beta)$ represents the change in the velocity distribution function f_α for the α particles caused by a particular collisional process with the β particles. The sum in Eq. (5.8) is extended over all particle species and elementary processes in the plasma discussed in Chapter (4) where the α particles are involved.

The collision term of the Boltzmann equation $C(f_\alpha, f_\beta)$ could be written in terms of the distribution function only in two ways. The first is applicable for dilute gases and plasmas where the particles are essentially subjected to individual binary collisions.

The other method applies to dense gases and plasmas when the particle is subjected to the attractive and repulsive forces from many other particles simultaneously and individual binary collisions do not exist. In this case the collision term of the Boltzmann equation is proportional to the first and higher derivatives of the distribution function, this is called the Fokker-Planck equation.

Here we are interested in dilute gases and plasmas where binary collisions are dominant and the collision term,

$$C(f_\alpha, f_\beta) = \left(\frac{\partial f_\alpha}{\partial t}\right)_{\alpha\beta}$$

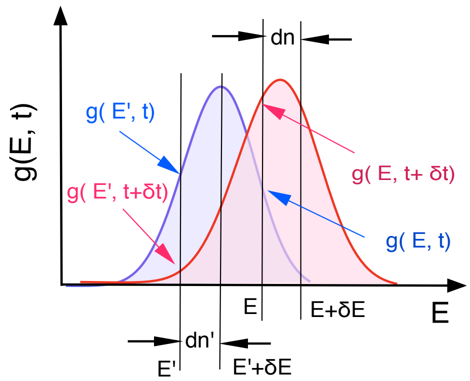

Figure 5.2: The time evolution of the distribution function $g(E, t)$.

represents the change in time of $f_\alpha(\boldsymbol{r}, \boldsymbol{v}_\alpha, t)$ of the projectile particles α for a given collision process with the target particles β. For binary collisions the change is equal to the difference between the rate at which the particles are added to the distribution function, $(\partial f_\alpha/\partial t)^+_{\alpha\beta}$ and the rate $(\partial f_\alpha/\partial t)^-_{\alpha\beta}$ at which are removed.

This process is illustrated in the scheme of Fig. (5.2) where the isotropic energy distribution function $g(E, t)$ which evolves in time between t and $t + \delta t$ under an unspecified collisional process. Within the energy interval $(E', E' + dE)$ the density $dn' = g(E', t + \delta t)\, dE$ of particles decreases, while in the range $(E, E + dE)$ the density $dn = g(E, t + \delta t)\, dE$ grows because $g(E, t + \delta t) > g(E, t)$.

In the case of Fig. (5.2) most particles are accelerated during δt because the distribution function $g(E, t)$ is shifted towards higher energies. The increment $[g(E, t + \delta t) - g(E, t)]\, dE$ gives,

$$\left(\frac{\delta g}{\delta t}\right) dE \simeq \frac{g(E, t + \delta t) - g(E, t)}{\delta t}\, dE > 0$$

that represents the variation in time of the number of particles by volume unit dn with energies within the interval $(E, E + dE)$.

Because the energy of an individual particle is usually different after and before the collision event, the variation $(\delta g/\delta t)$ comes from two sources. First, the loss of particles with original energies within $(E, E + dE)$ that are accelerated or retarded during δt and acquire different energies. In second place, those that after experience the collision, fall in the energy range $(E, E + dE)$.

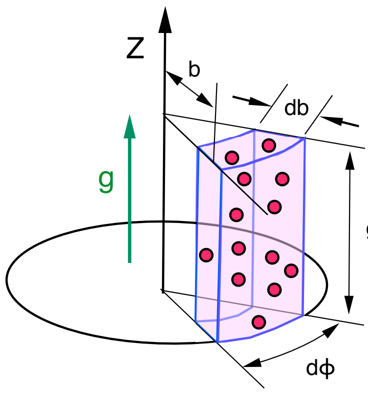

Figure 5.3: The projectile particles P inside the cylindrical section as in Fig. (4.4).

In more general terms, when the α particle with velocity $\boldsymbol{v}_\alpha$ collides with the β particle within the volume $\boldsymbol{r} + d\boldsymbol{r}$ it will usually get a different speed and is therefore removed from interval $f_\alpha(\boldsymbol{r}, \boldsymbol{v}_\alpha, t)\, d\boldsymbol{v}_\alpha$. The rate of removal $(\partial f_\alpha/\partial t)_{col}\, d\boldsymbol{v}_\alpha$ is proportional to the number of collisions per unit time that withdraw α particles within the volume $(\boldsymbol{r}, \boldsymbol{r} + d\boldsymbol{r})$ from the velocity range $(\boldsymbol{v}_\alpha,\, \boldsymbol{v}_\alpha + d\boldsymbol{v}_\alpha)$,

$$\left(\frac{\partial f_\alpha}{\partial t}\right)^-_{\alpha\beta} d\boldsymbol{v}_\alpha$$

In addition, collisions also bring particles within the range $(\boldsymbol{v}_\alpha,\, \boldsymbol{v}_\alpha + d\boldsymbol{v}_\alpha)$ and $(\boldsymbol{r}, \boldsymbol{r} + d\boldsymbol{r})$, and therefore,

$$\left(\frac{\partial f_\alpha}{\partial t}\right)_{\alpha\beta} d\boldsymbol{v}_\alpha = \left[\left(\frac{\partial f_\alpha}{\partial t}\right)^+_{\alpha\beta} - \left(\frac{\partial f_\alpha}{\partial t}\right)^-_{\alpha\beta}\right] d\boldsymbol{v}_\alpha$$

In order to evaluate this time variation we generalize the collision process discussed in Sec. (4.1) between two particles α and β, the latter could be regarded in first place as an scattering center. Their relative velocity is $\boldsymbol{g} = \boldsymbol{v}_\alpha - \boldsymbol{v}_\beta$ in the frame where the β particle remains at rest (also see Fig. 4.4) and $dn_\alpha = f_\alpha(\boldsymbol{r}, \boldsymbol{v}_\alpha, t)\, d\boldsymbol{v}_\alpha$ is the density of incident particles. These are enclosed within the cylindrical section of Fig. (5.3) with height $|\boldsymbol{g}|\,\delta t$ and area $b\, db\, d\epsilon$ has the volume,

$$\delta V = (|\boldsymbol{g}|\,\delta t) \times (b\, db) \times d\phi$$

defined by the impact parameter b that contains $dn_\alpha \times \delta V$ incident α particles inside. Therefore, the number of collisions with a single β particle with velocity $\boldsymbol{v}_\beta$ during δt is,

$$dN_\alpha = dn_\alpha \times \delta V \;= (\, f_\alpha(\boldsymbol{r}, \boldsymbol{v}_\alpha, t)\, d\boldsymbol{v}_\alpha\,) \times (\, |\boldsymbol{g}|\,\delta t \times b\, db \times d\phi\,)$$

The density of scattering β particles with speeds within $(\boldsymbol{v}_\beta,\, \boldsymbol{v}_\beta + d\boldsymbol{v}_\beta)$ is $dn_\beta = f_\beta(\boldsymbol{r}, \boldsymbol{v}_\beta, t)\, d\boldsymbol{v}_\beta$ and, consequently, the number of collisions by volume unit is obtained by multiplying dN_α by the density dn_β of collision centers,

$$dn_\beta \times dn_\alpha \times \delta V$$

As mentioned before, by *direct collisions* the particles α are *removed* from the velocity interval $(\boldsymbol{v}_\alpha,\, \boldsymbol{v}_\alpha + d\boldsymbol{v}_\alpha)$ and the total number of such *direct collisions* between α and β particles with during δt gives,

$$\left(\frac{\partial f_\alpha}{\partial t}\right)^-_{\alpha\beta} d\boldsymbol{v}_\alpha\, \delta t = f_\alpha(\boldsymbol{r}, \boldsymbol{v}_\alpha, t)\, f_\beta(\boldsymbol{r}, \boldsymbol{v}_\beta, t) \times (|\,\boldsymbol{g}|\, \delta t \times b\, db\, d\phi\,)\, d\boldsymbol{v}_\alpha\, d\boldsymbol{v}_\beta$$

However, the *inverse collisions* with β particles also increase the number of α particles with speeds with velocities in the range $(\boldsymbol{v}_\alpha,\, \boldsymbol{v}_\alpha + d\boldsymbol{v}_\alpha)$ within the volume δV. This increment results from α particles with initial speeds into $(\boldsymbol{v}'_\alpha,\, \boldsymbol{v}'_\alpha + d\boldsymbol{v}'_\alpha)$ which after the collision event reach velocities in the interval $(\boldsymbol{v}_\alpha,\, \boldsymbol{v}_\alpha + d\boldsymbol{v}_\alpha)$. Similar arguments as above apply to such *inverse collisions* and the number of α particles *added* to the velocity interval $(\boldsymbol{v}_\alpha,\, \boldsymbol{v}_\alpha + d\boldsymbol{v}_\alpha)$ during δt. Therefore,

$$\left(\frac{\partial f_\alpha}{\partial t}\right)^+_{\alpha\beta} d\boldsymbol{v}_\alpha\, \delta t = f_\alpha(\boldsymbol{r}, \boldsymbol{v}'_\alpha, t)\, f_\beta(\boldsymbol{r}, \boldsymbol{v}'_\beta, t) \times (\,|\boldsymbol{g}'|\, \delta t \times b\, db\, d\phi\,)\, d\boldsymbol{v}'_\alpha\, d\boldsymbol{v}'_\beta$$

where $\boldsymbol{g}' = \boldsymbol{v}'_\alpha - \boldsymbol{v}'_\beta$ and the term $(\,b\, db\, d\phi\,)$ remains unchanged because of the symmetry of collision process under time reversal. Using Eq. (4.7) we may replace,

$$b\, db\, d\phi = \sigma_{\alpha\beta}(g, \theta)\, d\theta\, d\phi = \sigma_{\alpha\beta}(g, \theta)\, d\Omega$$

where $d\Omega$ is the solid angle of figure (4.4). The change in the particle distribution function is,

$$C(f_\alpha, f_\beta)\, d\boldsymbol{v}_\alpha = \left(\frac{\partial f_\alpha}{\partial t}\right)_{\alpha\beta} d\boldsymbol{v}_\alpha = \left[\left(\frac{\partial f_\alpha}{\partial t}\right)^+_{col} - \left(\frac{\partial f_\alpha}{\partial t}\right)^-_{col}\right] d\boldsymbol{v}_\alpha$$

and writing, $f'_\alpha = f_\alpha(\boldsymbol{r}, \boldsymbol{v}'_\alpha, t)$ and $f'_\beta = f_\beta(\boldsymbol{r}, \boldsymbol{v}'_\beta, t)$ we obtain,

$$C(f_\alpha, f_\beta)\, d\boldsymbol{v}_\alpha = \left(f'_\alpha\, f'_\beta\, |\boldsymbol{g}'|\, d\boldsymbol{v}'_\alpha\, d\boldsymbol{v}'_\beta - f_\alpha\, f_\beta\, |\boldsymbol{g}|\, d\boldsymbol{v}_\alpha\, d\boldsymbol{v}_\beta\right)\, \sigma_{\alpha\beta}(g, \theta)\, d\Omega$$

The properties of each particular collision are introduced at this point, for example, in *elastic* collisions the energy is conserved and hence,

$$|\boldsymbol{g}| = |\boldsymbol{v}_\alpha - \boldsymbol{v}_\beta| = |\boldsymbol{v}'_\alpha - \boldsymbol{v}'_\beta| = |\boldsymbol{g}'|$$

and also $d\boldsymbol{v}_\alpha\, d\boldsymbol{v}_\alpha = d\boldsymbol{v}'_\alpha\, d\boldsymbol{v}'_\alpha$. Therefore, the Boltzmann collision integral $C(f_\alpha, f_\beta)$ for the elastic collisions between the α and β particles becomes,

$$C(f_\alpha, f_\beta) = \int \int \left(f'_\alpha\, f'_\beta - f_\alpha\, f_\beta\right)\, |\boldsymbol{g}|\, \sigma_{\alpha\beta}(g, \theta)\, d\Omega\, d\boldsymbol{v}_\beta \tag{5.9}$$

This collision integral connects the cross sections (see Sec. 4.1) of elementary processes described in Chap. (4) with the time evolution of the velocity distribution function. As we can see, the properties of collisions at microscopic level determine the macroscopic transport properties of the plasma.

5.2 The transport fluid equations

The following derivation of the transport fluid equations essentially comes from the classical Ref. [18] and an introductory approach is in Ref. [25]. An updated and rigorous formulation is found in Ref. [19].

The macroscopic fluid transport equations for a plasma are deduced by *taking moments* of the Boltzmann equation (5.5) where the low order moments are proportional to the averages of physical magnitudes. The moment $\boldsymbol{M}^{(k)}(\boldsymbol{r},t)$ of order k of the distribution function $g(\boldsymbol{v},\boldsymbol{r},t)$ is formally defined as the tensor,

$$\boldsymbol{M}^{(k)}(\boldsymbol{r},t) = \int_{-\infty}^{+\infty} \underbrace{(\boldsymbol{v} \otimes \boldsymbol{v} \otimes \cdots \otimes \boldsymbol{v})}_{\text{k times}}\, g(\,\boldsymbol{v},\,\boldsymbol{r},\,t)\, d\boldsymbol{v} \tag{5.10}$$

The complete set of moments $\boldsymbol{M}^{(k)}(\boldsymbol{r},t)$ for $k = 1, 2, \ldots$ characterizes $g(\boldsymbol{v},\boldsymbol{r},t)$ when the distribution function is smooth enough.

These moments are tensors or scalars related with the averages in the phase space of quantities of physical interest. For the particle specie α, the average of the function $H_\alpha(\boldsymbol{v},\boldsymbol{r},\,t)$ is defined in the phase space $(\boldsymbol{r},\boldsymbol{v})$ as,

$$< H_\alpha(\boldsymbol{v},\boldsymbol{r},\,t) >= \frac{1}{n_\alpha} \int_{-\infty}^{+\infty} H_\alpha(\,\boldsymbol{v},\,\boldsymbol{r},t\,)\, f_\alpha(\,\boldsymbol{v},\,\boldsymbol{r},\,t)\, d\boldsymbol{v} \tag{5.11}$$

Taking $H_\alpha(\boldsymbol{v},\boldsymbol{r},\,t) = 1$ we obtain the normalization condition $< H_\alpha >= 1$ (see Eq. 5.2) or equivalently,

$$n_\alpha(\,\boldsymbol{r},\,t) = \int_{-\infty}^{+\infty} f_\alpha(\,\boldsymbol{v},\,\boldsymbol{r},\,t)\, d\boldsymbol{v}$$

that corresponds to the local particle density of Eq. (5.1). Using $H_\alpha(\boldsymbol{v},\boldsymbol{r},\,t) = \boldsymbol{v}$ the average $< H_\alpha >= \boldsymbol{u}_\alpha(\boldsymbol{r},t)$ provides the flux of α particles,

$$\boldsymbol{\Gamma}_\alpha(\boldsymbol{r},t) = n_\alpha(\,\boldsymbol{r},\,t)\,\boldsymbol{u}_\alpha(\boldsymbol{r},t) = \int_{-\infty}^{+\infty} \boldsymbol{v}\, f_\alpha(\,\boldsymbol{v},\,\boldsymbol{r},\,t)\, d\boldsymbol{v} \tag{5.12}$$

and is related with the local velocity $\boldsymbol{u}_\alpha(\boldsymbol{r},t)$ of Eq. (5.3).

The second order moment is the tensor $H_\alpha(\boldsymbol{v},\boldsymbol{r},\,t) = \boldsymbol{v} \otimes \boldsymbol{v}$ provides the flux of momentum in the laboratory frame and is denominated *stress tensor*,

$$\widetilde{\boldsymbol{S}}_\alpha(\boldsymbol{r},t) = \int_{-\infty}^{+\infty} m_\alpha\,(\boldsymbol{v} \otimes \boldsymbol{v})\, f_\alpha(\,\boldsymbol{v},\,\boldsymbol{r},\,t)\, d\boldsymbol{v} \tag{5.13}$$

The average kinetic energy is proporcional to $H_\alpha(\boldsymbol{v},\boldsymbol{r},\,t) = (\boldsymbol{v} \cdot \boldsymbol{v}) = v^2$ while the *density flux of energy* is related with $H_\alpha(\boldsymbol{v},\boldsymbol{r},\,t) = v^2\,\boldsymbol{v}$,

$$\boldsymbol{K}_\alpha(\boldsymbol{r},t) = \int_{-\infty}^{+\infty} (\frac{m_\alpha\, v^2}{2})\,\boldsymbol{v}\, f_\alpha(\,\boldsymbol{v},\,\boldsymbol{r},\,t)\, d\boldsymbol{v} \tag{5.14}$$

We now face the problem of the *closure* of plasma fluid equations because the rigorous mathematical formulation requires the determination of *all* moments $\boldsymbol{M}^{(k)}(\boldsymbol{r}, t)$ of the particle distribution function for $k = 1, \ldots, N$. However, the fluid transport equations only make use of few averages, as $\boldsymbol{u}_\alpha(\boldsymbol{r}, t)$, $\widetilde{\boldsymbol{S}}_\alpha(\boldsymbol{r}, t)$, $\boldsymbol{K}_\alpha(\boldsymbol{r}, t)$, ... etc, which are related with measurable physical quantities. These equations will always be always incomplete because couple the low order with higher order moments. For example, the continuity equation relates n_α with the speed $\boldsymbol{u}_\alpha$, which in turn depends on $\widetilde{\boldsymbol{S}}_\alpha$ through the momentum transport equation, ... etc. We shall return in Sec. (5.2.5) to the problem of the *closure* which is inherent to the fluid description of a plasma.

Since the fluid equations result from averages, the transport phenomena over short times and length scales of microscopic level result smoothed out. Therefore, the fluid models are useful when the collisional mean free paths of all species are much shorter than the characteristic lengths of macroscopic motion of the plasma. The frequent collisions over short distances bring the plasma into a *local* or *partial equilibrium* as discussed in Sec. (4.6) where the macroscopic magnitudes $n_\alpha(\boldsymbol{r}, t)$, $k_B T_\alpha(\boldsymbol{r}, t)$, ...etc are not uniform and time dependent.

5.2.1 The averages of the distribution function.

In the fluid approximation the velocity of a particle $\boldsymbol{v} = \boldsymbol{u}_\alpha + \boldsymbol{w}$ is expressed as the sum of a streaming fluid speed $\boldsymbol{u}_\alpha(\,\boldsymbol{r},\, t)$ defined by Eq. (5.12) and a random or velocity $\boldsymbol{w}$. The averages over the components of $\boldsymbol{w}$ are $< w_x >=< w_y >=< w_z >= 0$, while $< w^2 >$ is always positive. Hence,

$$E_\alpha(\boldsymbol{r}, t) = \int_{-\infty}^{+\infty} \frac{m_\alpha v^2}{2}\, f_\alpha(\,\boldsymbol{v},\, \boldsymbol{r},\, t)\, d\boldsymbol{v}$$

is equivalent to,

$$E_\alpha = n_\alpha < \frac{m_\alpha}{2}\, v^2 >= n_\alpha\, \frac{m_\alpha}{2}\,(u_\alpha^2 + < w^2 >) = \rho_\alpha \frac{u_\alpha^2}{2} + E_{i\alpha} \tag{5.15}$$

The first term with $\rho_\alpha = m_\alpha n_\alpha$ represents the kinetic energy and the second $E_{i\alpha}$ is the corresponding local internal energy. Each plasma particle specie α may be regarded as an ideal gas and in this case, $E_{i\alpha} = \rho_\alpha\, k_B T_\alpha/(\gamma - 1)$.

We assume the existence of *local equilibrium* for each specie in the plasma (equivalently, its velocity distribution function could be approximated by a local Maxwellian as in Sec. 4.6.2). The local kinetic temperature [1] $k_B T_\alpha(\boldsymbol{r}, t)$ for the α particle specie is defined as,

$$\frac{3}{2}\, n_\alpha(\boldsymbol{r}, t) k_B T_\alpha(\boldsymbol{r}, t) = \int_{-\infty}^{+\infty} (\frac{m_\alpha\, w^2}{2})\, f_\alpha(\,\boldsymbol{v},\, \boldsymbol{r},\, t)\, d\boldsymbol{v} \tag{5.16}$$

Equivalently, the internal energy is calculated through Eq. (5.11) as the average of the scalar function $e_{i\alpha} =< H_\alpha >$ where,

$$H_\alpha = \frac{m_\alpha}{2}\, w^2$$

[1] For simplicity, the α particles are considered as an ideal monoatomic gas with $1/(\gamma - 1) = 3/2$.

The stress tensor (5.13) is given by the second order moment,

$$\widetilde{\boldsymbol{S}}_\alpha(\boldsymbol{r},t) = \int_{-\infty}^{+\infty} m_\alpha\,(\boldsymbol{v}\otimes\boldsymbol{v})\,f_\alpha(\,\boldsymbol{v},\,\boldsymbol{r},\,t)\,d\boldsymbol{v} = m_\alpha\,n_\alpha(\boldsymbol{r},t)\ <\boldsymbol{v}\otimes\boldsymbol{v}> \tag{5.17}$$

and in matrix notation the components are,

$$\begin{pmatrix} v_x^2 & v_xv_y & v_xv_z \\ v_yv_x & v_y^2 & v_yv_z \\ v_zv_x & v_zv_y & v_z^2 \end{pmatrix}$$

Again, using $\boldsymbol{v} = \boldsymbol{u}_\alpha + \boldsymbol{w}$ the average of the components of the stress tensor are of the form $<(u_{\alpha i} + w_i)(u_{\alpha j} + w_j)>$ hence,

$$S_{ij} = m_\alpha\,n_\alpha\,(< u_{\alpha i}u_{\alpha j} > + < w_iw_j > + u_{\alpha i} < w_j > + u_{\alpha j} < w_i >)$$

where $< w_i >$ are null. We have,

$$\widetilde{\boldsymbol{S}}_\alpha = m_\alpha\,n_\alpha\,(\boldsymbol{u}_\alpha\otimes\boldsymbol{u}_\alpha) + m_\alpha\,n_\alpha < \boldsymbol{w}\otimes\boldsymbol{w} >$$

The second term $\widetilde{\boldsymbol{G}}_\alpha = m_\alpha\,n_\alpha < \boldsymbol{w}\otimes\boldsymbol{w} >$ could be written as the sum of the two tensors, $\widetilde{\boldsymbol{G}}_\alpha = \widetilde{\boldsymbol{P}}_\alpha + \widetilde{\boldsymbol{\Pi}}_\alpha$ where,

$$\widetilde{\boldsymbol{P}}_\alpha = m_\alpha\,n_\alpha \begin{pmatrix} < w_x^2 > & 0 & 0 \\ 0 & < w_y^2 > & 0 \\ 0 & 0 & < w_y^2 > \end{pmatrix}$$

$$\widetilde{\boldsymbol{\Pi}}_\alpha = m_\alpha\,n_\alpha \begin{pmatrix} 0 & < w_xw_y > & < w_xw_z > \\ < w_yw_x > & 0 & < w_yw_z > \\ < w_zw_x > & < w_zw_y > & 0 \end{pmatrix} \tag{5.18}$$

Both $\widetilde{\boldsymbol{\Pi}}_\alpha$ and $\widetilde{\boldsymbol{G}}_\alpha$ are symmetric matrices where $< w_iw_j >=< w_jw_i >$ are equal. Because the speed $\boldsymbol{w}$ is random we have,

$$< w_x^2 >=< w_y^2 >=< w_z^2 >= \frac{< w^2 >}{3}$$

Then, the tensor $\widetilde{\boldsymbol{P}}_\alpha$ is proportional to the unity matrix $\widetilde{\boldsymbol{I}}$ and its trace may be identified with the usual scalar pressure,

$$p_\alpha = \frac{1}{3}Tr(\widetilde{P}_\alpha)$$

or equivalently using the Eq. (5.11) with,

$$p_\alpha(\boldsymbol{r},t) = \frac{m_\alpha}{3}\int_{-\infty}^{+\infty} w^2\,f_\alpha(\,\boldsymbol{v},\,\boldsymbol{r},\,t)\,d\boldsymbol{v} = \frac{m_\alpha n_\alpha}{3} < w^2 >$$

This is in agreement with the previous expression for the kinetic temperature (5.16) and both magnitudes are related by the equation of state for the ideal gas,

$$p_\alpha(\boldsymbol{r},t) = n_\alpha(\boldsymbol{r},t)\, k_B T_\alpha(\boldsymbol{r},t)$$

The components $< w_i\, w_j >$ outside the diagonal in the tensor $\widetilde{\mathbf{\Pi}}$ will be develop later and are related with other components of the *stress tensor*, as the viscosity in ordinary fluids. The final form of the stress tensor is,

$$\widetilde{\boldsymbol{S}}_\alpha = m_\alpha\, n_\alpha\, (\boldsymbol{u}_\alpha \otimes \boldsymbol{u}_\alpha) + p_\alpha\, \widetilde{\boldsymbol{I}} + \widetilde{\mathbf{\Pi}}_\alpha \tag{5.19}$$

Finally, for the vector of energy density flux $\boldsymbol{K}_\alpha(\boldsymbol{r},t)$ we have,

$$\boldsymbol{K}_\alpha(\boldsymbol{r},t) = \int_{-\infty}^{+\infty} (\frac{m_\alpha\, v^2}{2})\, \boldsymbol{v}\, f_\alpha(\, \boldsymbol{v},\, \boldsymbol{r},\, t)\, d\boldsymbol{v} = \frac{m_\alpha n_\alpha}{2}\ < v^2\, \boldsymbol{v} > \tag{5.20}$$

After substitution, the terms non null are,

$$< v^2\, \boldsymbol{v} >= (u_\alpha^2 + < w^2 >)\, \boldsymbol{u}_\alpha + < w^2 \boldsymbol{w} > + 2\ < (\boldsymbol{w} \cdot \boldsymbol{u}_\alpha)\, \boldsymbol{w} >$$

The first term proportional to the transport of the energy $E_\alpha\, \boldsymbol{u}_\alpha$ introduced in Eq. (5.15). The components of the last vector are of the form, $\boldsymbol{A} =< (\boldsymbol{w} \cdot \boldsymbol{u}_\alpha)\, \boldsymbol{w} >$,

$$\boldsymbol{A} =< (\sum_j w_j\, u_{\alpha j})\, \boldsymbol{w} >$$

for the k component,

$$A_k =< (\sum_j w_j u_{\alpha j})\, w_k >= \sum_j < w_j w_k > u_{\alpha j}$$

this is equivalent to the contraction of the symmetric second order tensor $\widetilde{\mathbf{G}}$ con $\boldsymbol{u}_\alpha$. Hence,

$$\boldsymbol{A} =< (\boldsymbol{w} \cdot \boldsymbol{u}_\alpha)\, \boldsymbol{w} >= \widetilde{\mathbf{G}} \colon \boldsymbol{u}_\alpha$$

The *heat flux density* vector for the particle specie α is defined as,

$$\boldsymbol{q}_\alpha = \int_{-\infty}^{+\infty} (\frac{m_\alpha w^2}{2})\, \boldsymbol{w}\, f_\alpha(\, \boldsymbol{v},\, \boldsymbol{r},\, t)\, d\boldsymbol{v} = \frac{m_\alpha n_\alpha}{2} < w^2 \boldsymbol{w} > \tag{5.21}$$

and we obtain,

$$\boldsymbol{K}_\alpha(\boldsymbol{r},t) = E_\alpha\, \boldsymbol{u}_\alpha + \boldsymbol{q}_\alpha + \widetilde{\mathbf{G}}_\alpha \colon \boldsymbol{u}_\alpha \tag{5.22}$$

5.2.2 The equation of continuity.

The continuity fluid equation for the α particle specie is obtained integrating the Eq. (5.5) over all possible velocities,

$$\int_{-\infty}^{+\infty} \frac{\partial f_\alpha}{\partial t}\, d\boldsymbol{v} + \int_{-\infty}^{+\infty} \nabla_{\mathbf{r}} \cdot (\boldsymbol{v}\, f_\alpha)\, d\boldsymbol{v} + \int_{-\infty}^{+\infty} \nabla_{\mathbf{v}} \cdot (\frac{\boldsymbol{F}_e}{m_\alpha}\, f_\alpha)\, d\boldsymbol{v} = \int_{-\infty}^{+\infty} C_s(f_\alpha)\, d\boldsymbol{v}$$

The details of the integral over the Boltzmann collision operator $C_s(f_\alpha)$ will be discussed later and for the two first terms the integrals over $\boldsymbol{v}$ can be permuted with the operators. Using the divergence theorem for the third term we obtain,

$$\frac{\partial}{\partial t}\int_{-\infty}^{+\infty} f_\alpha\, d\boldsymbol{v} + \nabla_{\mathbf{r}} \cdot \int_{-\infty}^{+\infty} (\boldsymbol{v}\, f_\alpha)\, d\boldsymbol{v} + \underbrace{\int_{s(v)} (\frac{\boldsymbol{F}_e}{m_\alpha}\, f_\alpha) \cdot d\boldsymbol{S}}_{f_\alpha \text{ is bounded} \rightarrow 0} = \int_{-\infty}^{+\infty} C_s(f_\alpha)\, d\boldsymbol{v}$$

The two first integrals are n_α y $n_\alpha \boldsymbol{u}_\alpha$, and because f_α is a bounded function the third integral is null. Finally we obtain the continuity equation for the specie α,

$$\frac{\partial n_\alpha}{\partial t} + \nabla_{\mathbf{r}} \cdot (n_\alpha \boldsymbol{u}_\alpha) = \int_{-\infty}^{+\infty} C_s(f_\alpha)\, d\boldsymbol{v}$$

The right term represents the moment of the Boltzmann collisional operator that will be discussed later in detail. This equation may be also interpreted as the time derivative of the particle number density $n_\alpha(\boldsymbol{r}, t)$ as,

$$\frac{dn_\alpha}{dt} = \frac{\partial n_\alpha}{\partial t} + \sum_i \left(\frac{\partial n_\alpha}{\partial x_i} \frac{dx_i}{dt} \right) = \int_{-\infty}^{+\infty} C_s(f_\alpha)\, d\boldsymbol{v}$$

Therefore, as discussed in Secs. (4.4.1.2) and (4.4.4.1) the above integral of the Boltzmann collision operator $C_s(f_\alpha)$ represents the difference between the source and sink term for the α particles,

$$\int_{-\infty}^{+\infty} C_s(f_\alpha)\, d\boldsymbol{v} = F_\alpha - S_\alpha \tag{5.23}$$

Using Eqs. (4.8) and (4.12) we have, $F_\alpha = \nu_I\, n_e$ y $S_\alpha = k_R n_i\, n_e$ respectively are the number α of particles produced or destroyed by time unit. Finally the fluid continuity equation becomes,

$$\frac{\partial n_\alpha}{\partial t} + \nabla_{\mathbf{r}} \cdot (n_\alpha \boldsymbol{u}_\alpha) = F_\alpha - S_\alpha \tag{5.24}$$

5.2.3 The momentum transport equation.

The next moment of the Boltzmann equation with physical meaning is obtained by multiplying the Eq. (5.5) by $m_\alpha \boldsymbol{v}$ and later integrating over the velocities $\boldsymbol{v}$,

$$\int_{-\infty}^{+\infty} m_\alpha \boldsymbol{v} \frac{\partial f_\alpha}{\partial t} d\boldsymbol{v} + \int_{-\infty}^{+\infty} m_\alpha \boldsymbol{v}\, \nabla_{\mathbf{r}} \cdot (\boldsymbol{v}\, f_\alpha)\, d\boldsymbol{v} + \int_{-\infty}^{+\infty} m_\alpha \boldsymbol{v}\, \nabla_{\mathbf{v}} \cdot (\boldsymbol{F}_e\, f_\alpha) d\boldsymbol{v} = \int_{-\infty}^{+\infty} m_\alpha\, \boldsymbol{v}\, C_s(f_\alpha)\, d\boldsymbol{v}$$

The first term is,

$$\int_{-\infty}^{+\infty} m_\alpha \boldsymbol{v} \frac{\partial f_\alpha}{\partial t} d\boldsymbol{v} = m_\alpha \frac{\partial}{\partial t}(n_\alpha < \boldsymbol{v} >) = m_\alpha \frac{\partial}{\partial t}(n_\alpha \boldsymbol{u}_\alpha)$$

while the second is transformed using the vector identity,

$$\nabla_{\mathbf{r}} \cdot [\boldsymbol{v} \otimes (\boldsymbol{v}\, f)] = [\boldsymbol{v}\ \cdot \nabla_{\mathbf{r}}]\, (\boldsymbol{v}\, f) + \underbrace{[(f\boldsymbol{v}) \cdot\ \nabla_{\mathbf{r}}]\ \boldsymbol{v}}_{0} = (\boldsymbol{v}\ \cdot \nabla_{\mathbf{r}})(\boldsymbol{v}\, f)$$

Hence,

$$\int_{-\infty}^{+\infty} m_\alpha \boldsymbol{v}\, \nabla_{\mathbf{r}}\ \cdot (\boldsymbol{v}\, f_\alpha)\, d\boldsymbol{v} = \nabla_{\mathbf{r}} \cdot \left[\int_{-\infty}^{+\infty} m_\alpha\, (\boldsymbol{v} \otimes \boldsymbol{v})\, f_\alpha\, d\boldsymbol{v}\right] = \nabla_{\mathbf{r}} \cdot (m_\alpha n_\alpha < \boldsymbol{v} \otimes \boldsymbol{v} >)$$

and we recover the stress tensor $\widetilde{\boldsymbol{S}}_\alpha(\boldsymbol{r}, t) = m_\alpha\, n_\alpha(\boldsymbol{r}, t)\ < \boldsymbol{v} \otimes \boldsymbol{v} >$ of Eq. (5.17). Again,

$$\nabla_{\mathbf{v}} \cdot [(\boldsymbol{F}_e f_\alpha) \otimes \boldsymbol{v}] = (\boldsymbol{v} \cdot \nabla_{\mathbf{v}})\, (\boldsymbol{F}_e\, f_\alpha) + (\boldsymbol{F}_e f_\alpha \cdot \nabla_{\mathbf{v}})\, \boldsymbol{v} = \boldsymbol{v}\, \nabla_{\mathbf{v}} \cdot (\boldsymbol{F}_e f_\alpha) + f_\alpha\, \boldsymbol{F}_e$$

where $(\boldsymbol{F}_e f_\alpha \cdot \nabla_{\mathbf{v}})\, \boldsymbol{v} = f_\alpha\, \boldsymbol{F}_e$. The third integral becomes the sum of two terms,

$$\int_{-\infty}^{+\infty} \boldsymbol{v}\, \nabla_{\mathbf{v}} \cdot (\boldsymbol{F}_e\, f_\alpha)\, d\boldsymbol{v} = \underbrace{\int_{-\infty}^{+\infty} \nabla_{\mathbf{v}} \cdot [f_\alpha\, (\boldsymbol{v} \otimes \boldsymbol{F}_e)]\, d\boldsymbol{v}}_{(\text{Div. Theor.} \to 0)} - \int_{-\infty}^{+\infty} f_\alpha \boldsymbol{F}_e\, d\boldsymbol{v}$$

Because the distribution function is bounded, the integral over the divergence is null again. Then,

$$n_\alpha < \boldsymbol{F}_e >= q_\alpha\, \boldsymbol{E} \int_{-\infty}^{+\infty} f_\alpha\, d\boldsymbol{v} + q_\alpha\, (\,[\int_{-\infty}^{+\infty} \boldsymbol{v}\, f_\alpha\, d\boldsymbol{v}] \wedge \boldsymbol{B}\,)$$

and using again the Eqs. (5.1) and (5.3) for n_α and $\boldsymbol{u}_\alpha$ we introduce the electric charge density $\rho_{e\alpha} = q_\alpha\, n_\alpha$ and current density $\boldsymbol{J}_{e\alpha} = q_\alpha\, n_\alpha\, \boldsymbol{u}_\alpha$ for the specie α,

$$n_\alpha < \boldsymbol{F}_e >= q_\alpha n_\alpha [\boldsymbol{E} + (\boldsymbol{u}_\alpha \wedge \boldsymbol{B})] = \rho_{e\alpha} \boldsymbol{E} + \boldsymbol{J}_{e\alpha} \wedge \boldsymbol{B}$$

Now, the equation for momentum transport reads,

$$m_\alpha \frac{\partial}{\partial t}(n_\alpha \boldsymbol{u}_\alpha) + \nabla_{\mathbf{r}} \cdot \widetilde{\boldsymbol{S}}_\alpha = \rho_{e\alpha} \boldsymbol{E} + \boldsymbol{J}_{e\alpha} \wedge \boldsymbol{B} + \boldsymbol{R}_\alpha$$

where the vector $\boldsymbol{R}_\alpha$ represents the first moment of the Boltzmann collision operator,

$$\boldsymbol{R}_\alpha = \int_{-\infty}^{+\infty} m_\alpha \, \boldsymbol{v} \, C_s(f_\alpha) \, d\boldsymbol{v} \tag{5.25}$$

that will be discussed later. The divergence of the stress tensor $\widetilde{\boldsymbol{S}}_\alpha$ becomes,

$$\nabla_{\mathbf{r}} \cdot \widetilde{\boldsymbol{S}}_\alpha = \nabla_{\mathbf{r}} \cdot [n_\alpha \, (\boldsymbol{u}_\alpha \otimes \boldsymbol{u}_\alpha)] + \nabla_{\mathbf{r}} \cdot (p_\alpha \, \widetilde{\boldsymbol{I}}) + \nabla_{\mathbf{r}} \cdot \widetilde{\boldsymbol{\Pi}}_\alpha$$

$$\nabla_{\mathbf{r}} \cdot \widetilde{\boldsymbol{S}}_\alpha = n_\alpha (\boldsymbol{u}_\alpha \cdot \nabla_{\mathbf{r}}) \, \boldsymbol{u}_\alpha + \boldsymbol{u}_\alpha \, [\nabla_{\mathbf{r}} \cdot (n_\alpha \boldsymbol{u}_\alpha)] + \nabla_{\mathbf{r}} \, p_\alpha + \nabla_{\mathbf{r}} \cdot \widetilde{\boldsymbol{\Pi}}_\alpha$$

Substituting in the above transport equation we have,

$$\begin{aligned} m_\alpha n_\alpha \frac{\partial \boldsymbol{u}_\alpha}{\partial t} + m_\alpha \boldsymbol{u}_\alpha \left[\frac{\partial n_\alpha}{\partial t} + \nabla_{\mathbf{r}} \cdot (n_\alpha \boldsymbol{u}_\alpha) \right] + m_\alpha n_\alpha (\boldsymbol{u}_\alpha \nabla_{\mathbf{r}} \cdot) \, \boldsymbol{u}_\alpha \\ + \nabla_{\mathbf{r}} \, p_\alpha + \nabla_{\mathbf{r}} \cdot \widetilde{\boldsymbol{\Pi}}_\alpha = \rho_{e\alpha} \boldsymbol{E} + \boldsymbol{J}_{e\alpha} \wedge \boldsymbol{B} + \boldsymbol{R}_\alpha \end{aligned}$$

The second term may be related with the fluid continuity equation (5.24),

$$m_\alpha \boldsymbol{u}_\alpha \left(\frac{\partial n_\alpha}{\partial t} + \nabla_{\mathbf{r}} \cdot (n_\alpha \boldsymbol{u}_\alpha) \right) = m_\alpha \boldsymbol{u}_\alpha (F_\alpha - S_\alpha)$$

This represents the increase or decrese of momentum associated with the production or loss of α particles. Finally, the momentum transport equation results as,

$$m_\alpha n_\alpha \frac{D \boldsymbol{u}_\alpha}{Dt} = -\nabla_{\mathbf{r}} \, p_\alpha - \nabla_{\mathbf{r}} \cdot \widetilde{\boldsymbol{\Pi}}_\alpha - m_\alpha \boldsymbol{u}_\alpha (F_\alpha - S_\alpha) + \rho_{e\alpha} \, \boldsymbol{E} + \boldsymbol{J}_{e\alpha} \wedge \boldsymbol{B} + \boldsymbol{R}_\alpha \tag{5.26}$$

where is introduced the operator $D/Dt = \partial/\partial t + (\boldsymbol{u}_\alpha \cdot \nabla_{\mathbf{r}})$.

The Eq. (5.26) is equivalent to the transport equation for a macroscopic fluid with electric charge density $\rho_{e\alpha}$ and current density $\boldsymbol{J}_{e\alpha}$. In addition to the Coulomb interaction, the motion of the particles in the plasma may be also eventually coupled by collisions with other particle species as neutrals. In fact, in Eq. (5.26) the vector $\boldsymbol{R}_\alpha$ and the tensor $\widetilde{\boldsymbol{\Pi}}_\alpha$ accounting for momentum exchange by collisions remain undetermined. Therefore, in order to complete the fluid transport equations, detailed models are required for the different particle collisions between in the collision operator $C_s(f_\alpha)$ and its moments as Eqs. (5.23) and (5.25).

5.2.4 The energy transport equation.

The moment of the Boltzmann equation related with the transport of energy is calculated by multiplying the Eq. (5.5) by $m_\alpha v^2/2$ and integrating and over the velocity as before,

$$\begin{aligned}&\frac{\partial}{\partial t}(n_\alpha < \frac{m_\alpha v^2}{2} >) + \nabla_{\mathbf{r}} \cdot (n_\alpha < \frac{m_\alpha v^2}{2} \boldsymbol{v} >)\\ +&\frac{m_\alpha}{2}\int_{-\infty}^{+\infty} v^2 \nabla_{\mathbf{v}} \cdot (\boldsymbol{F}_e\, f_\alpha) d\boldsymbol{v} = \int_{-\infty}^{+\infty} \frac{m_\alpha v^2}{2}\, C_s(f_\alpha)\, d\boldsymbol{v}\end{aligned} \tag{5.27}$$

In the following, Q_α represents the second moment of the collision operator $C_s(f_\alpha)$,

$$Q_\alpha = \int_{-\infty}^{+\infty} \frac{m_\alpha v^2}{2}\, C_s(f_\alpha)\, d\boldsymbol{v} \tag{5.28}$$

that will be discussed later in detail. The integrand of the third term is transformed by using,

$$\nabla_{\mathbf{v}} \cdot (\boldsymbol{F}\, v^2\, f) = v^2 \nabla_{\mathbf{v}} \cdot (\boldsymbol{F}\, f) + (f\, \boldsymbol{F}) \cdot (\nabla_{\mathbf{v}}\, v^2)$$

and therefore,

$$\int_{-\infty}^{+\infty} v^2 \nabla_{\mathbf{v}} \cdot (\boldsymbol{F}_e\, f_\alpha)\, d\boldsymbol{v} = \int_{-\infty}^{+\infty} \underbrace{\nabla_{\mathbf{v}} \cdot (v^2 \boldsymbol{F}_e\, f_\alpha)}_{(\text{Div. Theor.} \to 0)} \}\, d\boldsymbol{v} - \int_{-\infty}^{+\infty} (\boldsymbol{F}_e\, f_\alpha) \cdot \nabla_{\mathbf{v}}(v^2)\, d\boldsymbol{v}$$

The first integral is again null by using the divergence theorem and $\nabla_{\mathbf{v}}(v^2) = 2\, \boldsymbol{v}$,

$$-\int_{-\infty}^{+\infty} (\boldsymbol{F}_e\, f_\alpha) \cdot \nabla_{\mathbf{v}}(v^2)\, d\boldsymbol{v} = -\int_{-\infty}^{+\infty} (\boldsymbol{F}_e\, f_\alpha) \cdot (2\boldsymbol{v})\, d\boldsymbol{v} = -2 n_\alpha < \boldsymbol{F}_\alpha \cdot \boldsymbol{v} >$$

where the last term is related with the work of the electric field. Introducing the current density $\boldsymbol{J}_\alpha$ as before and using the Eq. (5.15) the transport equation reads,

$$\frac{\partial E}{\partial t} + \nabla_{\mathbf{r}} \cdot (\frac{m_\alpha n_\alpha}{2} < v^2 \boldsymbol{v} >) + \frac{m_\alpha}{2}(-\frac{2}{m_\alpha} \boldsymbol{J}_{e\alpha} \cdot \boldsymbol{E}) = Q_\alpha$$

The average $< v^2\, \boldsymbol{v} >$ is related with the second order moment $\boldsymbol{K}_\alpha(\boldsymbol{r}, t)$ previously introduced in Eq. (5.22) and we obtain,

$$\frac{\partial E}{\partial t} + \nabla_{\mathbf{r}} \cdot (E\, \boldsymbol{u}_\alpha) + \nabla_{\mathbf{r}} \cdot \boldsymbol{q}_\alpha + \nabla_{\mathbf{r}} \cdot (\widetilde{\mathbf{G}}_\alpha \colon \boldsymbol{u}_\alpha) = \boldsymbol{J}_{e\alpha} \cdot \boldsymbol{E} + Q_\alpha$$

This results into an energy transport equation, using $dE/dt = DE/Dt$ we find,

$$\frac{dE}{dt} = \frac{\partial E}{\partial t} + \nabla_{\mathbf{r}} \cdot (E\, \boldsymbol{u}_\alpha) = -\nabla_{\mathbf{r}} \cdot \boldsymbol{q}_\alpha - \nabla_{\mathbf{r}} \cdot (\widetilde{\mathbf{G}}_\alpha \colon \boldsymbol{u}_\alpha) + \boldsymbol{J}_{e\alpha} \cdot \boldsymbol{E} + Q_\alpha \tag{5.29}$$

The time variation of energy inside a volume V is calculated again by using the divergence theorem,

$$\frac{d}{dt}\int_V E\,d\boldsymbol{r} = -\int_S \boldsymbol{q}_\alpha \cdot d\boldsymbol{s} - \int_S (\widetilde{\mathbf{G}}_\alpha : \boldsymbol{u}_\alpha)\cdot d\boldsymbol{s} + \int_V \boldsymbol{J}_{e\alpha}\cdot \boldsymbol{E}\,d\boldsymbol{r} + \int_V Q_\alpha\,d\boldsymbol{r} \tag{5.30}$$

Therefore, the gain or loss of energy within the volume V is caused by the flux of energy $\boldsymbol{q}$ through the enclosing surface S and the work of the electric field associated to the charge transport term $\boldsymbol{J}_{e\alpha}\cdot\boldsymbol{E}$. Two additional terms $(\widetilde{\mathbf{G}}_\alpha : \boldsymbol{u}_\alpha)$ and Q_α account for the energy variation within V originated by the collisional interaction of the α particles.

Finally, by introducing $\widetilde{\boldsymbol{G}}_\alpha = p_\alpha \widetilde{\boldsymbol{I}} + \widetilde{\boldsymbol{\Pi}}_\alpha$ in the Eq. (5.29) we obtain,

$$\widetilde{\boldsymbol{G}} : \boldsymbol{u}_\alpha = p_\alpha \boldsymbol{u}_\alpha + \widetilde{\boldsymbol{\Pi}}_\alpha : \boldsymbol{u}_\alpha$$

and the usual energy fluid transport equation is deduced,

$$\frac{\partial}{\partial t}\left[\rho_\alpha(\frac{u_\alpha^2}{2} + e_{i\alpha})\right] + \nabla_{\mathbf{r}}\cdot\left[\rho_\alpha(\frac{u_\alpha^2}{2} + h_\alpha)\,\boldsymbol{u}_\alpha\right] = \boldsymbol{J}_{e\alpha}\cdot\boldsymbol{E} - \nabla_{\mathbf{r}}\cdot\boldsymbol{q}_\alpha - \\ -\nabla_{\mathbf{r}}\cdot(\widetilde{\boldsymbol{\Pi}}_\alpha : \boldsymbol{u}_\alpha) + Q_\alpha \tag{5.31}$$

where $h = e_i + p/\rho$ is the specific enthalpy of the particle specie α.

In this transport equation still remain undetermined the heath flux vector $\boldsymbol{q}_\alpha$, Q_α and the components of the tensor $\widetilde{\boldsymbol{\Pi}}_\alpha$. These terms account for the collisional energy exchange between the different species in the plasma and brings back again into the aforementioned problem of the *closure* of the fluid transport equations.

5.2.5 The closure of the fluid transport equations

The fluid transport equations (5.24), (5.26) and (5.31) for the α particles ($\alpha = e, i, a$) in a plasma have been derived from the Boltzmann equation (5.5) under the assumption of the *existence* of a *local equilibrium*,

$$\frac{\partial n_\alpha}{\partial t} + \nabla_{\mathbf{r}}\cdot(n_\alpha \boldsymbol{u}_\alpha) = F_\alpha - S_\alpha \tag{5.32}$$

$$\rho_\alpha \frac{D\boldsymbol{u}_\alpha}{Dt} = -\nabla_{\mathbf{r}}\, p_\alpha - \nabla_{\mathbf{r}}\cdot\widetilde{\boldsymbol{\Pi}}_\alpha - m_\alpha \boldsymbol{u}_\alpha(F_\alpha - G_\alpha) + \boldsymbol{F}_\alpha^e + \boldsymbol{F}_\alpha^g + \boldsymbol{R}_\alpha \tag{5.33}$$

$$\frac{DE_\alpha}{Dt} = -\nabla_{\mathbf{r}}\cdot(p_\alpha\,\boldsymbol{u}_\alpha) + \boldsymbol{J}_\alpha\cdot\boldsymbol{E} - \nabla_{\mathbf{r}}\cdot\boldsymbol{q}_\alpha - \nabla_{\mathbf{r}}\cdot(\widetilde{\boldsymbol{\Pi}}_\alpha : \boldsymbol{u}_\alpha) + Q_\alpha \tag{5.34}$$

Here, $E_\alpha = \rho_\alpha(u_\alpha^2/2 + e_{i\alpha})$ represents the energy the electromagnetic force is $\boldsymbol{F}_\alpha^e$ while $\boldsymbol{F}_\alpha^g$ are other additional external forces as the gravity, ...etc.

However, in Eqs. (5.32-5.34) still remain undetermined the heat flux vector $\boldsymbol{q}_\alpha$, the collisional momentum exchange vector $\boldsymbol{R}_\alpha$ the tensor $\widetilde{\boldsymbol{\Pi}}_\alpha$, and also Q_α. For macroscopic fluids this problem is solved for by using phenomenological expressions as for the heat flux,

$$\boldsymbol{q} = -\kappa \nabla_{\mathbf{r}} T$$

where κ is the thermal conductivity and T the local temperature. However this is not fully justified in the case of plasmas, where a different vector $\boldsymbol{q}_\alpha$ would be required for each $\alpha = e, i, a$ particle specie. In addition, the transport equations have been derived by averaging over an undetermined particle distribution function $f_\alpha(\boldsymbol{v}, \boldsymbol{r}, t)$. The explicit expression for this later would be required in Eq. (5.21),

$$\boldsymbol{q}_\alpha = \int_{-\infty}^{+\infty} (\frac{m_\alpha w^2}{2}) \boldsymbol{w}\, f_\alpha(\boldsymbol{v}, \boldsymbol{r}, t)\, d\boldsymbol{v}$$

to evaluate this integral. Similar arguments apply to the other indeterminate quantities that appear in Eqs. (5.32-5.34). We face the problem of the *closure* of the fluid transport equations.

In order to find the expressions for the undetermined variables in the fluid equations (5.32-5.34) is reauired the formulation of a particular *model* for the plasma – or equivalently – the specific form of the velocity distribution function $f_\alpha(\boldsymbol{v}, \boldsymbol{r}, t)$.

This represents an unavoidable problem in the fluid equations (5.24- 5.26) couple low order of with higher order moments of $f_\alpha(\boldsymbol{v}, \boldsymbol{r}, t)$. The particle density $n_\alpha(\boldsymbol{r}, t)$ is coupled with the speed $\boldsymbol{u}_\alpha$ in Eq. (5.32) which in turn depends on the tensor $\widetilde{\boldsymbol{\Pi}}_\alpha$ in Eq. (5.33), the latter is also found in Eq. (5.34) with $\boldsymbol{q}_\alpha$. The above derivation of the fluid equations only considers the first three moments of the Boltzmann equation with physical meaning, but the process could continue indefinitely. Any set *finite* transport equations will always contain more unknowns than equations.

The two available schemes to circumvent this difficulty is to *truncate* the moment expansion, assuming the higher order moments arbitrarily as zero, or on the basis of physical assumptions. The second possibility is to find a it small parameter ϵ and to develop an *asymptotic power approximation*. Despite its mathematical complexity, this procedure has the advantage of a systematic approach that provides an estimate of error made.

The classical asymptotic scheme is the Chapman-Enskog theory [17] valid for rarefied (low pressure) neutral gases dominated by collisions. The small parameter is the ratio $\epsilon = \lambda/L$ between the collisional mean free path λ and the macroscopic scale L. The velocity distribution function is developed in powers as,

$$f_a(\boldsymbol{v}, \boldsymbol{r}, t) = f_{0a}(\boldsymbol{v}, \boldsymbol{r}, t) + \epsilon\, f_{1a}(\boldsymbol{v}, \boldsymbol{r}, t) + \epsilon^2\, f_{2a}(\boldsymbol{v}, \boldsymbol{r}, t) + \cdots$$

where the functions f_{0a}, $f_{1a}, ...$ are assumed of the same order. On practical grounds only two expansion terms are calculated and the equilibrium Maxwell Boltzmann distribution corresponds to the zero order f_{0a} in ϵ,

$$f_{0\alpha}(\boldsymbol{v}, \boldsymbol{r}, t) = n_\alpha(\boldsymbol{r}, t) \left(\frac{m_\alpha}{2\pi k_B T_\alpha} \right)^{3/2} \exp\left(-\frac{(\boldsymbol{u}_\alpha - \boldsymbol{v})^2}{2k_B T_\alpha} \right)$$

The direct substitution of $f_{0\alpha}(\boldsymbol{v}, \boldsymbol{r}, t)$ in the Eqs. (5.21) and (5.18) for leads to $\boldsymbol{q}_a = 0$ and $\widetilde{\boldsymbol{\Pi}}_a = 0$. Therefore, the non Maxwellian distribution $f_{1a}(\boldsymbol{v}, \boldsymbol{r}, t)$ accounts for the particle transport and the departure from the equilibrium state of the plasma.

For neutral fluids the Chapman-Enskog theory applies for any type of intermolecular forces with shorter range than Coulomb forces and the unknowns in Eqs. (5.32-5.34) can be calculated. The results are similar to ordinary fluids, for the tensor components of $\widetilde{\mathbf{\Pi}}_a$ are,

$$\pi_{ij} = -\eta_a \left(\frac{\partial u_{ia}}{\partial x_j} + \frac{\partial u_{ja}}{\partial x_i} - \frac{2}{3} (\nabla_{\mathbf{r}} \cdot \boldsymbol{u}_a)\, \delta_{ij} \right) \qquad \text{and also} \qquad \boldsymbol{q}_a = -\kappa_a \nabla_{\mathbf{r}} T_a$$

For the mean free path λ and collision frequency ν_a between neutrals, the coefficients of thermal conductivity $\kappa_a = m_a n_a \chi_t$ and viscosity $\eta = m_a n_a \chi_v$ are calculated as, as,

$$\chi_v = \nu_a \lambda^2 \sqrt{\pi}\, \frac{75}{64} \left[1 + \frac{3}{202} + \cdots \right] = A_v\, \nu_a\, \lambda^2 \tag{5.35}$$

$$\chi_t = \nu_a \lambda^2 \sqrt{\pi}\, \frac{5}{16} \left[1 + \frac{1}{44} + \cdots \right] = A_t\, \nu_a\, \lambda^2 \tag{5.36}$$

where $\nu_a = V_{th}/\lambda$ is the collision frequency between neutral atoms.

These equations have a simple physical interpretation; as the viscosity and thermal conductivity can be understood in terms of random diffusion molecules. The particles perform random jumps of average length λ between two successive collisions ν_a times per unit time. The above expansions A_v and A_t are therefore constants of proportionality.

The application of the Chapman-Enskog theory to plasmas is more involved and constitutes and active field of research. The above expressions for neutral fluids are complicated by the presence of charged particles interacting through long range Coulomb forces. The collisions between different particle species introduce additional complexities.

5.2.6 The friction coefficients

In addtion to $\boldsymbol{q}_\alpha$ and $\widetilde{\mathbf{\Pi}}_\alpha$ the transport equations (5.32-5.34) involve the moments of the Boltzmann collision operator discussed in Sec. (5.1.1). The first integral is intuitive and related with the production F_α and loss rates S_α of the α particles,

$$\frac{dn_\alpha}{dt} = F_\alpha - S_\alpha = \int_{-\infty}^{+\infty} C_s(f_\alpha)\, d\boldsymbol{v}$$

The higher order moments involve the energy and momentum transfer,

$$\boldsymbol{R}_\alpha = \int_{-\infty}^{+\infty} m_\alpha\, \boldsymbol{v}\, C_s(f_\alpha)\, d\boldsymbol{v} \qquad\qquad Q_\alpha = \int_{-\infty}^{+\infty} \frac{m_\alpha v^2}{2}\, C_s(f_\alpha)\, d\boldsymbol{v}$$

coupling the motions of the different particle species in Eqs. (5.24), (5.26) and (5.31).

These calculations are difficult and require of an appropriate expression for the Boltzmann collision operator $C_s(f_\alpha) = (\partial f_\alpha / \partial t)_{col}$ with a detailed physical model for each collisional process involved. As we have seen in Chap. (4) they depend on the value of the cross section for and the energy range of interest.

The simplest scheme available to evaluate $\boldsymbol{R}_\alpha$ and Q_α is to make use of the so called *Krook* collisional model. The time evolution of $f_\alpha(\boldsymbol{v}, \boldsymbol{r}, t)$ for small departures from the plasma equilibrium state is,

$$C_s(f_\alpha) = \frac{df_\alpha}{dt} = -\frac{f_\alpha - f_{0\alpha}}{\tau_c} = \frac{1}{\tau_c}\, f_{1\alpha}(\boldsymbol{v}, \boldsymbol{r}, t_o)$$

where $\tau_c = 1/\nu_c$ is the characteristic relaxation time. Equivalently, the perturbed distribution function is,

$$f_\alpha(\boldsymbol{v}, \boldsymbol{r}, t) \simeq f_{0\alpha}(\boldsymbol{v}, \boldsymbol{r}, t_o) + f_{1\alpha}(\boldsymbol{v}, \boldsymbol{r}, t_o)\, e^{-t/\tau_c}$$

where τ_c is the collision time scale that brings the system back to the equilibrium state.

In plasmas with a low ionization degree the collisions of charged particles with the abundant background of neutral atoms are dominant. The Krook operator leads to the so called *friction coefficients* from which we can estimate the relevance of each collisional process.

From a macroscopic point of view, we can intuitively understand the collisional interaction between the plasma the species as a *friction* caused by their relative motion. The total friction force friction $\boldsymbol{R}_\alpha$ exerted on the specie α is the sum of those performed on the same all the others,

$$\boldsymbol{R}_\alpha = \sum_\beta \boldsymbol{R}_{\alpha\beta}$$

and the global momentum conservation requires, $\boldsymbol{R}_{\alpha\beta} = -\boldsymbol{R}_{\beta\alpha}$. and,

$$\sum_\alpha \boldsymbol{R}_\alpha = 0 \tag{5.37}$$

When the particle distribution function of particles can be approximated by a *local Maxwellian* (see Sec. 4.6.2) and the drift velocities $\boldsymbol{u}_\alpha$ y $\boldsymbol{u}_\beta$ are small compared with the thermal speeds $V_{Th} \gg u_\alpha, u_\beta$, the friction force between the two species could be approximated by,

$$\boldsymbol{R}_{\alpha\beta} = -A_{\alpha\beta}(\boldsymbol{u}_\alpha - \boldsymbol{u}_\beta) \tag{5.38}$$

where $A_{\alpha\beta} = A_{\beta\alpha} > 0$ represents the magnitude of the *friction force* between the α and β species. This friction force represents a momentum and energy transfer mechanism between the different particle species. The gain or loss of energy rate Q_α is the sum of the exchanged energies,

$$Q_\alpha = \sum_\beta Q_{\alpha\beta}$$

and because $\boldsymbol{R}_{\alpha\beta} = -\boldsymbol{R}_{\beta\alpha}$ we have,

$$Q_{tot} = Q_{\alpha\beta} + Q_{\beta\alpha} = -\boldsymbol{R}_{\alpha\beta} \cdot \boldsymbol{u}_\alpha - \boldsymbol{R}_{\beta\alpha} \cdot \boldsymbol{u}_\beta = -\boldsymbol{R}_{\alpha\beta} \cdot (\boldsymbol{u}_\alpha - \boldsymbol{u}_\beta)$$

The plasma momentum balance Eq. (5.37) is null, contrary to the above equation for the plasma energy rate. The energy balance is not satisfied because the plasma fluid equations apply for non equilibrium plasmas where elementary processes, as light emission, ionizations, ...etc dissipate energy. Therefore, an external source of energy , i.e. an electric field, is required to sustain this partial equilibrium plasma state.

5.2.6.1 Elastic collisions.

In the elastic collisions there is no change in neither the internal state nor in the kinetic energy of colliding particles. The strength of the friction force $A_{\alpha\beta}$ in Eq. (5.38) must be a function of the following quantities,

$$A_{\alpha\beta} \sim n_\alpha \, , n_\beta \, , \; \mu_{\alpha\beta} = \frac{m_\alpha m_\beta}{m_\alpha + m_\beta} \, , \, \sigma_{\alpha\beta} \, , \bar{V}_{col}$$

Here, $\bar{V}_{col}$ is a characteristic molecular velocity related with the temperature of colliding species, and $\sigma_{\alpha\beta}$ the total elastic cross section. It may be shown that,

$$A_{\alpha\beta} = n_\alpha n_\beta \, \mu_{\alpha\beta} \sigma_{\alpha\beta} \frac{4}{3} \left(\frac{8 k_B T}{\pi \mu_{\alpha\beta}} \right)^{1/2}$$

where $k_B T$ is the plasma kinetic temperature. For elastic collisions between electrons and neutral atoms, $\mu_{ea} \cong \mu_{ei} = m_e/2$ and hence,

$$A_{ea} \cong n_e n_a \, m_e \, \sigma_{ea} \frac{4\sqrt{2}}{3} \left(\frac{2 k_B T_e}{\pi m_e} \right)^{1/2}$$

where the characteristic energies are $k_B T = k_B T_e \ll k_B T_i$ for a cold and weakly ionized plasma. Introducing the *elastic collision frequency* (see Sec. 4.1) we have,

$$\nu_{ea} = n_a \, \sigma_{ea} \frac{4\sqrt{2}}{3} \left(\frac{2 k_B T_e}{\pi m e} \right)^{1/2} = n_a \, \sigma_{ea} \frac{2\sqrt{2}}{3} \bar{V}_{Te}$$

and $\bar{V}_{Te}$ is the electron thermal speed. Then, the friction force between electrons and neutrals (is similar for ion-neutral) becomes,

$$\boldsymbol{R}_{ea} = -m_e n_e \nu_{ea} (\boldsymbol{u}_e - \boldsymbol{u}_a)$$

In the general case, for two colliding species α and β we have,

$$\boldsymbol{R}_{\alpha\beta} = -m_\alpha n_\alpha \nu_{\alpha\beta} \, (\boldsymbol{u}_\alpha - \boldsymbol{u}_\beta)$$

However, an small exchange of energy $\Delta\epsilon$ occurs in the elastic collisions between electrons and neutral atoms [10] given by,

$$\Delta\epsilon = \frac{m_e^2}{2 m_a} (\Delta \boldsymbol{v}_e)^2$$

and averaging over all the possible collision angles θ we obtain,

$$\Delta\epsilon = \frac{m_e^2 v_e^2}{m_a} \left(1- < \cos(\theta) >\right)$$

In order to obtain the energy rate transfer by unit volume we multiply by the number of elastic collisions and the neutral atom density,

$$Q_{ea} = \frac{2m_e}{m_a} \nu_m n_a \epsilon_e$$

where we used the *effective collision frequency for momentum transfer* [10],

$$nu_m = \nu_{ea} \left(1- < \cos(\theta) >\right) \simeq \nu_{ea}$$

The fraction of electron energy gained by the the atom is small and proportional to the mass ratio $\delta_m = 2m_e/m_a \ll 1$. Because $\epsilon_e = 3k_B T_e/2$ we have,

$$Q_{ea} = \left(\frac{3}{2} k_B T_e\right) \nu_m \, n_a$$

and this term accounts for the energy transfer between the electrons and neutral gases being usually rather small. However it should be included in Eq. (5.31). when the collision frequency is large, as for high neutral gas pressures. The electrons gain energy form the electric field that is transferred to the neutral gas raising its temperature. This thermalization effect is evident in Fig. (4.11) where the gas temperature grows with the pressure and was discussed in Sec. (4.6.1) within the context of the *multithermal equilibrium*. While the energy transfer in an elastic collision is small, the number of collisions grows with the neutral gas pressure and becomes of an effective mechanism for gas heating.

5.2.6.2 Ionizing collisions.

In Eq. (5.33) the production or loss of a new particle also involves changes of energy and momentum. The ionizing electron loss an amount of energy E_I equal to the ionization potential of the neutral gas, and the new ion is created at rest with respect to the ion fluid. Therefore, the corresponding energy rate is,

$$Q_I = E_i \, \nu_I$$

where ν_i is the ionization frequency and is given by, $\nu_I \, n_e = k_I \, n_a \, n_e$. In the frame where both, ion and electron fluids move, the change of momentum for ions is,

$$\boldsymbol{R}_{Ii} = -m_i n_e \nu_I \left(\boldsymbol{u}_i - \boldsymbol{u}_e\right)$$

while for ions,

$$\boldsymbol{R}_{Ie} = -m_i n_e \nu_I \left(\boldsymbol{u}_e - \boldsymbol{u}_i\right)$$

and both terms were already considered in Eq. (5.33).

6

The boundaries of plasmas: the plasma sheaths.

6.1 Introduction.

The plasmas in nature and in the laboratory are limited by confining metallic or dielectric walls which in turn interact with this physical medium. In the experiments, the plasma is enclosed inside a vacuum tank or a glass discharge tube and the electrodes and/or the surfaces of measuring probes are boundaries for the plasma. The metallic external surfaces of orbiting vehicles also interact with the ionospheric plasma and, according to the electric polarity, a charged particle current may be drained that changes the electric potential of the vehicle with respect to its surroundings. This charging process may produce electric shocks and high altitude electric discharges in orbiting spacecrafts.

This interaction between the dielectric or metallic external surfaces of objects with the plasma constitutes a classical problem in plasma physics. The electric potential of a metallic wall generally differs from the bulk plasma potential. Both values are connected along a length scale through a plasma potential jump denominated *plasma sheath* where the quasineutrality condition is not fulfilled. The current collection from a plasma takes place through the plasma sheath and the dimension of this potential structure plays a key role in the charge collection process.

In the following we will discuss the classical model for a one dimensional collisionless plasma sheath in a fully ionized and cold ($k_BT_e \gg k_BT_i$) unmagnetized plasma. As we shall see, the structure of an stable plasma sheath is complex and separated in two different regions that scale with the plasma Debye length λ_D. The *presheath*, where ions are accelerated up to supersonic speed and the *plasma sheath* where the main plasma potential jump takes place.

This simple model does not apply apply to weakly ionized plasmas where collisions with neutrals are dominant. In this case the collisional mean free λ_c introduces new length scale that competes with the Debye length λ_D and complicates the structure of the plasma sheath.

6.2 The collisionless electrostatic plasma sheath.

In many experiments, the plasma is enclosed within a vacuum chamber of finite dimensions, and the walls held at a negatively bias potential $\varphi_w > \varphi_p$ with respect to the plasma bulk φ_p

as in Fig. (6.1) so that the electrons are reflected back inside. This is a common situation in laboratory plasmas because the metallic walls of the vacuum tanks are negatively biased in order to return the electrons to the plasma bulk to increase the ionization rate.

This situation in one dimension is represented in the scheme of Fig. (6.1). The plasma potential is uniform in the unperturbed plasma and its spatial variation from φ_w to φ_p is limited to a layer adjacent to the walls. This forms a potential barrier so that the more mobile electrons are confined inside the vacuum chamber.

The calculation of the plasma potential from φ_w at at the wall located at $x = 0$ up to the bulk plasma φ_p requires to solve the Poisson equation for $\varphi(x)$ with appropriate boundary conditions. In general, this leads to a complex nonlinear partial differential equation that becomes reduced to a one dimensional problem by making the following assumptions:

- The potential of the wall is negative for the plasma, $\varphi_w < \varphi_p$ so that ions are attracted and the electrons repelled.
- Within the plasma bulk (away from the wall) the quasineutrality condition os satisfied $n_e \cong n_i \cong n_{eo}$. The ions are considered cold ($k_B T_e \gg T_B K_I$) and the electrons have a Maxwell Boltzmann distribution.
- The ionization is negligible in the volume considered; all ions entering into the plasma sheath finally reach the wall. Then, the current density of ions $\Gamma_i = n_i\, u_i$ is constant in the sheath $d\Gamma_i/dx \approx 0$. Therefore, at each point x between plasma volume and the wall we have, $\Gamma_i = n_{io}\, u_{io} = n_i(x)\, u_i(x)$.

Under these conditions, the energy of an ion entering the sheath with velocity u_{io} is,

$$\frac{1}{2} m_i u_i^2(x) + e\,\varphi(x) = \frac{1}{2} m_i u_{io}^2$$

It follows that the ion density can be written as:

$$n_i(x) = \frac{n_{io}\, u_{io}}{\sqrt{u_{io}^2 - \frac{2e\,\varphi(x)}{m_i}}} \tag{6.1}$$

This expression along with the Maxwellian electron density is introduced in the Poisson equation for the plasma potential $\varphi(x)$,

$$\epsilon_o \frac{d^2\varphi}{dx^2} = e\, n_{eo} \left[\exp\left(e\varphi/k_B T_e\right) - \frac{u_{io}}{\sqrt{u_{io}^2 - \frac{2e\,\varphi(x)}{m_i}}} \right]$$

This expression is made dimensionless using ion sound speed $c_{is} = \sqrt{k_B T_e/m_i}$ and the following variables,

$$\phi = -\frac{e\varphi}{k_B T_e}, \quad N_e = n_e/n_{eo}, \quad N_i = n_i/n_{eo}, \quad V = u/c_{is}$$

With these changes the Poisson equation becomes,

$$\epsilon_o \frac{d^2}{dx^2}(-\frac{e\varphi}{k_B T_e}) = -\frac{e^2\, n_{eo}}{k_B T_e}\left[\exp(e\varphi/k_B T_e) - \frac{1}{\sqrt{1-2e\varphi(x)/m_i u_{io}^2}}\right]$$

where $2e\varphi/m_i u_{io}^2 = 2\phi/(u_{io}/c_{is})^2$ and finally,

$$\frac{d^2\phi}{dx^2} = -\lambda_D^{-2}\left[e^{-\phi} - \frac{1}{\sqrt{1+2\phi/V_o^2}}\right] \tag{6.2}$$

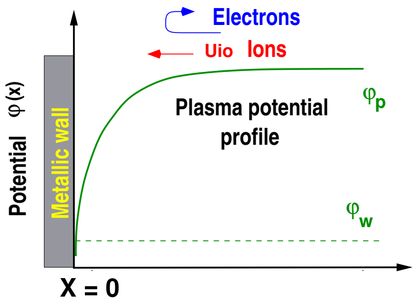

Figure 6.1: The plasma potential profile between the metallic wall and the undisturbed plasma.

The solutions of this nonlinear differential equation $\phi(x)$ provide the variation of the plasma potential $\varphi(x)$ in one dimension, normalized to the electron temperature value $k_B T_e$. We deliberately left aside the length x because the Eq. (6.2) shows that the natural normalization is $S = x/\lambda_D$ that defines the length scale of the electrostatic sheath.

It is obviously difficult to find general solutions of the differential equation (6.2) and therefore we only seek for approximate solutions in the limit $k_B T_e \gg e\varphi$ corresponding to $\phi < 1$, when the potential jump of the sheath is much lower than the thermal energy of electrons.

6.2.1 Bohm Criterion.

In the equation (6.2) with $s = x/\lambda_D$ multiplying by $d\phi/ds$ on both sides,

$$\int_{so}^{s} \frac{d^2\phi}{ds^2}\frac{d\phi}{ds}ds = \left[\int_{so}^{s}\left(1+\frac{2\phi}{V_o^2}\right)^{-1/2}\frac{d\phi}{ds}ds - \int_{so}^{s}\exp(-\phi)\frac{d\phi}{ds}ds\right]$$

where s_o correspond to the coordinate where ion enters with speed u_{io} and $s < s_o$ is any point inside the plasma sheath. Then,

$$\frac{1}{2}(\frac{d\phi}{ds})^2|_{s_o}^{s} = V_o^2\sqrt{1+\frac{2\phi}{V_o^2}}|_{s_o}^{s} + \exp(-\phi)|_{s_o}^{s}$$

where the lower limit of the left term is zero because the dimensionless electric field is negligible at the point where the ion enters into the sheath:

$$\frac{d\phi}{ds}|_{s=s_o} = -\frac{e}{k_B T_e}\frac{d\varphi}{ds}|_{s=s_o} = \frac{e}{k_B T_e}\mathcal{E}|_{s=s_o} \cong 0$$

Note that the expression $\mathcal{E} = -d\phi/ds$ represents an electric field normalized to the length scale that determines λ_D. Taking at the plasma bulk $\phi(s_o) \simeq \phi(\infty) = 0$ we obtain,

$$\frac{1}{2}(\frac{d\phi}{ds})^2 = V_o^2 \left[\sqrt{1+\frac{2\phi}{V_o^2}} - 1\right] + (\exp(-\phi) - 1) \tag{6.3}$$

This nonlinear equation do not have analytical solutions and only could be numerically solved. However, an approximate expression is found when the electron thermal energy is larger than the electrostatic energy $\phi \ll 1$. In this case the Taylor series expansion of the exponential gives,

$$\frac{1}{2}(\frac{d\phi}{ds})^2 = V_o^2 \left[\left(1+\frac{\phi}{V_o^2} - \frac{1}{2}\frac{\phi^2}{V_o^4} + ...\right) - 1\right] + \left[(1 - \phi + \frac{1}{2}\phi^2 + ...) - 1\right] > 0$$

This expression must always be positive, retaining only two terms of the expansion,

$$V_o^2 \left[\frac{\phi}{V_o^2} - \frac{1}{2}\frac{\phi^2}{V_o^4}\right] - \phi + \frac{1}{2}\phi^2 > 0$$

and finally we have,

$$\left[-\frac{1}{V_o^2} + 1\right] \frac{1}{2}\phi^2 > 0$$

In order to be positive, the normalized ion speed V_o needs to be,

$$V_o > 1, \quad u_{io} > c_{is}$$

This inequality is called *Bohm criterion*, and shows that ions must enter the sheath region with a higher velocity than ion acoustic speed.

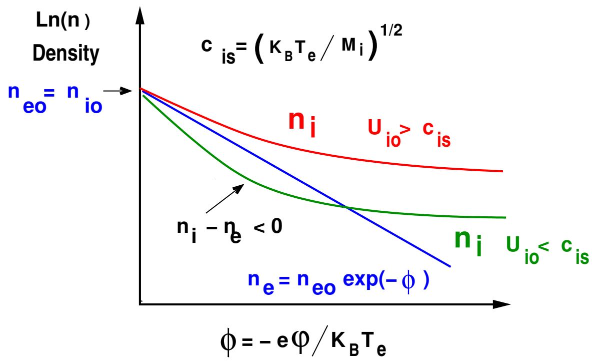

Figure 6.2: Comparison of $n_i(\phi)$ and $n_e(\phi)$ as a function of ϕ.

Therefore, the plasma potential profile close to the metallic wall needs to be divided in two different regions. The ions coming from the undisturbed bulk plasma before entering in the sheath need to be accelerated in order to satisfy $u_{io} > c_{ia}$. This implies the existence of a *presheath*, that is, an small electric field that accelerate the ions before the large potential drop corresponding to the *sheath*. As we made the condition of zero electric field in the volume plasma in Eq. (6.3), we have left the *presheath* included within the integration region between s_o and the generic point s.

The physical meaning of the condition $u_{io} > c_{is}$ could be understood by plotting the dimensionless electron $N_e(\phi)$ and ion $N_i(\phi)$ (see Eq. 6.1) densities as a function of the scaled plasma potential ϕ.

$$N_i(\phi) = \frac{1}{\sqrt{1+2\phi/V_{io}^2}} \quad \text{and,} \quad N_e(\phi) = \exp(-\phi)$$

In the unperturbed bulk plasma where $\phi = 0$ the quasineutrality condition $N_i = N_e = 1$ holds ($n_{eo} = n_{io}$) and the charged particle densities decrease inside the plasma sheath with ϕ. In logarithm scale the electron density reduces with slope -1 while,

$$\ln N_i(\phi) = -\frac{1}{2}\ln(1 + \frac{2\phi}{V_o^2})$$

decreases much slower as in Fig. (6.2).

The difference $N_i - N_e$ si proportional to the local charge density $\rho(\phi) = e\, n_{eo}(N_i - N_e) > 0$ that needs to be positive because the ions are attracted and the electrons repelled $n_i(\phi) > n_e(\phi)$ in the sheath. Then, close to the origin the slope of $N_i(\phi)$ needs to be over those of $N_e(\phi)$ as indicated in Fig. (6.2) and this occurs when $V_o > 1$.

6.2.2 Child-Langmuir current.

Since the electron density decreases rapidly with ϕ we focus our attention to the region close to the ion collecting electrode. We start again from the equation (6.2) and $V_o > 1$ is the dimensionless velocity of ions entering into the sheath,

$$\frac{d^2\phi}{ds^2} = -\left[e^{-\phi} - \frac{1}{\sqrt{1 + 2\phi/V_o^2}}\right]$$

We define an initial point $s_i < s_o$ inside the plasma sheath where we can neglect the decreasing term $exp(-\phi)$ for $s_i < s \leq s_w$. That is, the electron density could be neglected for $s \geq s_i$ or equivalently, $2\phi/V_o^2 \gg 1$, the electrostatic energy dominates over the ion kinetic energy, and therefore,

$$\frac{d^2\phi}{ds^2} = \left(1 + \frac{2\phi^2}{V_o^2}\right)^{-1/2} \cong \frac{V_o}{\sqrt{2\phi}}$$

Multiplying by $d\phi/ds$ on both sides we can integrate between s_i and generic point $s \leq s_w$ in the sheath before the location of the collecting electrode $s_w = x_w/\lambda_D$,

$$\int_{s_i}^{s} \frac{d^2\phi}{ds^2}\frac{d\phi}{ds}ds = \int_{s_i}^{s} \frac{V_o}{\sqrt{2\phi}}\frac{d\phi}{ds}ds$$

$$\frac{1}{2}(\frac{d\phi}{ds})^2|_{s_i}^{s} = \sqrt{2}\, V_o \sqrt{\phi}\,|_{s_i}^{s}$$

As before the dimensionless electric field is $\mathcal{E} = -d\phi/ds$ and the above equation becomes,

$$\frac{1}{2}\left[\mathcal{E}^2(s) - \mathcal{E}_i^2\right] = \sqrt{2}\, V_o \left(\sqrt{\phi(s)} - \sqrt{\phi_i}\right)$$

Again, we neglect the electric field $\mathcal{E}_i$ in the point s_i compared with $\mathcal{E}(s)$ and also $\phi(s) \gg \phi_i$. This simplifies the last equation,

$$\frac{1}{2}(\frac{d\phi}{ds})^2 = \sqrt{2}\, V_o \sqrt{\phi}$$

and for values of s in the vicinity of the electrode ($s_i < s \sim s_w = 0$) we have,

$$\frac{d\phi}{\phi^{1/4}} = 2^{3/4}\sqrt{V_o}\,ds$$

Integrating from the generic point $s \leq s_w$, up to the location s_w [1] of the collecting metal wall at the electric potential $\phi_w = \phi(s_w) = \phi(0)$ we obtain,

$$\frac{4}{3}\left(\phi_w^{3/4} - \phi^{3/4}\right) = 2^{1/2}\sqrt{V_o}\,(s_w - s)$$

and taking $\phi_w \gg \phi(s)$ we can solve V_o,

$$V_o = \frac{4\sqrt{2}}{9}\frac{\phi_w^{3/2}}{(s_w - s)^2}$$

Finally, if we undo the previous change of variable we $s_w - s = d/\lambda_D$ where d is then the distance point $x = s\,\lambda_D$ we have considered the electrode is finally:

$$u_{io} = \frac{4\sqrt{2}}{9}\left(\frac{\epsilon_o k_B T_e}{e^2 n_{eo}}\right)\frac{1}{d^2}\sqrt{\frac{k_B T_e}{m_i}}\left(\frac{e\,\varphi_w}{k_B T_e}\right)^{3/2}$$

Since the ion current density is constant in the sheath can then write $J_i = e\,n_i u_i = n_{io}u_o$ so we get,

$$J_i = n_{io}u_{io} = \frac{4}{9}\sqrt{\frac{2e}{m_i}}\frac{\epsilon_o}{e^2}\frac{\varphi_w^{3/2}}{d^2}$$

which is precisely the Child-Langmuir space charge limited current for a plane diode.

This expression predicts the maximum ion current density J_i that reach the collecting electrode for a potential difference φ_w between its surface and the background plasma separated a distance $d = x_w - x$. This current density current scales with the power $3/2$ of the potential difference φ_w between the bulk plasma and the collecting electrode.

[1] In Fig. (6.1) the metallic wall is located at $x = 0$, we retain the coordinate $s_w = 0$ to evidence the location of the ion collecting wall.

Bibliography

[1] F.F. Chen. Introduction to plasma physics and controlled fusion. Vol. 1: Plasma physics. 2nd ed. Plenum Press New York, USA (1984).

[2] J.M. Rax. Physique des Plasmas. Dundod, Paris, France (2007).

[3] G.K. Parks. Chaps. 1 and 6. Physics of Space plasmas. An introduction (2nd Ed.). Addison Wesley, Redwood City, USA, (2004).

[4] W. Baumjohann and R.A. Treumann. Chaps. 1-4 and 6. Basic Space Plasma Physics. Imperial College Press, London, UK, (2006).

[5] R.J. Walker and C.T. Russell. Solar wind interactions with magnetized planets, pp. 164-181 in *Introduction to Space Physics*, Edited by, M.G. Kivelson and C.T. Russel. Cambridge University Press, New York, USA (1995).

[6] J.G. Luhmann. Ionospheres, pp. 183-202 in *Introduction to Space Physics*, Edited by, M.G. Kivelson and C.T. Russel. Cambridge University Press, New York, USA (1995).

[7] M.C. Kelley. The Earth's ionosphere: Plasma Physics and Electrodynamics. International Geophysical Series, Academic Press, San Diego, USA (1989).

[8] H. Cho and Y.S. Parks. Low energy electron scattering from Argon. J. Korean Phys. Soc. **55** (2) pp. 459-462 (2009).

[9] R. Rejoub, B.G. Lindsay and R.F. Stebbings. Determination of the absolute partial and total cross sections for electron impact ionization of the rare gases. Phys. Rev. A **65**, 042713 (2002).

[10] Y.P. Raizer. Gas discharge physics. Springer Verlag, Berlin, Germany (1991).

[11] A. Fridman and L.A. Kennedy. Plasma Physics and Engineering. Taylor and Francis, New York, USA (2004).

[12] M.A. Lieberman and A.J. Lichtenberg. Principles of plasma discharges and materials processing. Wiley and Sons, New York, USA (1994).

[13] S.C. Brown. Basic data of plasma physics. The fundamental data on electrical discharges in gases. American Vacuum Society Classics. AIP Press, New York, USA (1994).

[14] R.G. Jahn. Chaps. 1-5. Physics of electric propulsion. Dover Publication. New York, USA (1966)

[15] D.M. Goebel and I. Katz. Chaps. 1,2,4 and 5. Fundamentals of electric propulsion. Ion and Hall Thrusters. Wiley and sons. Hoboken, New Jersey, USA (2008).

[16] N.H. Stone. The aerodynamics of bodies in rarefied ionized gas with applications to spacecraft environmental dynamics. NASA Technical paper 1933 (1981).

[17] S. Chapman y T.G. Cowling. The Mathematical Theory of Non-uniform Gases. Cambridge University Press, Cambridge, UK (1953).

[18] S.I. Braginskii. Transport processes in a plasma. Reviews of Plasma Physics, **1**, pp. 205-311 (1965).

[19] L.C. Woods An introduction to the kinetic theory of gases and magnetoplasmas Oxford Science Publications. Oxford University Press, Oxford, UK (1993).

[20] A.V. Phelps. Cross sections and swarm coefficients for nitrogen ions and neutrals in N_2 and argon ions and neutrals in Ar for energies from 0.1 eV to 10 KeV J. Phys. Chem. Ref. Data. **20** (3) pp. 557-573 (1991).

[21] A.V. Phelps The application of scattering cross section to ion flux models in discharge sheaths. *J. Appl. Phys.* **76** (2) pp. 747-753 (1994).

[22] D.E. Hastings. A review of plasma interactions with spacecraft in low Earth orbit . *J geophys. Res.* **79**, (A13), 1871-1884, (1986).

[23] Plasma physics formulary. Naval Research laboratory, NRL publication 0084-4040, Washington DC, (1986).

[24] R.J. Goldston y P.H. Rutherford. Introduction to plasma physics. Institute of Physics, Bristol, UK (1995).

[25] A. Rai Choudhuri. Physics of Fluids and Plasmas. An Introduction for Astrophysicists. Cambridge University Press, Cambridge, UK (1998).